

**UC Davis**

**UC Davis Electronic Theses and Dissertations**

**Title**

A NEW APPROACH TO ASSESS WATER BALANCES AND DROUGHT CONDITIONS OVER THE TRANSBOUNDARY REGION, LO RIVER WATERSHED, VIETNAM

**Permalink**

<https://escholarship.org/uc/item/0vv9t4nr>

**Author**

Nguyen, Anh

**Publication Date**

2022

Peer reviewed|Thesis/dissertation

A New Approach to Assess Water Balances and Drought Conditions over the  
Transboundary Region, Lo River Watershed, Vietnam

By

ANH THUY NGUYEN

DISSERTATION

Submitted in partial satisfaction of the requirements for the degree of

DOCTOR OF PHILOSOPHY

In

Civil and Environmental Engineering

In the

OFFICE OF GRADUATE STUDIES  
of the  
UNIVERSITY OF CALIFORNIA  
DAVIS

Approved:

Professor. M. Levent Kavvas, Chair

---

Dr. Ali Ercan

---

Professor. Holly Oldroyd

Committee in Charge  
2022

## ACKNOWLEDGEMENT

I would like to express my most sincere thanks to my advisor, Professor M. Levent Kavvas for his continued support and guidance that helped me complete the program. His enthusiasm, energy, and patience in guiding me will go a long way and I will never forget his kindness in my whole life.

I would like to express my sincere thanks to Dr. Ali Ercan and Professor Holly Oldroyd for serving as my dissertation committee members and providing valuable suggestions. In addition, I would like to thank Dr. Kara Carr, Ms. Lauren K. Worrell, and my colleagues for their time and kind support given to me during my studies.

To my husband Toan Trinh, my two lovely kids, Mia Trinh and Dan Trinh, my parents, my brother and sisters, I would like to express my deepest thanks for their lifelong love and support. Without their dedication and constant encouragement, I would not have been able to complete this study.

## ABSTRACT

Water balance and drought analysis are crucial practices to reduce the effects of hydro-meteorological risks on human society in an economically and environmentally sustainable manner. Water withdrawal and water supply are changing dramatically in Vietnam due to the escalating pressure from socioeconomic development, environmental requirements, and climate change impacts. The IPCC has identified Vietnam to be amongst the countries most affected by climate change, predicting an increase in the frequency and magnitude of natural disasters, especially droughts and floods. Water resources in Vietnam are highly dependent on external sources, with over 60 percent of the total average surface water discharge generated outside of the country. The reliance on external sources poses an alarming threat of water scarcity, requiring immediate actions to cope with droughts and increase the resilience of Vietnam's water resources. Thus, assessment of drought conditions over transboundary river regions is considered one of the most crucial tasks of the Government of Vietnam.

The Lo River watershed (LRW), a tributary of the Red River watershed, is a transboundary watershed with a catchment area of 39,000 km<sup>2</sup>. The watershed is composed of upstream and downstream regions. The upstream region, located in China, accounts for 52% of the total area, while the downstream region, located in Vietnam, accounts for 48% of the total area.

The main goal of this study is to assess drought conditions in the transboundary watershed LRW, based on long-term projected water supply and water demand under different 21st century climate change scenarios. The projected water supply is obtained by coupling a hydroclimate model whose inputs are provided by GCM projection outputs. Water demand, including municipal and industrial (M&I), environmental (E), and agricultural (AG), is collected

from reliable sources. Future municipal and industrial (M&I) water demand and environmental water demand are collected from the Vietnamese Ministry of Natural Resources and Environment (MONRE), and the Ministry of Agriculture and Rural Development (MARD), respectively. Before projecting water supply, bias correction methods are investigated and applied. Bias correction combined with outputs from the hydroclimate model provide realistic flow data for the downstream region. Once projected water supply and water demand are obtained, a drought analysis is applied over the target watershed.

Results of the drought analysis show future drought events are projected to be more intense and severe than past events. Increased understanding of the impact of climate change on future water resources aids policymakers in developing more effective plans to increase the resilience to climate change and sustain the water security of the region and the country.

## TABLE OF CONTENTS

CHAPTER 1. INTRODUCTION .....	15
1.1 Introduction.....	15
1.2 Study Area .....	19
1.3 Overview of Study Goals.....	23
References.....	26
CHAPTER 2. RECONSTRUCTING HISTORICAL HYDROCLIMATE DATA FOR LO RIVER WATERSHED REGION.....	29
2.1 Introduction.....	29
2.2 Methodology .....	32
2.2.1 Weather Research and Forecasting – WRF.....	33
2.2.2 WEHY Hydrologic Model .....	36
2.2.3 WEHY Reservoir model .....	40
2.3 Calibration and Validation of WEHY-WRF model for LRW .....	44
2.3.1 WRF over LRW: Atmospheric Processes.....	44
2.3.2 The WEHY model over the LRW: Hydrology processes .....	51
2.4 Assessment of atmospheric and hydrologic conditions over the LRW during 1901–201459	
2.5 Conclusions.....	66
References.....	68
CHAPTER 3. PRECIPITATION AND STREAM FLOW BIAS CORRECTION.....	73
3.1 Introduction.....	73
3.2 Methodology .....	73
3.2.1. Precipitation Bias Correction .....	74
3.2.2. Streamflow Bias Correction .....	75
3.3 Results.....	77
3.3.1. Precipitation Bias Correction Results .....	77
3.3.2. Streamflow Bias Correction Results .....	82
3.4 Conclusions.....	91
References.....	92
CHAPTER 4. DYNAMICAL DOWNSCALING OF GLOBAL CLIMATE MODELS TO PROJECT WATER SUPPLY OVER THE LO RIVER WATERSHED.....	93
4.1 Introduction.....	94
4.2 Methodology .....	96
4.3 Results.....	99

4.4	Conclusion .....	106
	References .....	108
CHAPTER 5. WATER DEMAND .....		110
5.1	Introduction.....	110
5.2	Key Assumptions .....	111
	5.2.1. Agricultural Production.....	111
	5.2.2. Tourism .....	113
	5.2.3. Industry.....	113
	5.2.4. Population forecasts .....	114
	5.2.5. Domestic water use .....	115
5.3	Demand forecasting scenarios .....	116
	Scenario 1 – Low economic growth .....	116
	Scenario 2 – Average economic growth .....	117
	Scenario 3 – High economic growth.....	117
	5.3.1. Comparison of scenarios .....	118
5.4	Conclusions.....	120
	References .....	121
CHAPTER 6. WATER BALANCE AND FUTURE DROUGHT ANALYSIS.....		122
6.1	Introduction.....	122
6.2	Methodology .....	123
	6.2.1 Estimation of water supply.....	123
	6.2.2 Water balance analysis .....	127
6.3	Result and Discussion .....	129
6.4	Conclusion .....	136
	References .....	138
CHAPTER 7. DISCUSSION AND CONCLUSIONS .....		140
7.1	Summary .....	140
7.2	Future Perspectives .....	143
7.3	Conclusion .....	143

## LIST OF FIGURES

Figure 1.1 Geographic location of Lo River Watershed in Vietnam .....	20
Figure 1.2 Topographic variation in Lo River Watershed.....	22
Figure 2.1 Methodology of historical data reconstruction process.....	33
Figure 2.2 Schematic showing the data flow and program components in WRF-AWR (Skamarock et al, 2008) .....	34
Figure 2.3 ARW $\eta$ coordinate (Skamarock et al, 2008) .....	35
Figure 2.4 Structural description of WEHY hydrologic model and description of land surface processes within this model (Kavvas et al., 2004) .....	37
Figure 2.5 Flow processes over a longitudinal cross section of a hillslope, as conceptualized in hydrologic module (Kavvas et al., 2004).....	38
Figure 2.6 Hydrologic model's depiction of hillslope surface and subsurface flow processes (Kavvas et al., 2004).....	38
Figure 2.7 The description of WEHY reservoir operation .....	41
Figure 2.8 Relationship among Surface area, water elevation, and storage at Tuyen Quang and Thac Ba reservoirs .....	42
Figure 2.9 The current reservoir operation rule includes minimum and maximum reservoir water levels for Tuyen Quang and Thac Ba reservoirs.....	43
Figure 2.10 The description of the three nested WRF domains for dynamical downscaling .....	46
Figure 2.11 Comparison of the model-simulated basin average monthly precipitation over the LRW in Vietnam's territories against the corresponding ground observations .....	48

Figure 2.12 Comparison of model-simulated precipitation and the VNGP data over the study region from 1980 to 2010.....	50
Figure 2.13 Comparison of model-simulated precipitation and APHRODITE data over the study region from 1990 to 2001 at resolution of 0.25° .....	51
Figure 2.14 Delineated MCUs map for LRW.....	52
Figure 2.15 Land parameter maps of surface roughness (SR) and root depth for Lo River Watershed .....	53
Figure 2.16 Month averages of Leaf Area Index (LAI) data over the LRW .....	54
Figure 2.17 Computed soil hydraulic conductivity parameter maps for the LRW.....	55
Figure 2.18 Comparison of the monthly mean discharge between the WEHY hydrology model simulations and observations at Vu Quang station during: Jan 1972 to Dec 1980 for calibration .....	56
Figure 2.19 Comparison of the monthly mean discharge between the WEHY hydrology model simulations and observations at Vu Quang station from Jan 2008 to Dec 2012 for validation.....	59
Figure 2.20 Annual basin average precipitation depths over LRW during 1900–2015 with their 10-year moving averages.....	60
Figure 2.21 Comparison of monthly basin average precipitation during 1900–1950 and 1951–2015.....	61
Figure 2.22 Annual basin-average temperature over LRW during 1900–2015.....	62
Figure 2.23 Comparison of monthly basin average temperature during 1900–1950 and 1951–2015.....	63
Figure 2.24 Location of Ham Yen and Chiem Hoa stations.....	64

Figure 2.25 Historical mean monthly results at Ham Yen from 1972 to 2005, for calculated and observed evapotranspiration .....	65
Figure 2.26 Historical mean monthly results at Chiem Hoa from 1972 to 2005, for calculated and observed evapotranspiration .....	65
Figure 2.27 Annual basin-average evapotranspiration over LRW during 1900–2015.....	66
Figure 3.1a Comparisons of WRF-simulated monthly precipitation versus VNGP monthly precipitation from water year 1980 to water year 2005 for the LRW (before precipitation bias-correction).....	78
Figure 3.2a Comparisons of WRF-simulated annual precipitation versus VNGP annual precipitation from water year 1980 to water year 2005 for the LRW (before precipitation bias-correction).....	79
Figure 3.3a Comparisons of 5-year moving LRW average annual precipitation between VNGP and WRF-simulated precipitation during water year 1980 to water year 2005 (before precipitation bias-correction).....	80
Figure 3.4 Monthly observation data and simulated flow data using four different climate inputs (before and after bias-correction downscaled atmospheric data from CCSM4 and MIROC5) at Tuyen Quang station.....	83
Figure 3.5 Mean monthly observation data and simulated flow data using four different climate inputs (before and after bias-correction downscaled atmospheric data from CCSM4 and MIROC5) at Tuyen Quang station.....	84
Figure 3.6 Observed and WEHY-simulated annual flow data during water year 1980 to water year 2005 (before and after precipitation bias-correction of downscaled atmospheric data from CCSM4 and MIROC5) at Tuyen Quang station.....	85

Figure 3.7 Observed and WEHY-simulated 5-year moving average annual flow data during water year 1980 to water year 2005 (before and after precipitation bias-correction of downscaled atmospheric data from CCSM4 and MIROC5) at Tuyen Quang station.....	85
Figure 3.8 Time series data of Standardized flow data under observation and simulation conditions.....	87
Figure 3.9 Monthly climatology of mean flow data at Tuyen Quang in three periods.....	88
Figure 3.10 Monthly climatology of standard deviation flow data at Tuyen Quang in three periods.....	89
Figure 3.11 Observed and bias-corrected simulation flow data at Tuyen Quang (2007-2015).....	89
Figure 3.12 Bias-corrected simulation flow data at Tuyen Quang (2007-2015) and lower and upper band of monthly observed (corresponding to 5 and 95 % confidence band).....	90
Figure 3.13 Bias-corrected simulation flow data at Tuyen Quang (2016-2019) and lower and upper band of monthly observed (corresponding to 5 and 95 % confidence band).....	90
Figure 4.1 Structure and components of WEHY-WRF (Watershed Environmental Hydrology Hydro-Climate Model) (Kavvas et al. 2013).....	99
Figure 4.2 Historical and future GCM (MIROC5 and CCSM4)-based WRF projection of ensemble average annual precipitation for the LRW.....	100
Figure 4.3 Future mean monthly precipitation in the early 21st century, mid-21st century and end of the 21st century and historical mean monthly precipitation during WY 1990 - WY1999 over the LRW.....	101
Figure 4.4 Comparison of the spatial change of precipitation against control run (10 years mean annual precipitation).....	102

Figure 4.5 Historical and future GCM (MIROC5 and CCSM4)-based WRF projection of ensemble average annual air temperature for the LRW.....	103
Figure 4.6 Comparison of historical and future GCM (MIROC5 and CCSM4)-based WRF projection of ensemble average annual solar radiation for Lo River watershed.....	104
Figure 4.7 Comparison of historical and future GCM (MIROC5 and CCSM4)-based WEHY projection of ensemble average annual flow for Lo River watershed.....	105
Figure 4.8 Comparison of the future mean monthly flow at early 21st century, at mid-21st century and at the end of the 21st century against the historical mean monthly flow during wy1990-wy1999 over the LRW.....	106
Figure 5.1 Total cereal production – Vietnam (Reproduced from the Food and Agriculture Organisation of the United Nations, 2021).....	111
Figure 5.2 Water Demand Forecasts.....	117
Figure 5.3 Comparison of forecasts - total water demand.....	118
Figure 5.4 Comparison of forecasts - urban and industrial demand.....	118
Figure 6.1 Water supply calculation (MONRE, 2019).....	124
Figure 6.2 Characteristics of a reservoir: relationship between water level and storage capacity (Trinh et al., 2017).....	126
Figure 6.3 Exceedance probability of flow data at Vu Quang station.....	126
Figure 6.4 Estimation of water supply for the LRW.....	127
Figure 6.5 The concept and definition of water surplus and deficit duration and volume (Trinh et al., 2017).....	128
Figure 6.6 Comparison between future average water supply and water demand.....	130

Figure 6.7 Comparison of the monthly climatology of historical and the future water surplus and deficit based on current water demand .....	130
Figure 6.8 Comparison of the monthly climatology of historical and future water surplus and deficit for the LRW based on different water demand scenarios.....	131
Figure 6.9 Comparison of the total historical and the future water deficit during the dry season.....	132
Figure 6.10 Comparison of the total historical and the future water surplus during the wet season.....	132
Figure 6.11 Relationship between drought duration and severity based on the current demand.....	134
Figure 6.12 Relationship between drought duration and severity based on 2025 water demand.....	134
Figure 6.13 Relationship of drought duration and severity based on 2050 demand.....	135
Figure 6.14 Evolution of the drought intensity as function of return period during historical and future conditions.....	136

## LIST OF TABLES

Table 2.1 WRF model configuration .....	47
Table 2.2 Statistics for comparison of the daily mean discharge at Vu Quang Station....	58
Table 3.1 Mean, standard deviation, and correlation coefficient of LRW average monthly precipitation observations and WRF-simulations with CCSM4 and MIROC5 inputs .....	82
Table 3.2 Mean monthly flow data at Tuyen Quang in each of the three periods.....	88
Table 3.3 Standard deviation of monthly flow data at Tuyen Quang in each of the three periods.....	88
Table 5.1 Irrigation water use generating exports (Vietnam General Statistics Office, 2021) .....	112
Table 5.2 Assumed improvement in agricultural water use efficiency .....	113
Table 5.3 Tourist water demand forecasting assumptions (Vietnam General Statistics Office, 2021).....	113
Table 5.4 Economic growth scenarios (Vietnam General Statistics Office, 2021) .....	114
Table 5.5 Assumed GDP elasticity of industrial demand – all scenarios .....	114
Table 5.6 Population forecasts (World Population Review, 2021) .....	114
Table 5.7 Assumed urban service area coverage (World Bank, 2019).....	115
Table 5.8 Assumed urban per capita demands (L/person/day).....	115
Table 5.9 Estimated water demand for LRW in 2019 (unit: $10^9$ m <sup>3</sup> ).....	119
Table 5.10 Estimated water demand for LRW in 2025 (unit: $10^9$ m <sup>3</sup> ).....	119
Table 5.11 Estimated water demand for LRW in 2030 (unit: $10^9$ m <sup>3</sup> ).....	119
Table 5.12 Estimated water demand for LRW in 2050 (unit: $10^9$ m <sup>3</sup> ).....	119

## Abbreviations

LRW:	Lo River Watershed
ECMWF:	European Centre for Medium-Range Weather Forecasts
WRF:	Weather Research and Forecasting
GCMs:	Global Climate Models
WEHY:	Watershed Environmental Hydrology
GIS:	Geographic Information system
IPCC:	Intergovernmental Panel on Climate Change
ERA-20C:	ECMWF's first atmospheric reanalysis of the 20th century
RCP:	Representative Concentration Pathways
WPS:	WRF Preprocessing System
MONRE:	Ministry of Natural Resources and Environment
MARD:	Ministry of Agriculture and Rural Development
FAO:	Food and Agriculture Organisation of the United Nations

## **CHAPTER 1. INTRODUCTION**

### **1.1 Introduction**

Water is critical to life on Earth than water. Yet, in the face of rapid population growth, strong socio-economic development, and increasing quality of life standards, freshwater resources are facing a critical shortages and lack sustainable integrated management. In many regions of the world, water demand currently exceeds supply, and this imbalance is predicted to worsen in the near future. Water is required for agricultural, industrial, household, recreational and environmental uses (Vairavamoorthy et al., 2008). The world's population is growing at the rate of 80 million people each year (Chakkaravarthy & Balakrishnan, 2019). Recently, according to the WWF (World Wildlife Fund), 1.1 billion people in the world lack access to clean water, and 2.7 billion people have to face water scarcity for at least one month each year.

Economic development is also one of the greatest pressures on water balance. Fast economic development leads to increased natural resource consumption and requires stable water resources while simultaneously generating considerable volumes of polluted wastewater which affects the quality of water sources (Development Bank, 2009). Under continued development, and without appropriate measures to manage water resources, water scarcity will become increasingly severe.

Water resources have long been recognized as a key resource for the development of Vietnam. Historically, the Vietnamese government has undertaken considerable work to develop water infrastructure for settlements; enhance food security; and protect communities from flooding, drought, and other natural disasters. However, during this development period, the crucial role of water in the nation's sustainable development and the protection of human health and life has not been fully appreciated. Further, the recognition of water as an economic good

has not been properly recognized. As a result, insufficient attention has been paid to water resources management and protection. Recently, numerous examples of serious degradation in both the water quality and quantity have occurred. In particular, the historical droughts of 2016 and 2019 caused losses of billions of U.S. dollars for the economy of Vietnam (William et al. 2019).

Vietnam has 3,450 rivers and streams, each with a length of 10 km or more spread across 16 major river basins. Their total annual average flow is about 830-840 billion cubic meters. The country has more than 7,160 irrigation reservoirs, with an estimated total capacity of about 70 billion cubic meters. Underground water sources have a reserve of about 189.3 million cubic meters per day and the potential to be exploited, on average, for about 61.2 million cubic meters per day and night. The average annual rainfall of Vietnam is about 1,940-1,960 mm (equivalent to 640 billion cubic meters per year), ranking Vietnam among the countries with the highest rainfall in the world. However, due to the lack of both physical infrastructure for water storage and financial capacity to build storage, there is low utilization of the rainfall supply. This lack of utilization is coupled with an unevenly temporal and spatial distribution of rainfall, resulting in water shortages throughout the country. Although Vietnam has improved its water supply situation in the past few decades, many rural parts of the country, which are often the poorest communities, have not seen significant improvement (World Bank. 2019).

The goal of this study is to obtain the water balance of a Vietnamese basin by means of comparison between future water supply and water demand. Based on the estimation of water balance, it is possible to assess climate change effects, water resource conditions, and develop strategic adaptations with the purpose of reducing risk to human society in an economically and environmentally sustainable manner.

Long-term, high-resolution spatial and temporal atmospheric and hydrologic data are being increasingly recommended for regional water balance assessment (Ohara *et al.* 2011; Trinh *et al.* 2016; He & Gautam 2016; Jang *et al.* 2017). Herein, estimates of future water supply are based on future atmospheric, hydrologic conditions. Water supply estimates are initiated by obtaining Global Climate model (GCM) data that provide climatic variables at coarse resolution (100-500 km). These global atmospheric reanalysis data are too coarse for direct use in local impact studies. Therefore, they must be downscaled to the scale of the studied watershed with a finer spatial and temporal resolution. A regional climate model (RCM) was applied to the watershed in order to obtain atmospheric conditions in finer resolution. The RCM was implemented based on the physical boundaries of the study region and GCM data. The RCM was configured based on existing ground observation data in Vietnam. The global climate data used to configure the RCM were taken from the European Centre for Medium-Range Weather Forecasts (ECMWF) – Atmospheric Reanalysis coarse climate data of the 20th century (ERA-20C), known as “Reanalysis data”. The ERA-20C was selected because it provides three-dimensional data at 3-hour time increments for the required atmospheric and surface variables throughout the 20th century (Poli *et al.* 2013, 2015, 2016). In addition, this dataset is long enough, stable, and continuous, and can uniformly cover the globe at a spatial resolution of 1.25° (~165 km) at the equator and consistently capture dry and wet events.

Two Global Climate Models, CCSM4 and MIROC5, were used to simulate future climate. These two scenarios are recommended by the Ministry of Natural Resources and Environment in Vietnam (MONRE, 2016). Similar to ERA20C, these two, CCSM4 and MIRC05 GCMs, are only available at coarse resolution of 1.25° and 1.41° respectively. Due to the coarse scale of the ERA-20C, CCSM4, and MIROC5 datasets, they were dynamically

downscaled to a fine spatial resolution over the studied watershed (<10 km) by means of the Weather Research and Forecasting (WRF, Skamarock *et al.* 2005) model. The configured-downscaled atmospheric data were then used to simulate hydrologic conditions through application of the Watershed Environmental Hydrology (WEHY) model, producing future water supply estimates. The future water supply was compared to water demand in order to identify water balance trends and characteristics in space and time through statistical analyses. Such information is meaningful for strategic planning and climate change adaptation in water resources management. One important note is that while GCMs might be considered the best tool for estimation of future climatic conditions, they introduce uncertainty due to their coarse resolutions in space. One recommended technique in handling uncertainty is bias correction to quantify the differences between historical simulated data and observed data. Two bias-correction processes are applied: precipitation bias-correction which quantifies the differences between the WRF simulation and observation data, and streamflow bias-correction which quantifies differences between the WEHY-hydrologic module and observed flow data.

In summary, this study is conducted as follows:

1. Historical and future global climate data are obtained, including ERA-20C, CCSM4 and MIROC5.
2. WRF is applied to dynamically downscaled global climate data, and the model is calibrated and validated.
3. Bias corrections for both precipitation and stream flow are implemented.
4. Water supply of the watershed is reconstructed and projected.
5. Future water demand for the selected watershed is estimated.

6. Future water balance analysis and drought analysis are conducted to identify the characteristics of potential drought conditions in the watershed over the 21st century.

7. Conclusions and recommendations to adapt to future drought of the region are provided.

## **1.2 Study Area**

The LRW is located in Northern Vietnam (downstream section) and Southwest China (upstream section) with a catchment area of 39,000 km<sup>2</sup> (Figure 1.1). The Lo River is considered one of the major international rivers in Vietnam. The upstream section of the LRW is located in China with 52% of the watershed's total area, while the downstream section is located in Vietnam with 48% of the area. While the basin has an important political and military strategic position, it is also considered a key economic and agricultural region of Vietnam. However, because there is no data sharing mechanism or agreement between the two countries and the monitoring network is inadequate, the investigation and assessment of surface water resources in the Lo River basin are limited. Due to increasing climate change impacts, escalating exploitation of water resources by the upstream country, and rising water demand for socio-economic development activities, the LRW has faced serious water-related issues such as flash-floods, severe droughts, and water scarcity. Thus, conducting more research on water resources is crucial for the region.

The Lo River, one of the two main tributaries of the Red River, originates in the high mountains (above 2000 m) of the southwest of Vinh Son town in the Yanshan district, Chau Van Son area in China's Yunnan province. The upstream section, Ban Long Giang, flows from northwest to southeast through Van Son city, Son Sa town, Nam On Ha, and into Vietnam's territory at Thanh Thuy, Vi Xuyen district. It continues to flow through Ha Giang, Vinh Tuy,

Ham Yen, Tuyen Quang town, and finally into the Red River at Bach Hac, Viet Tri city. There is no upstream reservoir in China.



Figure 1.1 Geographic location of Lo River Watershed in Vietnam

The rainy season, commonly defined as being from May to October, represents 85–90% of the total annual rainfall. The dry season prevails from November to April, representing only 10–15% of the total annual rainfall. Thus, drought and lack of surface water in the dry season can be severe, especially on the leeward highlands deeper in the continent, such as Dong Van and Hoang Su Phi.

Average evaporation in the region ranges from 480 to 960 mm/year, depending on location, topography, temperature characteristics, and number of sunshine hours. Areas with small evaporation rates are Muong Khuong (485 mm/year), Bac Ha (568 mm/year) and Ham Yen (558 mm/year). Areas with higher evaporation volume are Vinh Yen (955 mm/year), Hoang Su Phi (926 mm/year), and Viet Tri (912 mm/year).

The majority of terrain is mountainous and strongly divided, creating a well-developed network of rivers and streams with a river network density of about 0.60-0.70 km/km<sup>2</sup>. Within its Vietnam territory, the LRW has roughly 230 rivers and streams of more than 10 km in length. The topography of the watershed slopes from northwest to southeast. Mountainous terrain over the east and north dominates the upper catchment area and tends to decrease in a northwest–southeast direction with elevation that ranges from 44 - 2,900 m (Figure 1.2). Land use and land cover are diverse from upstream to downstream. The area is mostly covered by crops and forests, and industrial crops dominate (58%) in the watershed. Together with topography, wind speed also heavily affects the distribution of rainfall in the watershed.

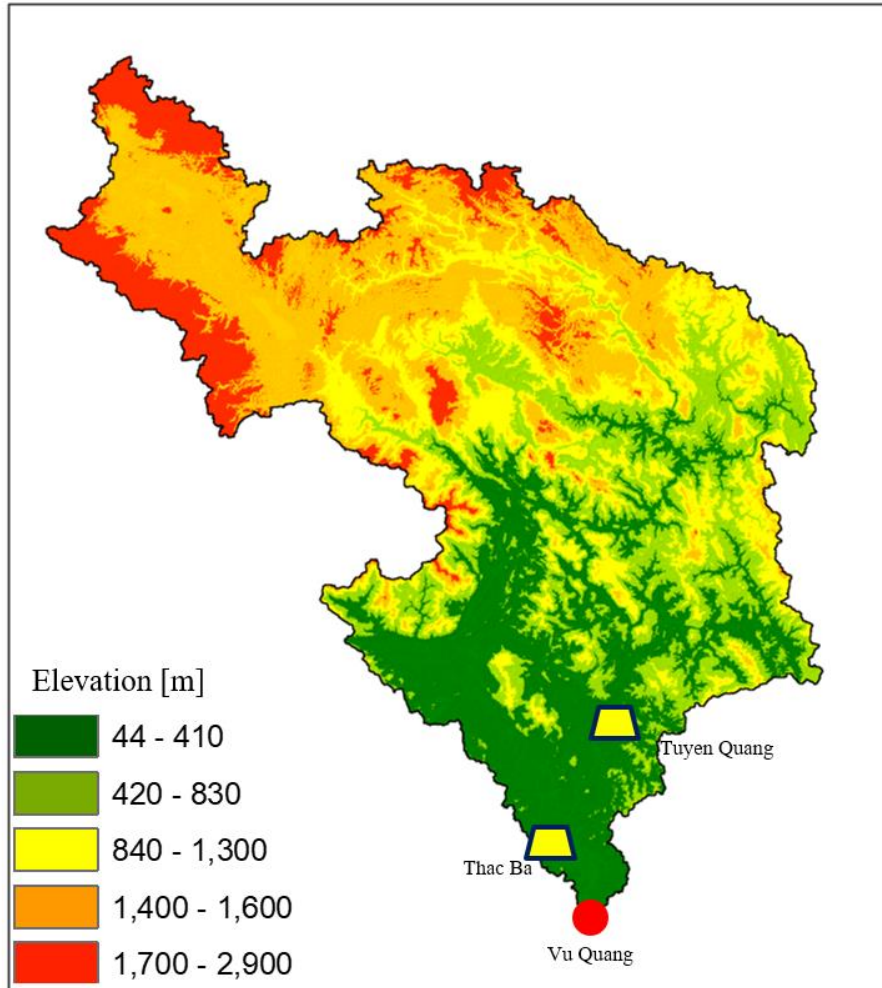


Figure 1.2 Topographic variation in Lo River Watershed

The LRW is a key economic and agricultural region in Vietnam. The main economies of the region are industry, services, agriculture, forestry and fisheries. Water resources in the Lo River basin are affected in terms of water quality and water quantity by the actions of the upstream country. Conflicts in water use among sectors, between upstream and downstream areas, and between localities are consistently increasing. In the dry season, serious deficits in water supply exist for industry, agriculture, mining and mineral processing, and hydroelectricity

and navigation. While in the rainy season, floods, flash floods, and mud floods often occur in areas with high rainfall due to the lack of forest cover and steep slopes.

There are two main reservoirs impacted downstream at the LRW. They are Thac Ba and Tuyen Quang hydropower reservoirs (Figure 1.2). Thac Ba is a major reservoir in Yen Bai Province Vietnam, created by construction of the Thac Ba hydroelectric plant in the 1960s. The maximum capacity of Thac Ba reservoir is 4 billion cubic meters. The Tuyen Quang (Na Hang) reservoir is located in Tuyen Quang province. Its construction started in 2002 and completed in 2008. Its maximum capacity is 2 billion cubic meters. Both reservoirs serve as flood prevention and provide water supply for their respective downstream regions as well as for the Red River Delta.

As Vietnam aspires to become a modern, industrialized economy by 2035, the water resources in the country, including the Lo River region, have been placed under unrelenting pressure. There is an emerging gap between water supply and demand, both in certain locations and seasons, that will intensify in coming years, especially under a changing climate. Research into the current and future status of water resources within the country is essential. In particular, a better understanding of drought conditions in the region will help to provide solutions, recommendations, and better preparation for adapting and mitigating negative impacts from climate change conditions over the 21st century. The supply and demand gap and climate change are expected to not only have a significant effect on natural systems, but also on social systems and economies of this region.

### **1.3 Overview of Study Goals**

Under the theme of coordinated water supply and water demand during the 21<sup>st</sup> century over the Lo River watershed, this research has five independent but related pieces:

**Chapter 1.** Introduction of the study area, overview of research objectives and methodologies.

**Chapter 2.** Implementation, calibration and validation processes for atmospheric and hydrologic models over the target watershed. First, the WRF model was implemented to downscale the ERA-20C reanalysis data based on the physical boundaries of the study region. The model was configured based on existing ground observation data in Vietnam. After successfully configuring and evaluating the WRF model, the downscaled atmospheric data were input into the watershed model-WEHY for estimation of hydrologic conditions over the LRW. It is noted that there are three main processes in configuring and evaluating WEHY-WRF models including: (1) setting up the models with boundary conditions; (2) preparing model inputs; and (3) conducting model calibration and validation to check model plausibility.

**Chapter 3.** This chapter presents a novel methodology of bias correction by using two different bias-correction applications: (1) precipitation bias-correction in which a bias-correction method to quantify differences between WRF simulation and observation data is applied; (2) streamflow bias-correction in which differences between WEHY-hydrologic module and observed flow data are quantified. The precipitation and streamflow bias-correction were applied over the control-run (historical) period. After implementation of the bias correction methods, the model was validated through comparison of the bias-corrected data against available corresponding observations during recent years.

**Chapter 4.** This chapter presents the projection of water supply from the LRW over the 21<sup>st</sup> century. By applying the bias-correction procedure for the future period, the WEHY-WRF model provides future atmospheric and hydrologic conditions over the LRW. The two global climate simulations, CCMS4-RCP 4.5 and MIROC5-RCP 8.5, are downscaled during both the

historical and future periods. These future climate scenarios are recommended for the region by the Vietnam Ministry of Natural Resources and Environment (MONRE). Future fine-scale atmospheric and hydrologic data were analyzed with the purpose of identifying historical trends and characteristics in space and time, by means of statistical analyses. The simulated outflow from Vu Quang station (outlet point at LRW), considered as a water supply, is compared to the corresponding water demand (estimated in chapter 5).

**Chapter 5.** This chapter presents the water demand estimation for the Lo River basin. Several mathematical methods are used for estimating future demand, including extrapolating historical trends, correlating demand with socio-economic variables, and calculating development plans for each sector. Data sources include; the national development plan of water-using sectors, such as agriculture and industry; local development plans of provinces within the watershed; statistical books and reports from MONRE.

**Chapter 6.** In this chapter, water balance analyses of historical and future water supply and water demand are conducted to determine water deficits that may lead to future droughts. Drought characteristics analyzed include drought duration, severity, and drought inter-arrival time using multiple indexes. Drought assessments play an essential role in addressing risk that can mitigate the effect of droughts in the study region of the LRW.

**Chapter 7.** This chapter summarizes the research results of the above chapters and presents conclusions and recommendations to mitigate negative impacts of future droughts and other water related risks. Suggestions for possible future research on the extension of this study are also included.

## References

- Bozorg-Haddad, O., Bahrami, M., Kazemi, M., Abdi, B., Yari, P., Chu, X., & Loáiciga, H. A. (2019). Water Security and Sustainability: Global Threats and Conflicts. *Encyclopedia of Water*, 1–6. <https://doi.org/10.1002/9781119300762.wsts0090>
- Chakkaravarthy, D. N., & Balakrishnan, T. (2019). Water Scarcity-Challenging the Future. *International Journal of Agriculture, Environment and Biotechnology Citation: IJAEB*, 12(3), 187–193. <https://doi.org/10.30954/0974-1712.08.2019.2>
- Development Bank, A. (2009). Water: Vital for Vietnam's Future.
- NAWAPI. (n.d.). *Cần thiết phải điều tra, đánh giá tài nguyên nước lưu vực sông Lô – Gâm*. Retrieved November 16, 2021, from [http://nawapi.gov.vn/index.php?option=com\\_content&view=article&id=4165%3Acn-thit-phi-iu-tra-anh-gia-tai-nguyen-nc-lu-vc-song-lo-gam&catid=70%3Anhim-v-chuyen-mon-ang-thc-hin&Itemid=135&lang=vi](http://nawapi.gov.vn/index.php?option=com_content&view=article&id=4165%3Acn-thit-phi-iu-tra-anh-gia-tai-nguyen-nc-lu-vc-song-lo-gam&catid=70%3Anhim-v-chuyen-mon-ang-thc-hin&Itemid=135&lang=vi)
- Nguyen, D. H. (2010). *An ninh nguồn nước là vấn đề hàng đầu của an ninh Môi trường trên toàn cầu - Cục Quản lý tài nguyên nước*. <http://dwrn.gov.vn/index.php/vi/news/Nhin-ra-The-gioi/An-ninh-nguon-nuoc-la-van-de-hang-dau-cua-an-ninh-Moi-truong-tren-toan-cau-1243/>
- Ribbe, L., & Haarstrick, A. (2021). Towards Water Secure Societies. In *Towards Water Secure Societies*. <https://doi.org/10.1007/978-3-030-50653-7>
- Vairavamoorthy, K., Gorantiwar, S. D., & Pathirana, A. (2008). *Managing urban water supplies in developing countries-Climate change and water scarcity scenarios*. <https://doi.org/10.1016/j.pce.2008.02.008>

- VNMHA. (n.d.). *Những thách thức về an ninh nguồn nước ở Việt Nam*. Retrieved November 19, 2021, from <http://vmha.gov.vn/tin-tuc-tai-nguyen-nuoc-va-moi-truong-114/nhung-thach-thuc-ve-an-ninh-nguon-nuoc-o-viet-nam-9854.html>
- Vörösmarty, C. J., McIntyre, P. B., Gessner, M. O., Dudgeon, D., Prusevich, A., Green, P., Glidden, S., Bunn, S. E., Sullivan, C. A., Liermann, C. R., & Davies, P. M. (2010). Global threats to human water security and river biodiversity. *Nature*, *467*(7315), 555–561. <https://doi.org/10.1038/nature09440>
- Ministry of Natural Resources and Environment (MONRE), Climate Change and Sea Level rise scenarios for Vietnam, summary for policymakers. (2016)
- He, M. and Gautam, M., 2016. Variability and trends in precipitation, temperature and drought indices in the State of California. *Hydrology*, *3*(2), p.14.
- Trinh, T., Ishida, K., Fischer, I., Jang, S., Darama, Y., Nosacka, J., Brown, K. and Kavvas, M.L., 2016. New methodology to develop future flood frequency under changing climate by means of physically based numerical atmospheric-hydrologic modeling. *Journal of Hydrologic Engineering*, *21*(4), p.04016001.
- Jang, S., Kavvas, M.L., Ishida, K., Trinh, T., Ohara, N., Kure, S., Chen, Z.Q., Anderson, M.L., Matanga, G. and Carr, K.J., 2017. A performance evaluation of dynamical downscaling of precipitation over northern California. *Sustainability*, *9*(8), p.1457.
- Ohara, N., Chen, Z.Q., Kavvas, M.L., Fukami, K. and Inomata, H., 2011. Reconstruction of historical atmospheric data by a hydroclimate model for the Mekong River basin. *Journal of Hydrologic Engineering*, *16*(12), pp.1030-1039.
- Poli, P., Hersbach, H., Tan, D., Dee, D., Thepaut, J.N., Simmons, A., Peubey, C., Laloyaux, P., Komori, T., Berrisford, P. and Dragani, R., 2013. *The data assimilation system and initial*

*performance evaluation of the ECMWF pilot reanalysis of the 20th-century assimilating surface observations only (ERA-20C)*. European Centre for Medium Range Weather Forecasts.

Poli P. Hersbach H. Dee D. Berrisford P. Simmons A. Laloyaux P . 2015 ERA-20C Deterministic. ECMWF ERA Rep. 20, pp. 48. Available from [www.ecmwf.int/en/elibrary/11700-era-20c-deterministic](http://www.ecmwf.int/en/elibrary/11700-era-20c-deterministic).

Skamarock, W.C., Klemp, J.B., Dudhia, J., Gill, D.O., Barker, D.M., Wang, W. and Powers, J.G., 2005. *A description of the advanced research WRF version 2*. National Center For Atmospheric Research Boulder Co Mesoscale and Microscale Meteorology Div.

William R. Sutton, Jitendra P. Srivastava, Mark Rosegrant, James Thurlow, and Leocardio Sebastian. 2019. *Striking a Balance: Managing El Niño and La Niña in Vietnam's Agriculture*. RepNo 132068. World Bank, Washington, DC. License: Creative Commons Attribution CC BY 3.0 IGO

World Bank. 2019 "Vietnam: Toward a Safe, Clean, and Resilient Water System". World Bank Washington, DC.

## **CHAPTER 2. RECONSTRUCTING HISTORICAL HYDROCLIMATE DATA FOR LO RIVER WATERSHED REGION**

### **Abstract**

This chapter introduces a reliable tool from atmospheric-hydrologic-reservoir models to reconstruct and project water supply based on future coarse atmospheric data.

High spatial and temporal resolution atmospheric-hydrologic data were reconstructed by means of the Weather Research and Forecasting Model-WRF and the Watershed Environmental Hydrology-WEHY models, with inputs from the global atmospheric reanalysis dataset of the 20th century (ERA-20C) over the LRW watershed. The WRF model was implemented over the study region based on ERA-20C reanalysis data and was configured based on existing ground observation data in Vietnam's territories and global Aphrodite precipitation data. The WEHY model was evaluated based on comparisons with observation data at the outlet station.

Model results analysis suggested no significant trend in the annual accumulated precipitation depth, while there were upward trends in annual temperature. These results can later be used for the projection of LRW future water supply utilizing atmospheric inputs from global climate models' future climate projections.

### **2.1 Introduction**

Reliable atmospheric and hydrologic data, such as precipitation, air temperature, humidity, wind, air pressure, solar radiation, and net radiation are crucial for water balance studies. However, in many cases, it is hard to obtain dependable data with adequate spatial resolution, temporal resolution, spatial coverage, observation period, data quality, or completeness, due to political, historical, and financial reasons. Field observation data are affected by various factors such as noise of sensors, management of equipment, local effect of

the land cover and topography, and quality control policy (Ohara et al 2011, Trinh et al, 2016). This chapter focuses on reconstruction of historical hydro-climate data over the LRW as a part of the study to estimate water balance in the LRW during the 21<sup>st</sup> century. Further, study efforts to provide a reliable hydro-climate model WEHY-WRF that can be used to project reliable water supply based on the future coarse atmospheric data from the GCMs is introduced.

Previously, there have been attempts to reconstruct and project hydro-climate data over the target region. Hydro-climate information may be reconstructed from global atmospheric reanalysis data (Krishnamurti *et al.* 1997; Compo *et al.* 2006; Brower *et al.* 2013; Fuka *et al.* 2014). However, these global atmospheric reanalysis data are too coarse, preventing them from direct application in local impact studies. Research efforts have therefore focused on downscaling these coarse data to the scale of a studied watershed. Some studies apply statistical approaches (statistical or stochastic downscaling) to reconstruct historical data, relying heavily on gauge observations. Therefore, these statistical approaches are not applicable in ungauged or sparsely gauged watersheds (Anderson *et al.* 2007; Jang & Kavvas 2013). In addition, stochastic methods assume stationarity in the hydroclimatic regime, and do not account for the ongoing change in the world's hydro-climate conditions (Milly *et al.* 2008; Trinh *et al.* 2016). Consequently, these statistical downscaling approaches have not been effective for investigating atmospheric conditions in limited data conditions and under changing atmospheric conditions, especially on the climate scale. The alternative method, dynamical downscaling (DD), uses conservation equations of mass, momentum, and energy in the form of a regional climate model (RCM) to spatially and temporally refine future atmospheric conditions. This approach is known as a suitable technology for areas with complex topography, and for estimating atmospheric data under limited data or no-data conditions (Kavvas *et al.* 2013; Jang *et al.* 2017). Furthermore, the

DD technique can couple with land surface and hydrologic models to further simulate hydrologic conditions over a specific watershed.

In this context, this study applies the DD technique with input provided from the ECMWF – ERA-20C to reconstruct atmospheric data including precipitation, temperature, and wind speed at fine spatial and time resolutions. ERA-20C was selected because it provides three-dimensional data at 3-hour time increments for the required atmospheric and surface variables throughout the 20th century (Poli *et al.* 2013, 2015, 2016). In addition, this dataset has sufficient duration, is stable and continuous, and can uniformly cover the globe at a spatial resolution of  $1.25^\circ$  ( $\sim 165$  km) at the equator, and consistently capture dry and wet events. Due to its coarse scale atmospheric data, ERA-20C was first dynamically downscaled to a fine spatial resolution over the studied watershed ( $< 10$  km) by means of the Weather Research and Forecasting (WRF) model. The downscaled atmospheric data were then input to the WEHY model for simulation of hydrologic and reservoir operation in the LRW.

In summary, this chapter applies the following steps: 1) Obtain the global reanalysis data ERA20C; 2) implement and configure the selected regional climate model, WRF; 3) implement and configure the selected hydrology model, WEHY, in consideration of two main reservoirs in the LRW; 4) Reconstruct water supply data including atmospheric, evapotranspiration, streamflow data over LRW. After successfully configuring and reconstructing the hydro-climate data over LRW, the reconstructed data can be analyzed to identify historical trends and characteristics in space and time, by means of statistical analyses.

## 2.2 Methodology

The LRW is a transboundary region between China and Vietnam. Because there is no formal data sharing agreement between the two countries, assessing the atmospheric hydrologic conditions over the watershed, especially areas outside of Vietnam, is a great challenge. In order to achieve a more comprehensive understanding of the historical drought condition over the watershed, the historical water supply was reconstructed.

Water supply reconstruction starts with obtaining and downscaling the global reanalysis ERA-20C data by means of WRF. Data from this reanalysis dataset are available for download directly from their associated organizations. WRF is implemented by incorporating the physical boundaries of the study region and configured using ground observation data in Vietnam. Utilized were the Aphrodite precipitation data version of APHRO\_V1101 datasets for monsoon Asia (APHRODITE) (Yatagai et al. 2009, 2012), and the Vietnam Gridded Precipitation, VNGP. APHRODITE was developed by the Research Institute for Humanity and Nature (RIHN) and the Meteorological Research Institute of Japan Meteorological Agency (MRI/JMA), Japan ([www.chikyu.ac.jp/precip/](http://www.chikyu.ac.jp/precip/)) (Yatagai *et al.* 2012). Meanwhile, the VNGP is a daily gridded rainfall dataset, interpolated by means of the sphere map interpolation technique from 481 rain gauges. This dataset has a resolution of  $0.1^\circ$  and covers the whole of Vietnam (Nguyen et al., 2016). The VNGP values were validated by comparing them with gauge observations through correlations, mean absolute errors, root mean square errors, and spatial distribution. The validation results show that the VNGP is matched well with rainfall observations when compared to different interpolation techniques (Nguyen et al., 2016). The spatially-distributed daily rainfall data of VNGP are available from Jan 1980 to December 2010.

After configuring and evaluating the WRF model, WRF outputs can be input into the hydrologic model-WEHY over the Lo River watershed, including both upstream and downstream areas in China and Vietnam. The simulated water supply over LRW is then compared to water demand which is discussed in CHAPTER 5. Figure 2.1 presents a flow diagram of the reconstruction process. The following is an introduction of applications in this study.

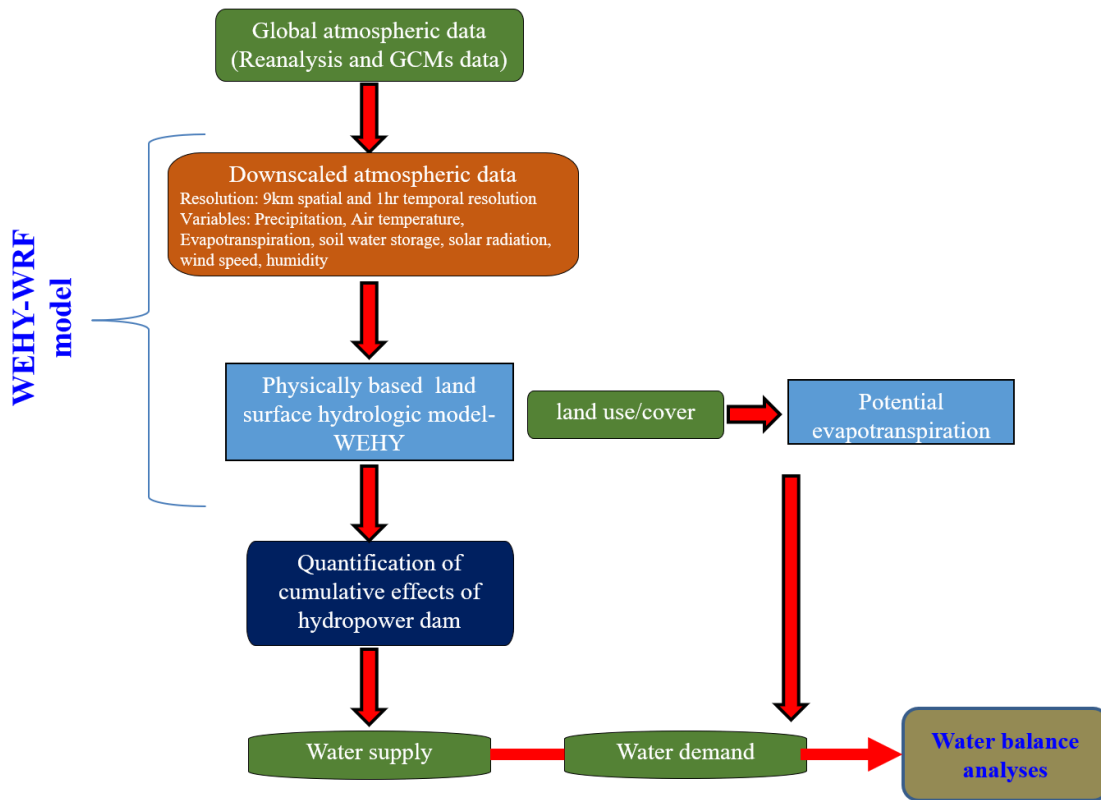


Figure 2.1 Methodology of historical data reconstruction process

### 2.2.1 Weather Research and Forecasting – WRF

The Weather Research and Forecasting (WRF) Model is a next-generation regional-scale numerical weather prediction system designed for operational forecasting and atmospheric research. The model provides researchers a tool to produce simulations on both real data, such as

from observations and on idealized atmospheric conditions (Skamarock et al, 2008). WRF is currently in operational use at the National Centers for Environmental Protection (NCEP) and other forecasting centers internationally (Predictia.es/en). With its advantages, WRF has been considered as one of the most used models with over 30,000 registered users in the world ((Jucker et al, 2020).

Generally, WRF has two main components including preprocessing-WPS and the main program WRF (Figure 2.2). The WPS program's functions are to implement the simulated domain, preparing input atmospheric data for the main program-WRF. The WRF program includes two sub-components (1) REAL-to create initial and boundary conditions; (2) WRF- to simulate atmospheric data according to the setup domain. The input of WPS data is raw atmospheric data such as reanalysis or GCMs outputs data. These global data can be Grib data or netCDF format. Thus, libraries such as grib, netCDF libraries should be used during the WPS program.

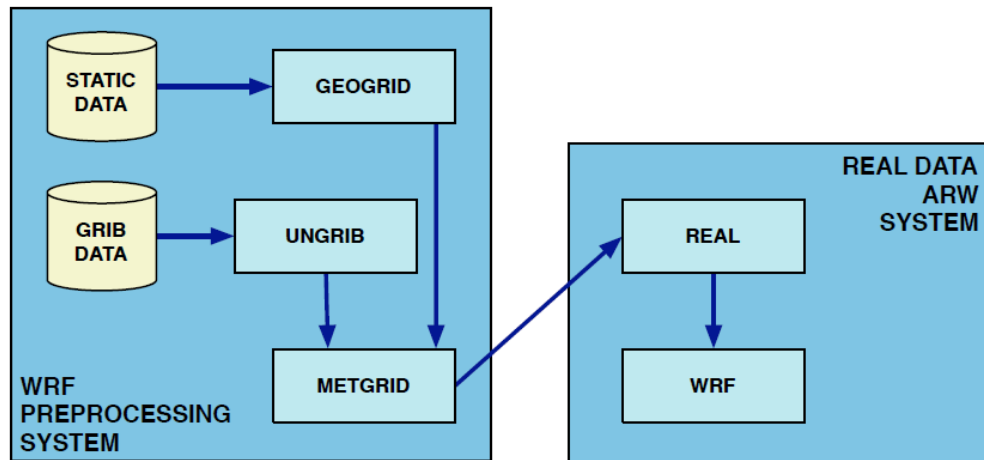


Figure 2.2 Schematic showing the data flow and program components in WRF-AWR

(Skamarock et al, 2008)

There are 16 main Features of the WRF-ARW System, written by Skamarock et al, 2008, such as equations, prognostic variables, vertical coordinate, horizontal grid, etc.

WRF Software Framework is single-source code for maintainability and highly modular. The model coupling Application Program Interface (API) enabling WRF to be coupled with other models such as land ocean models.

The ARW equations in WRF are formulated using a terrain-following hydrostatic-pressure vertical coordinate denoted by  $\eta$  and defined by Skamarock et al, 2008 as

$$\eta = (P_h - P_{ht})/\mu \text{ where } \mu = P_{hs} - P_{ht}.$$

$P_h$  is the hydrostatic component of the pressure, and  $P_{hs}$  and  $P_{ht}$  refer to values along the surface and top boundaries, respectively.  $\eta$  varies from a value of 1 at the surface to 0 at the upper boundary of the model domain (Fig. 2.3).

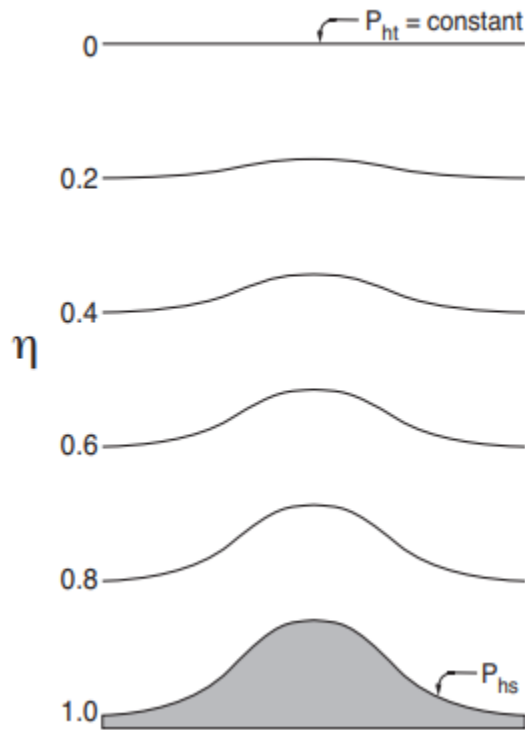


Figure 2.3 ARW  $\eta$  coordinate (Skamarock et al, 2008)

### **2.2.2 WEHY Hydrologic Model**

For its hydrologic component, the WEHY-WRF hydro-climate model utilized the WEHY model, a physically based model derived from the conservation equations of mass, momentum, and/or energy for water flows in various domains (Chen et al., 2004a; Chen et al., 2004b; Kavvas et al., 2004; Kavvas et al., 2012; Kavvas et al., 2006). The WEHY model was originally introduced as a scalable physically-based hydrologic model, able to upscale point-scale processes at grid points to the scale of the model computational unit (MCU) areas throughout the watershed domain (Chen et al., 2004a; Chen et al., 2004b; Kavvas et al., 2004). These MCUs are either individual hillslopes or first-order-subwatersheds within a watershed. MCU identification and delineation is described in Chen et al. (2004a). The WEHY model represents flow processes through two subprograms: the hillslope flow processes and the channel routing processes. The hillslope flow subprogram of the WEHY model describes unsaturated flow, subsurface stormflow, overland flow, groundwater flow, and hillslope channel flow; these flows are computed in parallel. The channel routing subprogram describes the transport of water in a stream network of the watershed. If dams are present in the target watershed, the dam operation subprogram is enabled, and works in conjunction with the channel routing subprogram. Since model parameters are related to the physical features of a watershed, the WEHY model is able to account for the effect of spatial heterogeneity in land surface and subsurface conditions on the hydrologic flow processes.

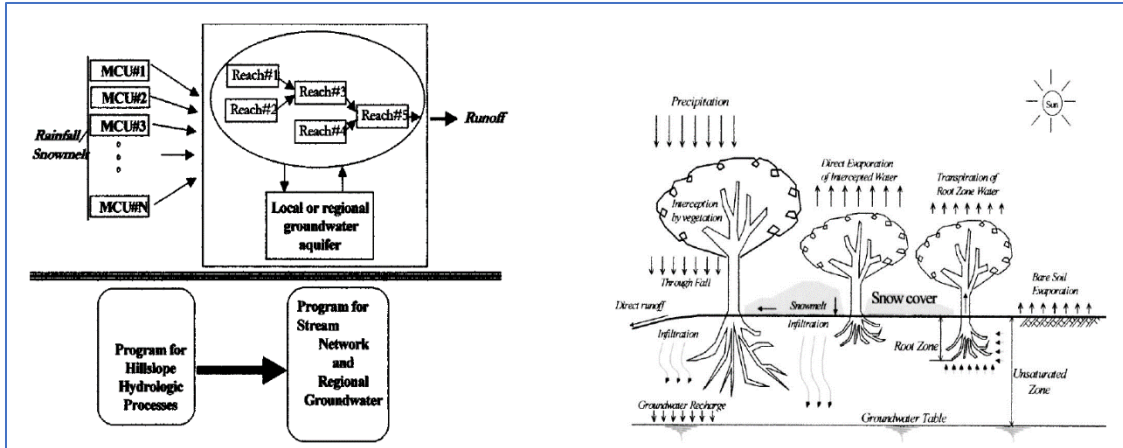


Figure 2.4 Structural description of WEHY hydrologic model and description of land surface processes within this model (Kavvas et al., 2004)

Figure 2.4 shows a structural description of the WEHY model: a description of MCU discharge into a neighboring channel network. The WEHY model has two main programs including hillslope and stream network-regional ground water programs. In the hillslope program, the WEHY model has separated the hydrologic processes into three computational components including, unsaturated flow, subsurface stormflow, and overland flow. The network-regional ground water program contains groundwater flow, and channel flow that are computed in parallel.

A conceptualized representation of the hillslope program showing surface and subsurface flow components is presented in Figure 2.5. It is noted that this watershed model is able to simulate both the Hortonian as well as variable source area flow mechanisms. Furthermore, although the subsurface soil root zone may not be saturated to the soil surface, Hortonian overland flow may still occur due to ponding of infiltration-excess rainfall/snowmelt water over the land surface.

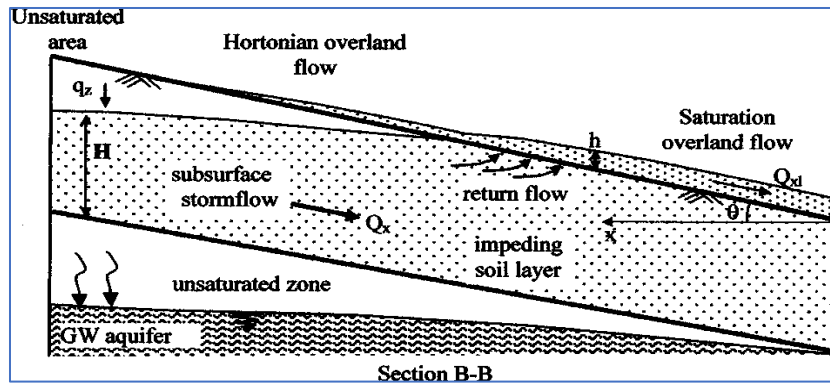


Figure 2.5 Flow processes over a longitudinal cross section of a hillslope, as conceptualized in hydrologic module (Kavvas et al., 2004)

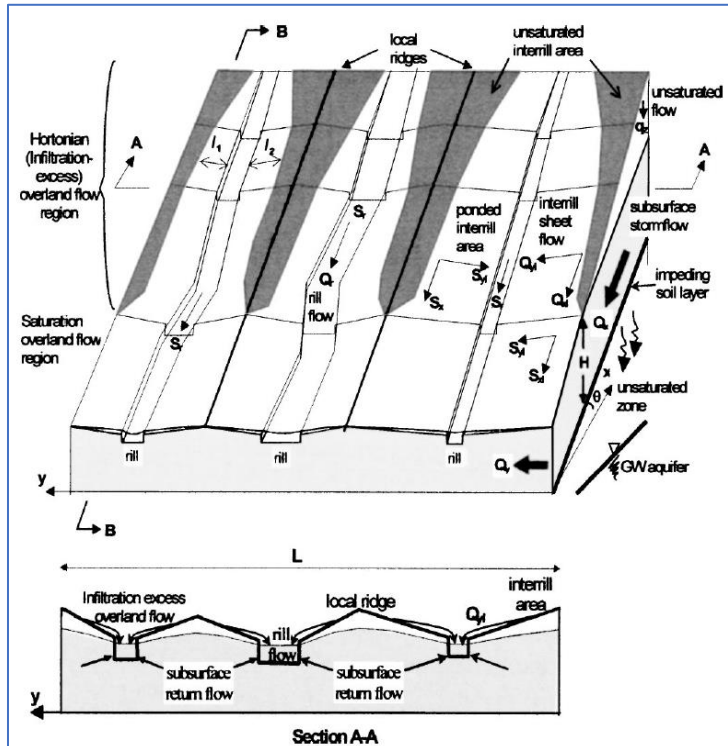


Figure 2.6 Hydrologic model's depiction of hillslope surface and subsurface flow processes (Kavvas et al., 2004)

Meanwhile, over vegetated landscape regions, water from rainfall can infiltrate vertically downward to the deeper soil layers as unsaturated flow until it reaches a hardened soil layer

underneath the plant roots. At this layer, the soil hydraulic conductivity decreases extensively to obstruct the vertical soil water flow. Thus, over this soil impeding layer, the soil water begins to pond and to saturate soil pores. When soil water attains “saturation state”, a flow referred to as the “subsurface stormflow” (Dunne 1978) shifts downslope inside a hillslope and remains replenished with the aid of vertical unsaturated flow. Subsurface stormflow is a fundamental hydrologic flow process that (1) contributes water for rill/gully flow in humid, vegetated landscapes; and (2) determines the dynamic place of saturation overland flow in variable source regions (Kavvas et al, 2004). If this unsaturated flow inside the subsurface area maintains a vertical path through the unsaturated quarter under the soil impeding layer, then it may create an underlying groundwater aquifer. In this way, a deep unconfined groundwater aquifer can be replenished. If the subsurface stormflow exceeds the transmission potential of the soil horizon, then a return flow from the subsurface to the surface will occur, forming overland flow (Kavvas et al, 2004).

The WEHY model requires two main types of data input: 1) atmospheric data (rain, temperature, wind speed, radiation, geopotential height, humidity; 2) physical surface information (topography, geomorphology, soil, land cover). Execution of the WEHY model entails four main steps: (1) processing of GIS data and hydro-meteorological data; (2) model configuration (delineation of the circulate community and model computational units (MCUs) and choice of particular hydrologic additives); (3) estimation of model parameters (model calibration); and (4) model validation (simulated vs. observation data). These steps have been applied to implement the model to the focus watershed.

The initial step of data processing entails the collection, assembly, and evaluation of GIS data and the hydro-meteorological data. Model configuration entails delineation of the stream

network and model computational units (MCUs) that become defined (Chen et al., 2004a; Chen et al., 2004b; Kavvas et al., 2004; Kavvas et al., 2012; Kavvas et al., 2006), and choice of the particular hydrologic components for the application at hand. Estimation of model parameters, or calibration, entails the assessment of the parameters of the WEHY model in large part from the compiled land information directly, without a rainfall-runoff fitting exercise (Chen et al., 2004a). For model validation, the simulated runoff from the WEHY hydrologic module is compared to observed data, especially at the outlet point of the observed region.

To confirm the validity of WEHY-HCM for the LRW, the atmospheric-hydrologic model is applied to the LRW and is calibrated and validated. Calibration is the adjustment of model parameters in order that the model simulations match observation data. Validation applies the calibrated model during a time period outside of the period used for calibration, again comparing simulated results to observation data. The historical reconstructed streamflow for LRW, simulated by the WEHY-HCM, was then input to a reservoir operation model (Hec-ResSim) to generate outflow from the reservoirs based on the present operation rules (USBR, 2004).

### **2.2.3 WEHY Reservoir model**

In the WEHY watershed model, there is an option for incorporation of reservoir operation in a watershed as a subprogram, which needs to be customized for each reservoir in the LRW (Thac Ba and Tuyen Quang reservoirs). Accurate representation of the two dams' operations is crucial to reliably estimate the flow conditions over the LRW. Using the simulated inflow and water levels, the two dams' operations were implemented and used to estimate outflow discharge. The operation rules for Thac Ba and Tuyen Quang were obtained from the Vietnam Department of water resources management (DWRM). The operation information for Thac Ba and Tuyen Quang including the relationship between water surface area, storage, and water level

are exhibited in Figure 2.8. WEHY's dam operation subprogram is based on relationship functions among surface area ( $F$ ), water elevation ( $Z$ ), and storage ( $W$ ) as shown in Figure 2.8, and the current operation rule as shown in Figure 2.9.

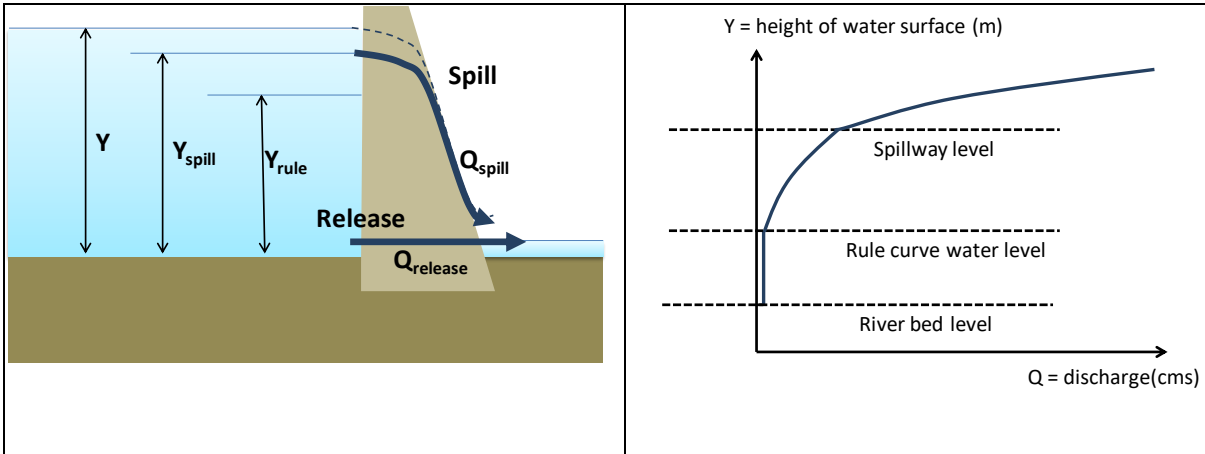


Figure 2.7 The description of WEHY reservoir operation

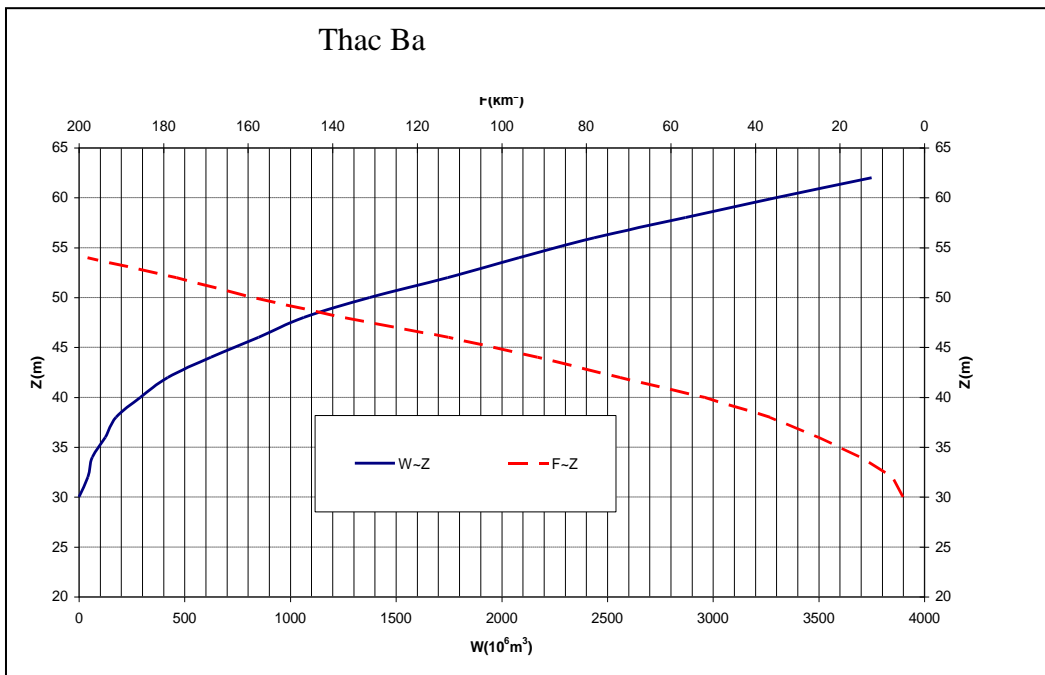
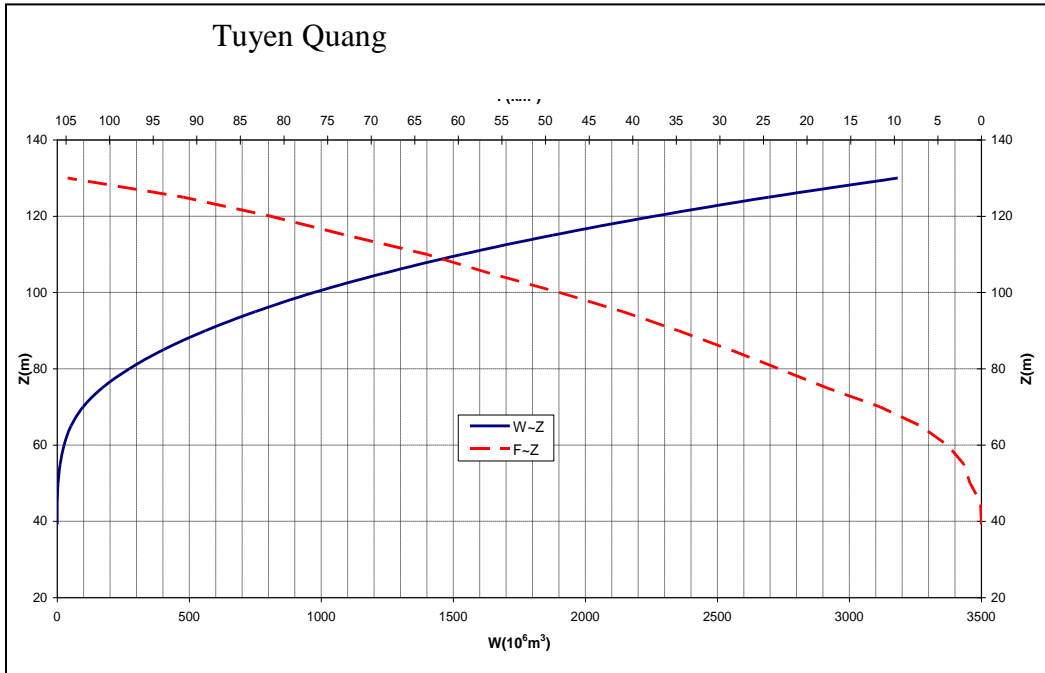


Figure 2.8 Relationship among Surface area, water elevation, and storage at Tuyen Quang and Thac Ba reservoirs

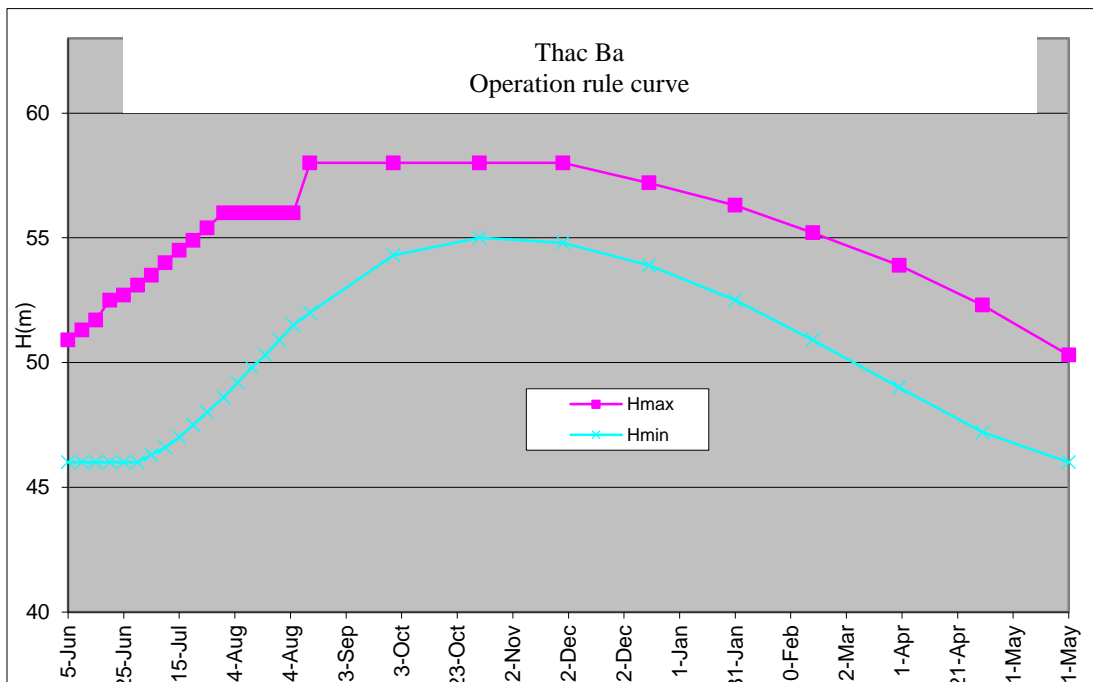
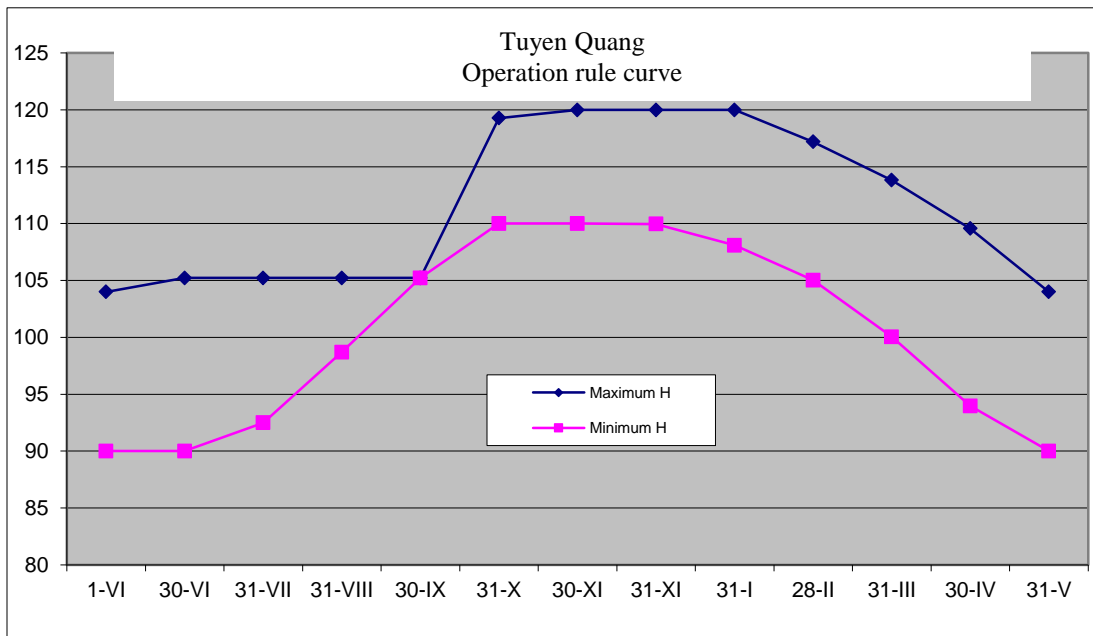


Figure 2.9 The current reservoir operation rule includes minimum and maximum reservoir water levels for Tuyen Quang and Thac Ba reservoirs

Outflow from each reservoir was calculated based on WEHY simulated inflow and the changes in monthly storage in each reservoir. The changes in monthly storage were obtained from current reservoir operation rules and the relationship among surface area, water elevation, and storage at Tuyen Quang and Thac Ba Reservoirs. The outflows were then incorporated into WEHY's channel flow component to route these outflows to the outlet point of the LRW (Vu Quang station).

## **2.3 Calibration and Validation of WEHY-WRF model for LRW**

### **2.3.1 WRF over LRW: Atmospheric Processes**

The historical reanalysis data, ERA-20C, was selected to define the initial and boundary conditions in WRF simulations, allowing derivation of finer scale variables over LRW. ERA-20C was developed in the European Centre for Medium Range Weather Forecasts with the same surface and atmospheric forcing as the final version of the atmospheric model integration ERA-20CM (Hersbach et al. 2013, 2015). The spatio-temporal evolution of ERA-20C includes 91 atmospheric vertical levels between the surface and 0.01 hPa, four soil layers of the land surface, 25 frequencies and 12 directions of ocean waves. The ERA-20C is a public dataset and is available for downloading directly from its associated organizations. For a description of the contents of ERA-20C, see Hersbach et al. (2015). Based on ERA-20C and the physical boundaries of the LRW, WRF was employed to dynamically downscale coarse scale ERA-20C atmospheric data to the scale of the studied watershed. Figure 2.10 depicts three nested domains used for the WRF simulations. The spatial resolution of each of the nested domains is one-third of that of its parent domain. The first domain (D1) has a spatial grid resolution of 81 km with  $26 \times 29$  horizontal grid points, the second (D2) is 27 km with  $48 \times 57$  horizontal grid points, the third (D3) is 9 km with  $105 \times 78$  horizontal grid points (for the entire Red River) and 9km with

42 x 33 horizontal grid points (for the entire LRW). In order to simulate atmospheric processes in each domain, parameterization options in the WRF model need to be configured for all three domains. The selected physical parameterizations are the Goddard scheme (Tao et al. 1989) for the microphysics processes option, the new Simplified Arakawa–Schubert scheme (Han & Pan 2011) for the cumulus parameterization option, the BouLac scheme (Bougeault & Lacarrere 1989) for the planetary boundary layer option, the New Goddard scheme (Chou & Suarez 1999) for both the short-wave and long-wave radiation options, and the RUC Land Surface Model (Benjamin et al. 2004) for the land surface model option (Table 2.1). The initial and boundary conditions for the climate variables over the LRW were set up by means of WRF based on ERA-20C reanalysis data at 3-hourly intervals.

Two observation datasets were used for evaluation of WRF simulations. One is ground observation data that were taken from the Vietnam Gridded Precipitation, (VNGP). The other dataset is the global high resolution (0.25°) dataset for precipitation, APHRODITE, developed by the Research Institute for Humanity and Nature (RIHN) and the Meteorological Research Institute of Japan Meteorological Agency (MRI/JMA), Japan ([www.chikyu.ac.jp/precip/](http://www.chikyu.ac.jp/precip/)) (Yatagai *et al.* 2012).

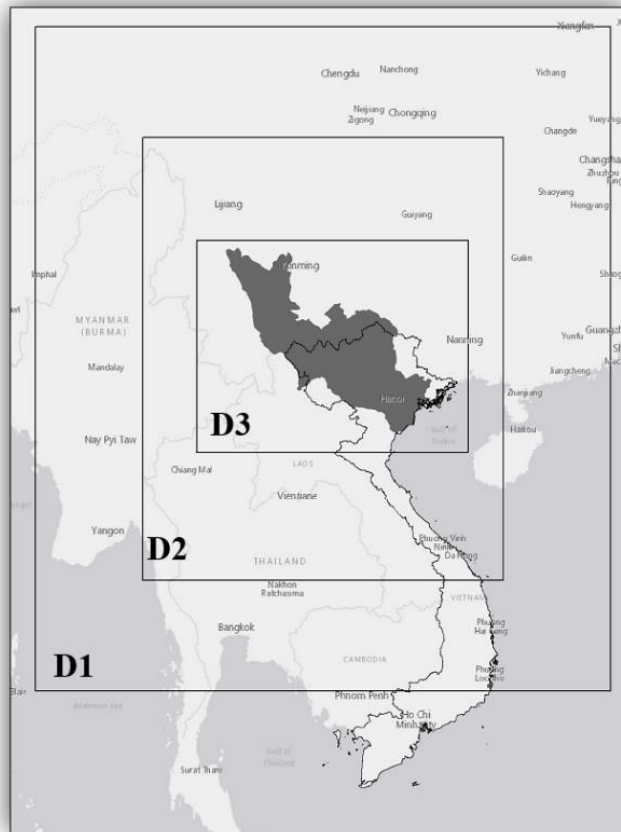


Figure 2.10 The description of the three nested WRF domains for dynamical downscaling

Table 2.1 WRF model configuration

WRF model configuration	The selected option
Microphysics processes	Goddard scheme (Tao et al., 1989)
Cumulus parameterization	New Simplified Arakawa-Schubert scheme (Han and Pan, 2011)
Planetary boundary layer scheme	BouLac scheme (Bougeault and Lacarrere, 1989)
radiation scheme	New Goddard scheme (Chou and Suarez, 1999)
Surface scheme	RUC Land Surface Model (Benjamin et al., 2004)

First, the WRF-downscaled precipitation data were compared to corresponding ground observations from the VNGP data in the downstream part of the LRW. Figure 2.11 shows the comparison of ground observations and model-simulated monthly basin average precipitation over the LRW in Vietnam during 1980–2010. Based on the correlation coefficient (R), 0.86, and Nash–Sutcliffe efficiency coefficient, 0.712, the simulated monthly precipitation data are highly correlated to the corresponding ground observations (monthly precipitation data).

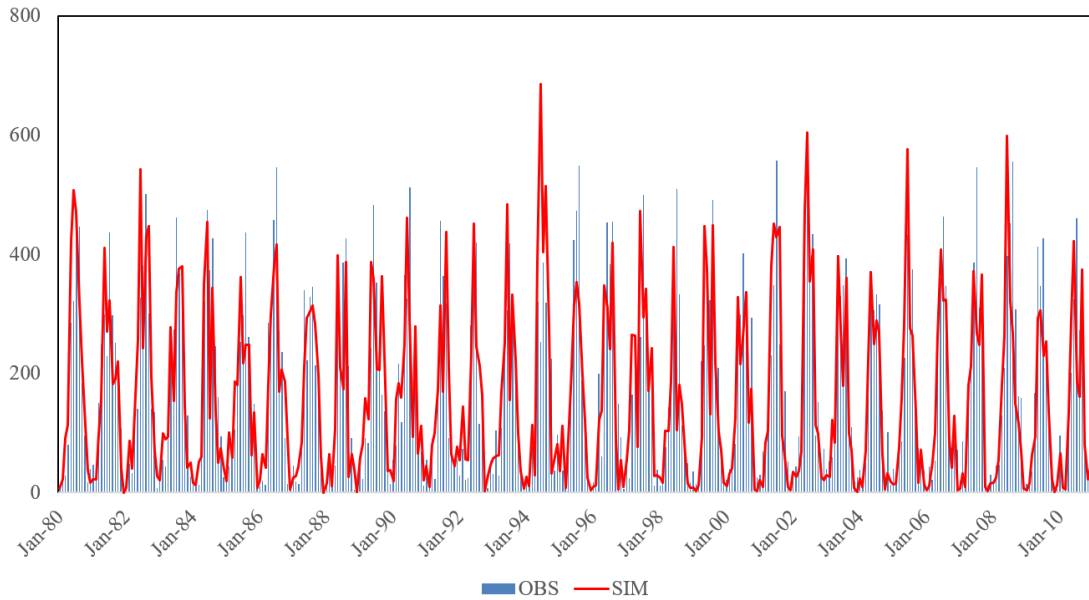
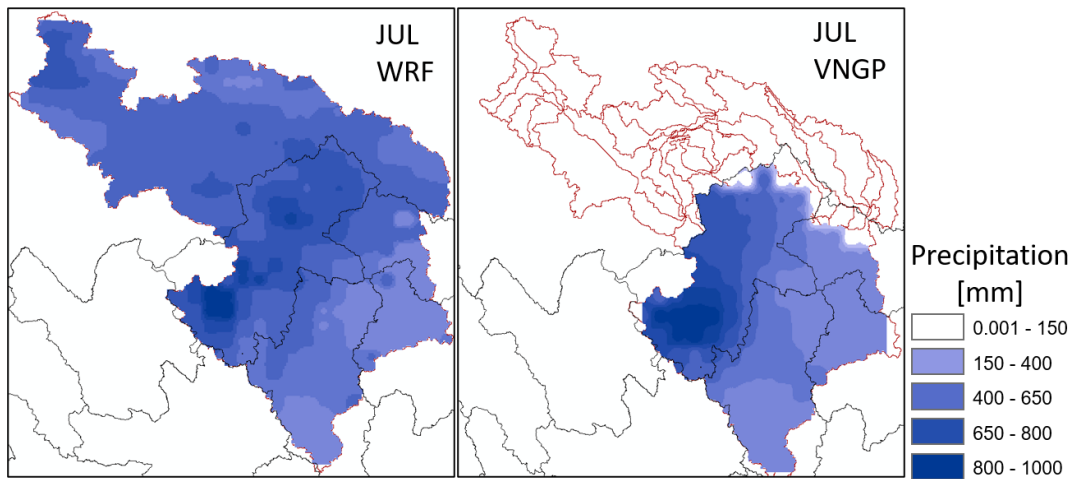
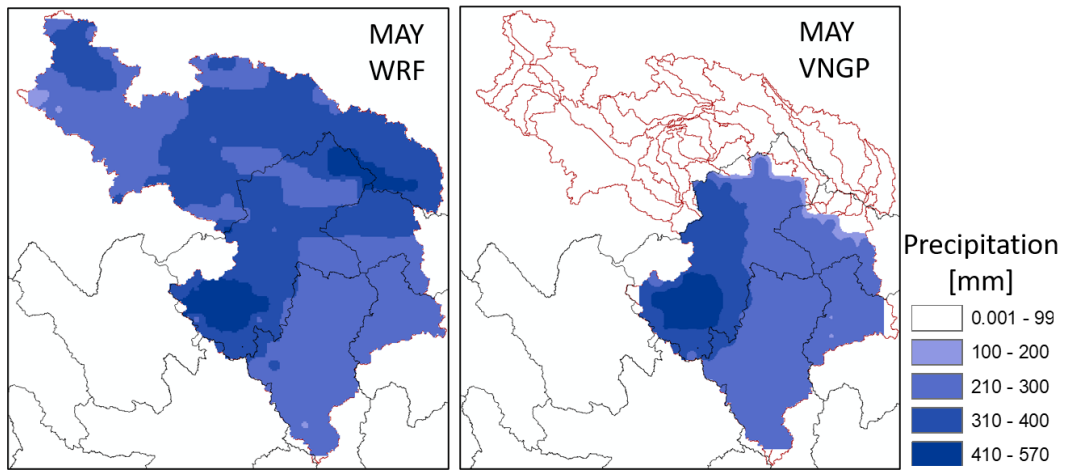
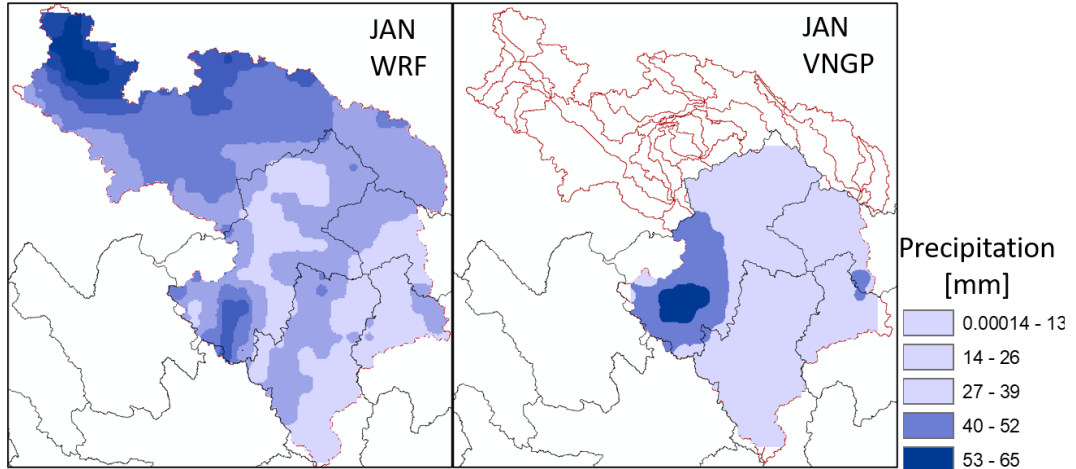


Figure 2.11 Comparison of the model-simulated basin average monthly precipitation over the LRW in Vietnam's territories against the corresponding ground observations

The WRF model simulations were also compared with spatial observation data under the monthly climatological precipitation spatial distribution maps. Figure 2.12 shows monthly climatological precipitation spatial distribution maps of WRF simulation and the VNGP during a 31-year period (1980-2010), with the largest precipitation typically occurring in July, and the lowest precipitation in January. The simulated precipitation distribution shown in Figure 2.12 contains all grid data from D3, whereas the VNGP data are more limited. There is a good agreement in all comparisons. Model-simulated precipitation matches the corresponding observation data well with respect to high and low precipitation areas.



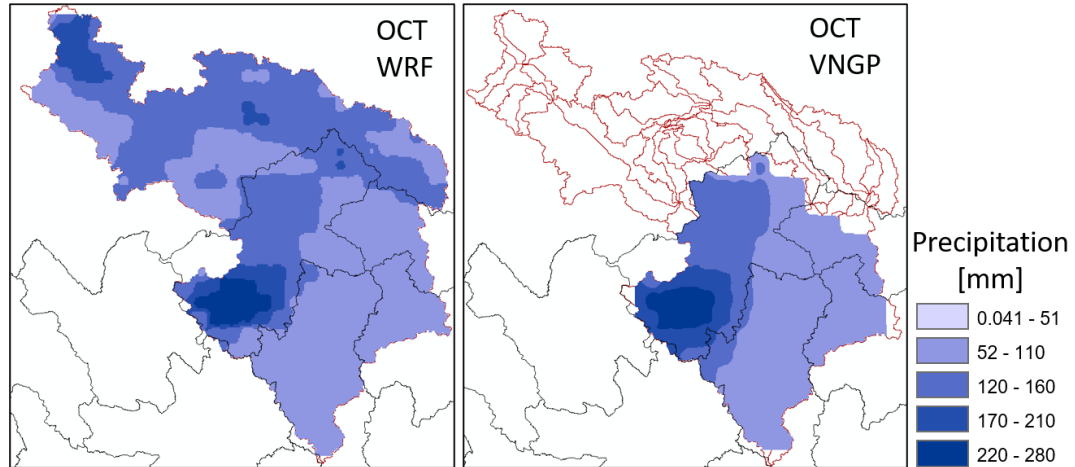


Figure 2.12 Comparison of model-simulated precipitation and the VNGP data over the study region from 1980 to 2010

Because there is no atmospheric observation data over the upstream part of the LRW in China's territories, the WRF simulations are evaluated based on the global high resolution ( $0.25^\circ$ ) datasets for precipitation, APHRODITE. The spatial distribution of the mean monthly WRF-simulated historical precipitation fields and the corresponding precipitation fields from APHRODITE data were also compared, as shown in Figure 2.13. In general, the model-simulated precipitation matches the corresponding APHRODITE data well with respect to magnitude and spatial distribution from 1990 to 2001. However, because APHRODITE is a spatial precipitation data set that is interpolated from the ground-based observations that are mostly located at easily accessible and relatively low-elevation areas (Kure et al. 2013), there are some slight differences in this comparison. Therefore, it is suspected that APHRODITE data may underestimate the precipitation at high-elevation locations. Despite this difference, it is confirmed that the atmospheric simulations of WRF can successfully produce historical climate data over the LRW in both the upstream and downstream areas.

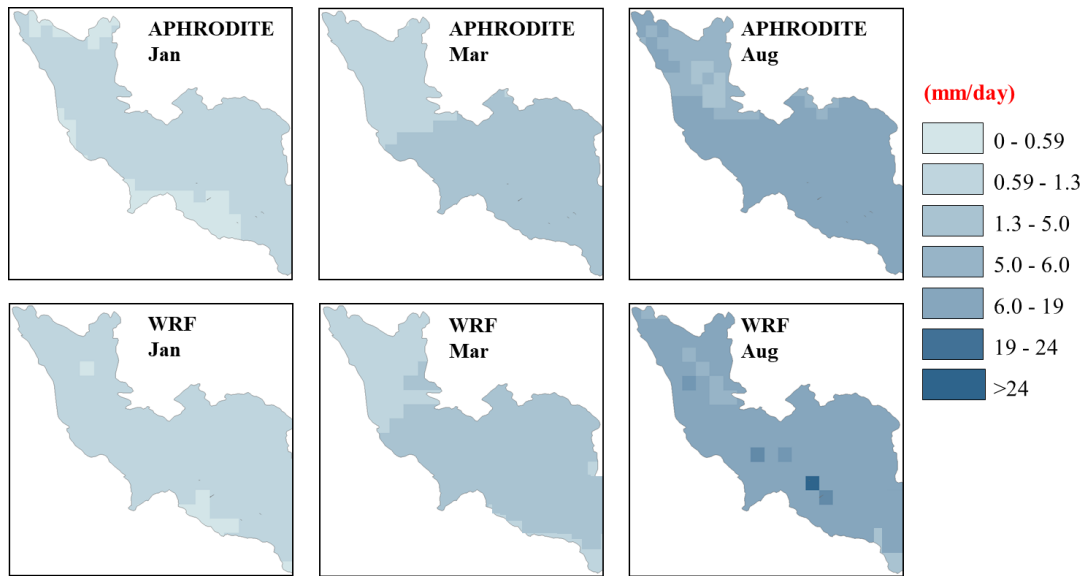


Figure 2.13 Comparison of model-simulated precipitation and APHRODITE data over the study region from 1990 to 2001 at resolution of  $0.25^\circ$

### 2.3.2 The WEHY model over the LRW: Hydrology processes

The WEHY model's input requires both atmospheric data and physical surface information such as topography, soil, and land cover. The first step of the WEHY application is delineation of the stream network. The delineation was based on Geographic information system (GIS) software Arc-GIS 10.1 utilizing elevation information, known as digital elevation model (DEM) data. In this study, the delineation in Arc-GIS 10.1 was based on the ASTER Global Digital Elevation Model (DEM) with spatial resolution of 30 m (Tachikawa et al. 2011). The LRW was delineated into 76 model computational units (MCUs), and 38 reaches as shown in Figure 2.14.

After delineation, data processing is performed consisting of estimation of soil hydraulic and land cover parameters. Soil and land parameters were estimated for each MCU. Soil parameters are significant components of the WEHY model. These data were obtained from the global SoilGrids data (1 km) from the International Soil Reference and Information Centre

(ISRIC) (Hengl et al., 2014; Trinh et al., 2018). Land cover parameters are also important for the hydrologic model implementation, and were collected from the Global Land Cover Characterization (GLCC) dataset (Loveland et al., 2000). The soil parameters include hydraulic conductivity, pore size index, soil depth, bubbling pressure, and porosity, while the land cover parameters include emissivity, albedo, leaf area index (LAI), surface roughness, and root depth, etc. (Kavvas et al., 2013). Land, LAI and soil parameters were estimated for model computational units (MCUs) as shown in Figure 2.15, 2.16 and 2.17.

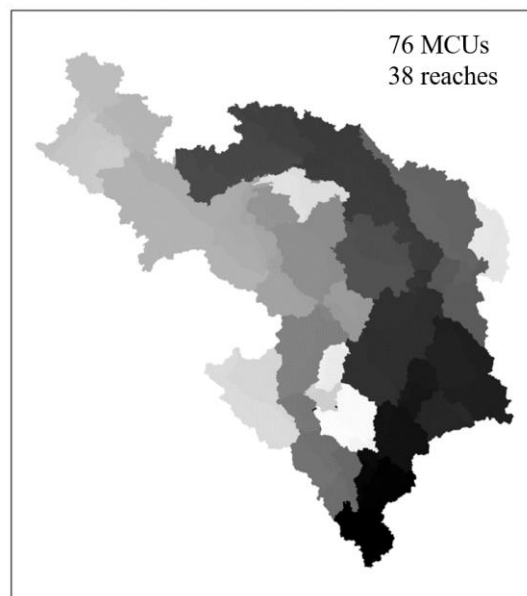


Figure 2.14 Delineated MCUs map for LRW

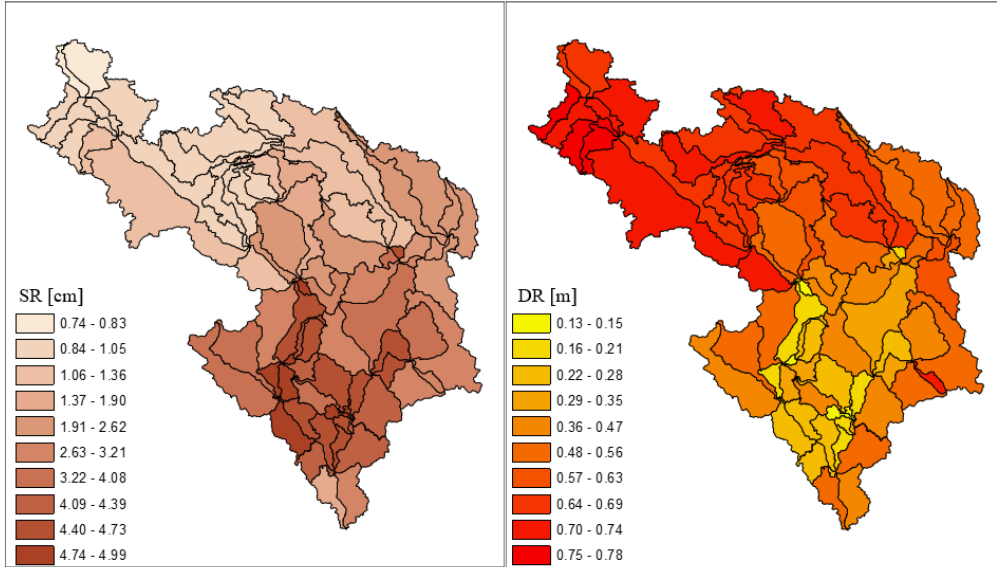
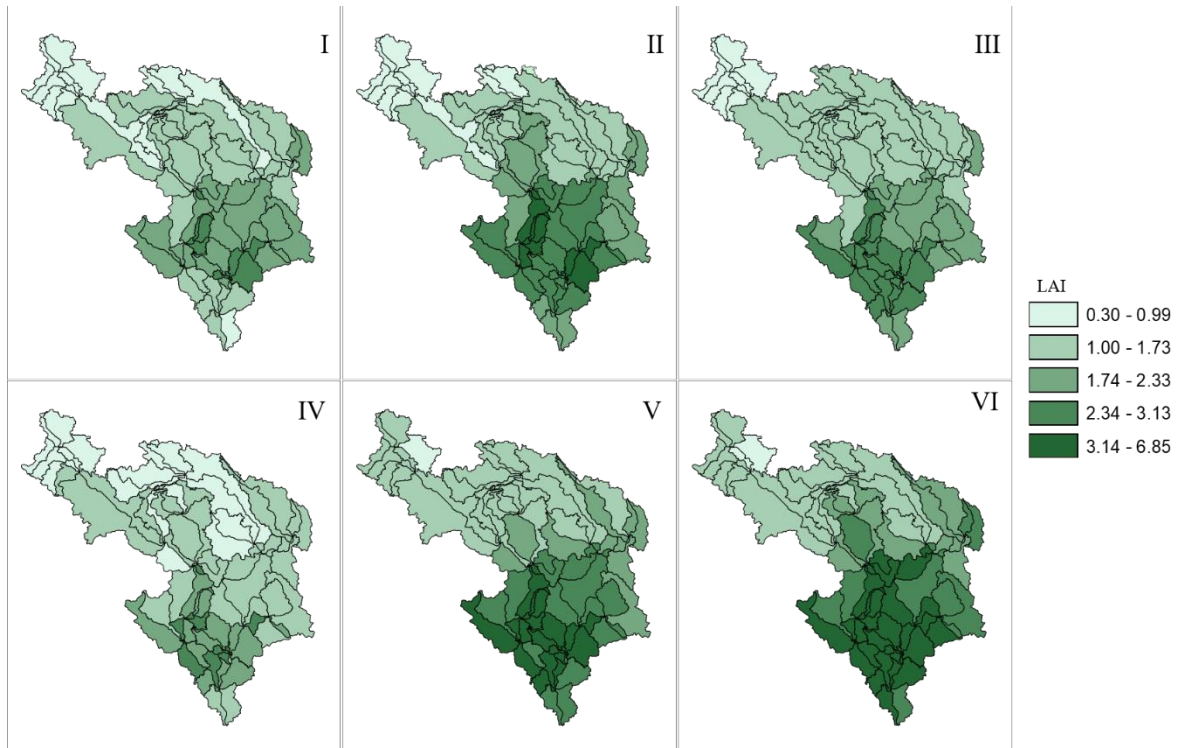


Figure 2.15 Land parameter maps of surface roughness (SR) and root depth for Lo

River Watershed



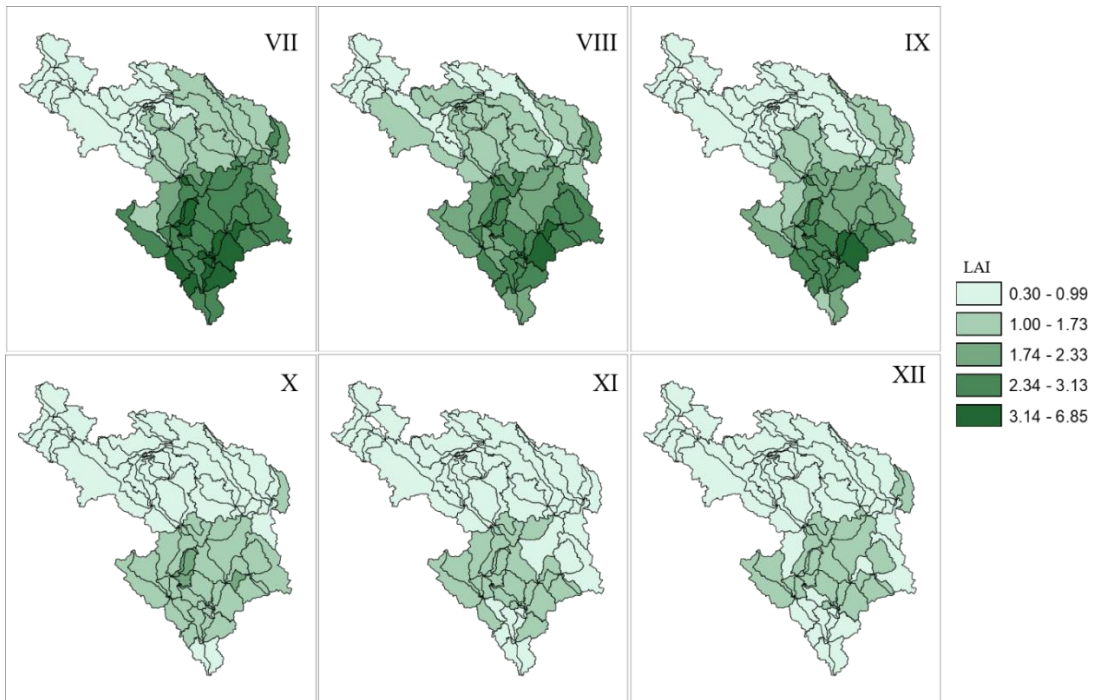


Figure 2.16 Month averages of Leaf Area Index (LAI) data over the LRW

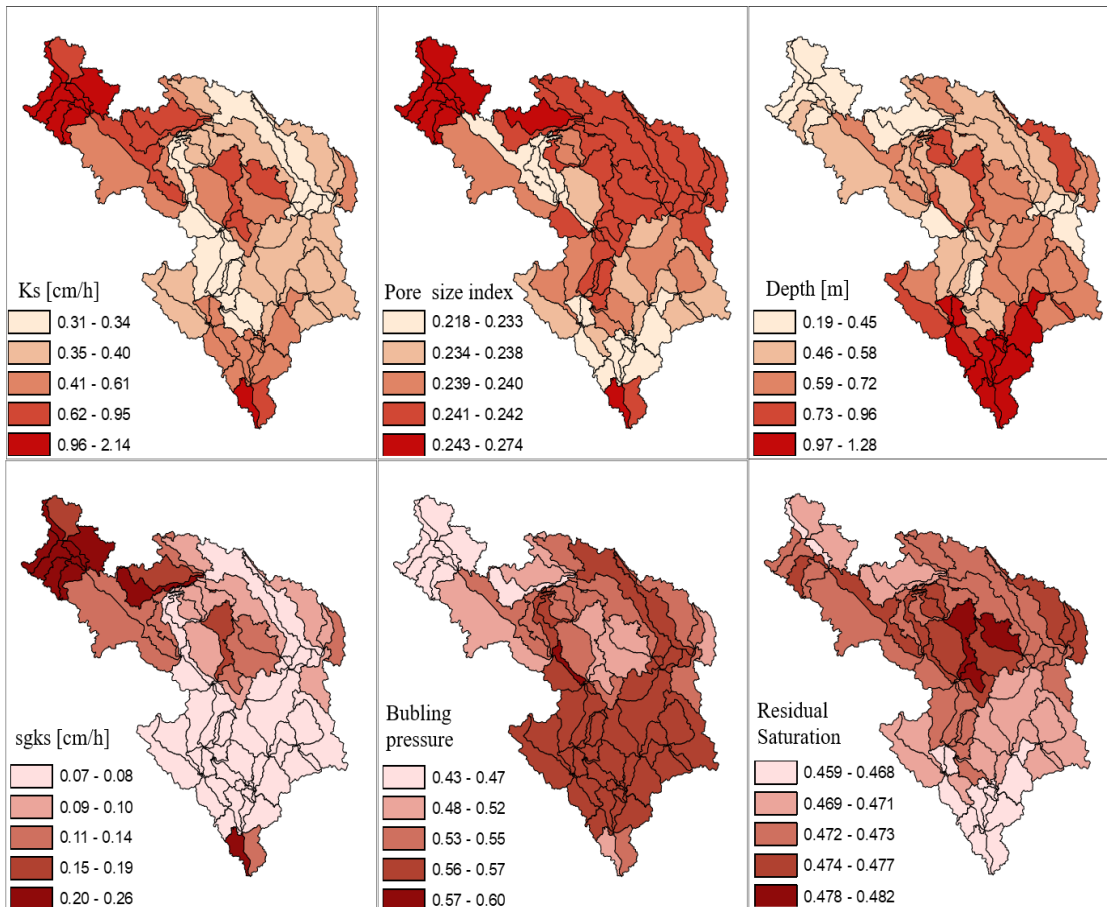


Figure 2.17 Computed soil hydraulic conductivity parameter maps for the LRW

After successful estimation of the geomorphologic and land cover parameters for the LRW, atmospheric data from the validated WRF-downscaled ERA-20C were applied to the WEHY model in order to simulate hydrologic conditions over the LRW. In order to calibrate and validate WEHY, the simulated flow data were compared with the corresponding observations (figure 2.18). Vu Quang is the outlet station of LRW, and its data were used for calibration and validation. Observation data at Vu Quang were available from 1972-2019 at a monthly interval. The observation data from 1972-1980 were selected for calibration and data from 1981-2012 were selected for validation. As presented previously, the WEHY simulation requires incorporation of the WEHY reservoir sub-program. Thac Ba reservoir has been operated since

the 1960s. Therefore, both calibration and validation processes need to consider the Thac Ba operation rule. However, the Tuyen Quang reservoir has only operated since 2008. Therefore, 5 years of the validation period (2008-2012) requires consideration of both the Thac Ba and Tuyen Quang operation rules.

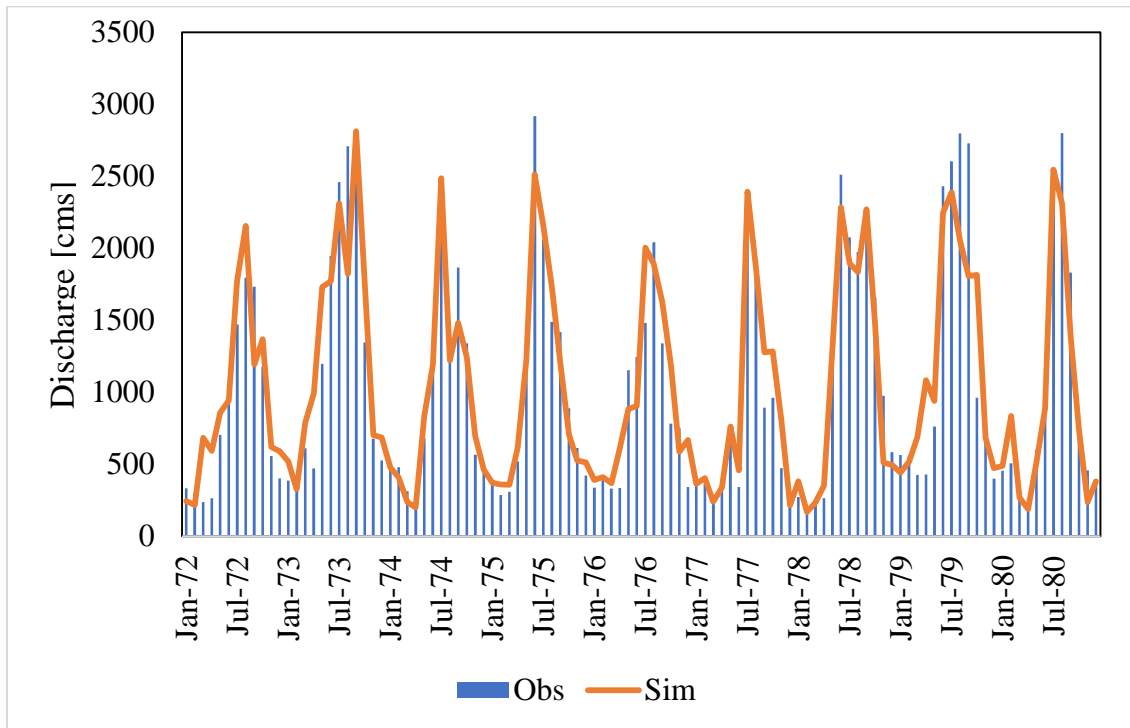


Figure 2.18 Comparison of the monthly mean discharge between the WEHY hydrology model simulations and observations at Vu Quang station during: Jan 1972 to Dec 1980 for calibration

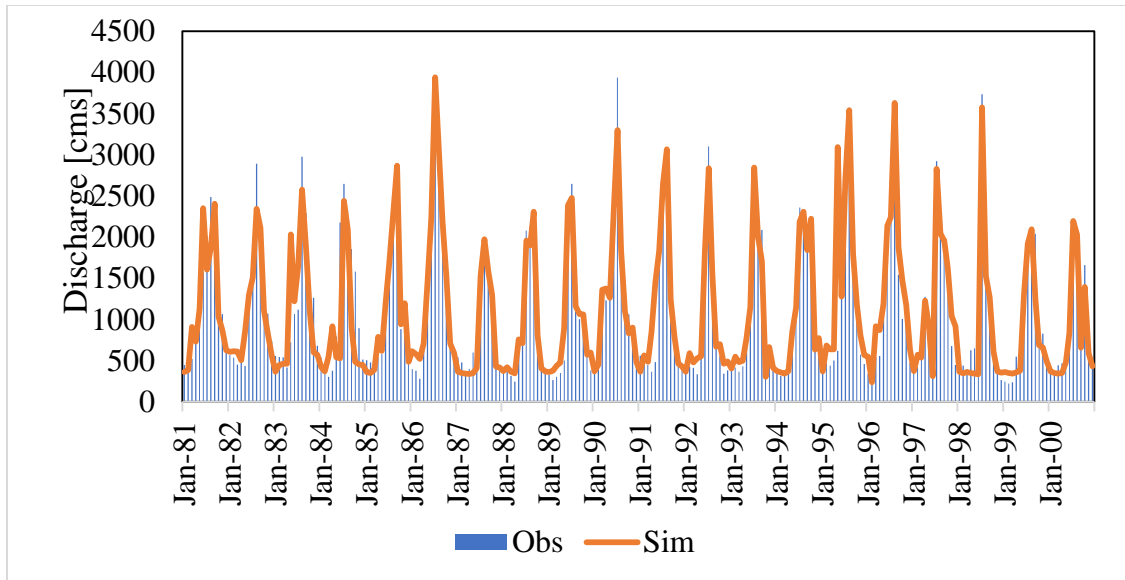


Figure 2.18. Comparison of the monthly mean discharge between the WEHY hydrology model simulations and observations at Vu Quang station from Jan 1981 to Dec 2000 for validation

Visual inspection of the observations and simulations shows fairly good reproduction (Figures 2.18 and 2.19) for both the calibration and validation periods. The WEHY model satisfactorily simulated both timing and general magnitude of streamflow. During the calibration period, in which only the operation rules of the Thac Ba reservoir were needed, the Nash Coefficient was 0.83 and the correlation coefficient was 0.92. During the validation period, in which both reservoir operation rules were applied from 2008 on, the Nash-Sutcliffe coefficient was 0.79 and the correlation coefficient was 0.89, indicating a satisfactory model performance (Table 2.2). Comparison of the observed and simulated outflow at Vu Quang is shown in Figure 2.19. The WEHY hydrologic model and reservoir sub-programs are reliable techniques to simulate hydrologic conditions over the LRW.

Table 2.2 Statistics for comparison of the daily mean discharge at Vu Quang Station

<b>Evaluation statistics</b>	Calibration (1972-1980)	Validation (1981-2000)
<b>Mean by Observation [m<sup>3</sup>/s]</b>	1018.02	1082.47
<b>Mean by Simulation [m<sup>3</sup>/s]</b>	1035.75	1078.93
<b>Standard Deviation by Observation[m<sup>3</sup>/s]</b>	778.94	802.10
<b>Standard Deviation by Simulation [m<sup>3</sup>/s]</b>	711.13	807.43
<b>Correlation Coefficient</b>	0.92	0.89
<b>Nash Coefficient</b>	0.83	0.79

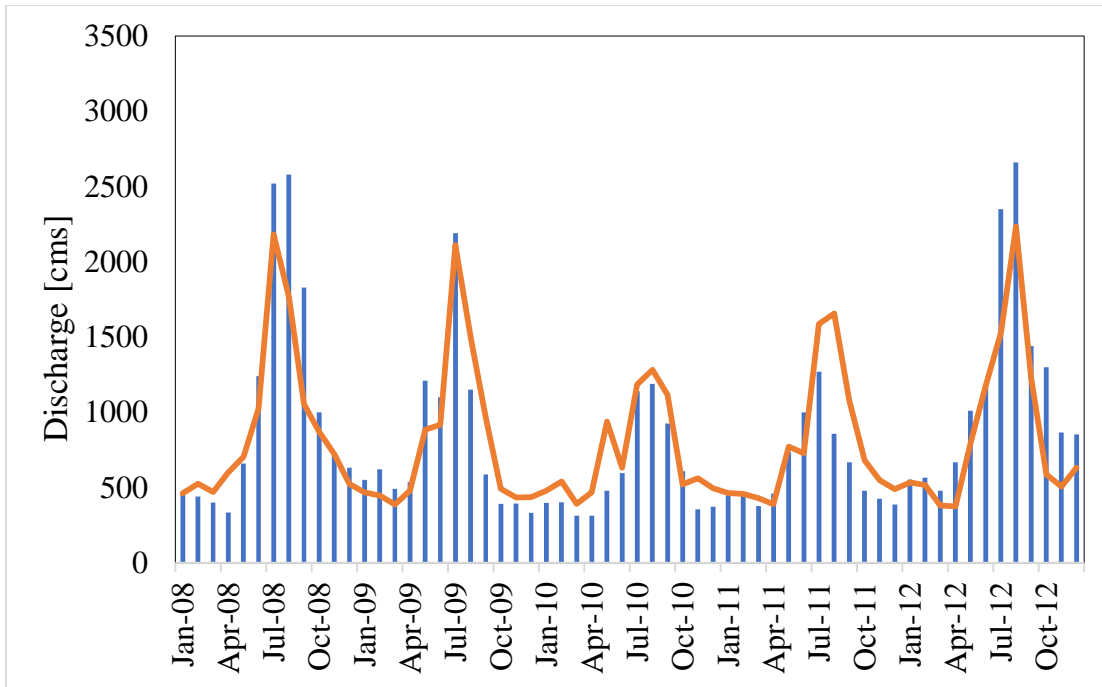


Figure 2.19 Comparison of the monthly mean discharge between the WEHY hydrology model simulations and observations at Vu Quang station from Jan 2008 to Dec 2012 for validation.

#### 2.4 Assessment of atmospheric and hydrologic conditions over the LRW during 1901–2014

Basin average precipitation data were first analyzed in terms of annual precipitation during the period from 1900–2015, and then depicted by a trend line of annual precipitation to determine overall changes, as seen in Figure 2.20. By visual inspection of the trend line, it is seen that there were no significant trends in annual precipitation over LRW.

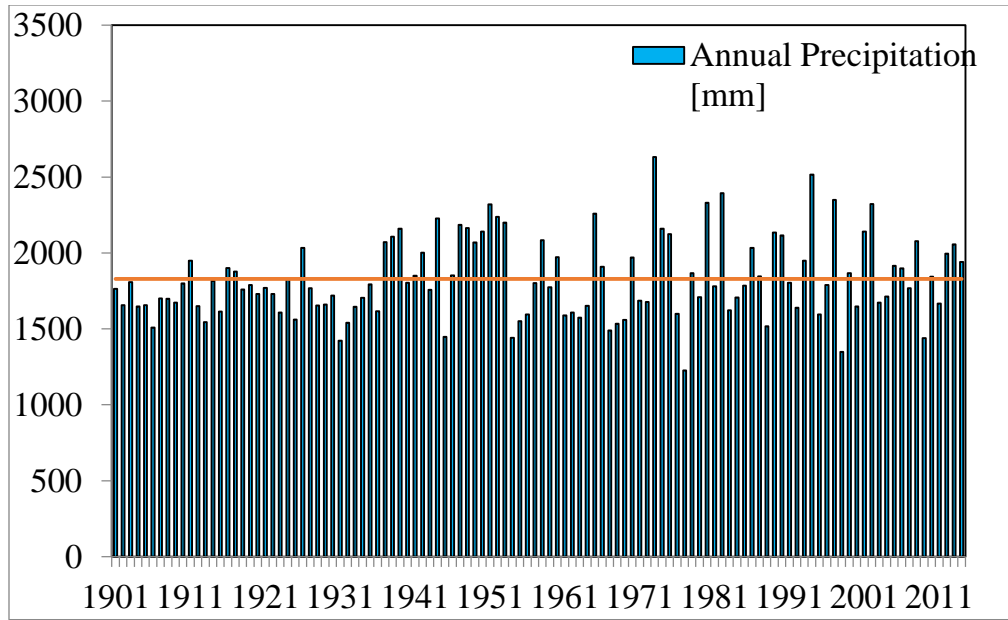


Figure 2.20 Annual basin average precipitation depths over LRW during 1900–2015 with their 10-year moving averages

In order to analyze changes in the precipitation regime during the period from 1950–2010, the monthly basin average of annual precipitation was divided into two time windows, 1900–1950 and 1951–2015, as shown in Figure 2.21. It is also clearly seen from this figure that the wet season lasts for six months from May to September, and the dry season occurs from October to April of the following year. As shown in Figure 2.21, there is no significant difference, and no seasonal shift between the first- and second-time windows for either the dry or wet seasons.

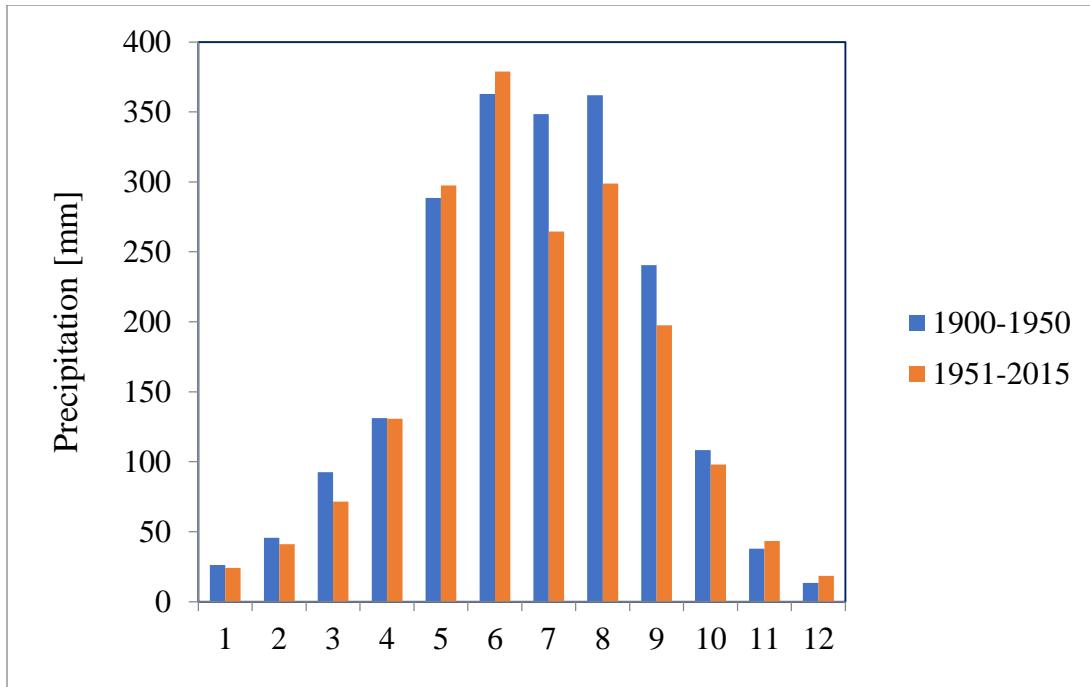


Figure 2.21 Comparison of monthly basin average precipitation during 1900–1950 and 1951–2015

For the assessment of temperature, similar analyses were applied over the LRW for the period from 1900–2015. Figure 2.22 shows annual basin average temperature over the LRW with a trend line. By visual inspection of the trend line, it is seen that temperature is increasing.

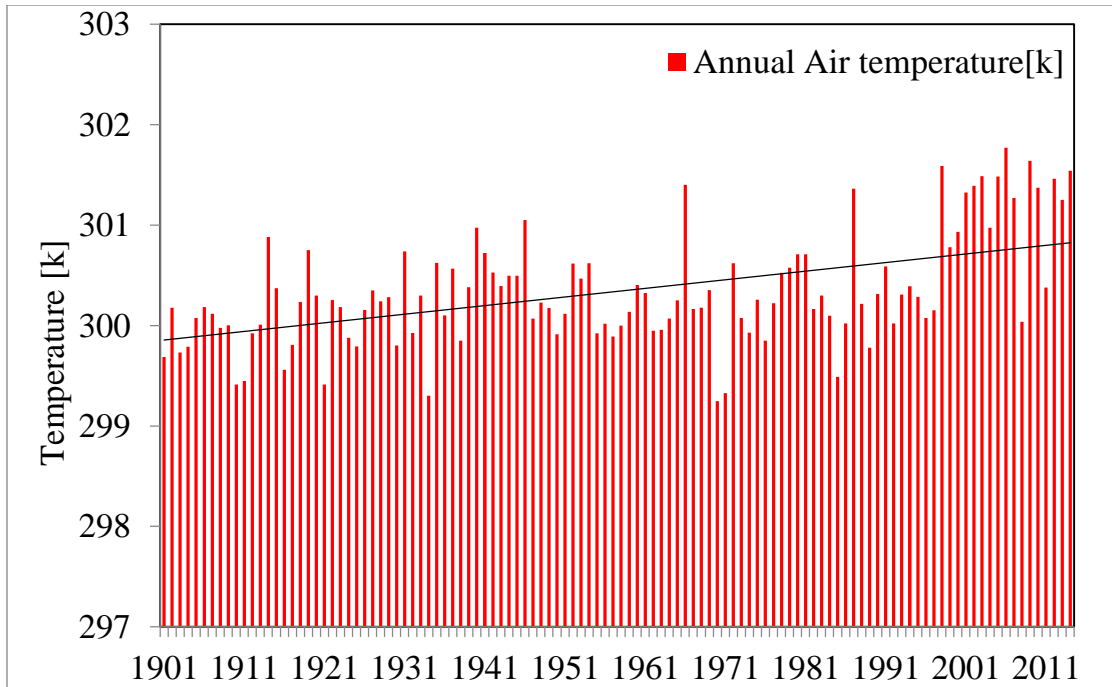


Figure 2.22 Annual basin-average temperature over LRW during 1900–2015

In terms of the comparison of temperature between the two-time windows, 1900–1950 and 1951–2015, it is inferred from Figure 2.23 that the temperature increased in each month of the year, except January and February. Temperature magnitude grew by 1–5% from the first time window to the second time window. It is also noted that there is no seasonal shift between the first and second time windows with respect to cold and hot seasons.

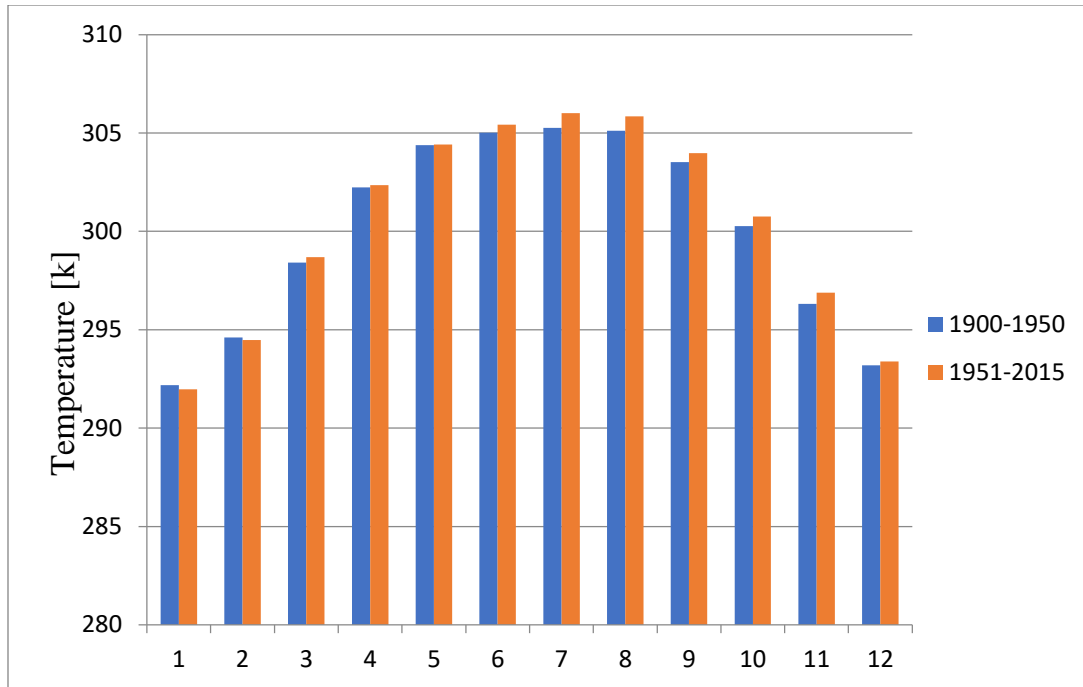


Figure 2.23 Comparison of monthly basin average temperature during 1900–1950 and 1951–2015

#### Comparison of monthly basin average temperature during 1900–1950 and 1951–2015

Together with precipitation and temperature, evapotranspiration is one of the most vulnerable variables in the atmospheric cycle with respect to climate change. These circulation features are also important as they are contributing factors to rainfall dynamics, soil moisture, and water demand estimation. In this study, evapotranspiration was calculated externally using the FAO56 Penman-Monteith method which utilized climate variables, such as the temperature and wind speed, from the WRF model to calculate evapotranspiration. Observation data are available at two locations, Chiem Hoa and Ham Yen (Figure 2.24). Comparison between calculated and observed evapotranspiration at Ham Yen and Chiem Hoa is presented in Figures 2.25 and 2.26. By visual inspection, it can be seen that calculated data were matched well with observations. Statistical analysis also shows high correlation between the calculated and

observed monthly evapotranspiration at Ham Yen and Chiem Hoa with correlation coefficients and the Nash–Sutcliffe coefficients of 0.82 and 0.84, and 0.65 and 0.67.

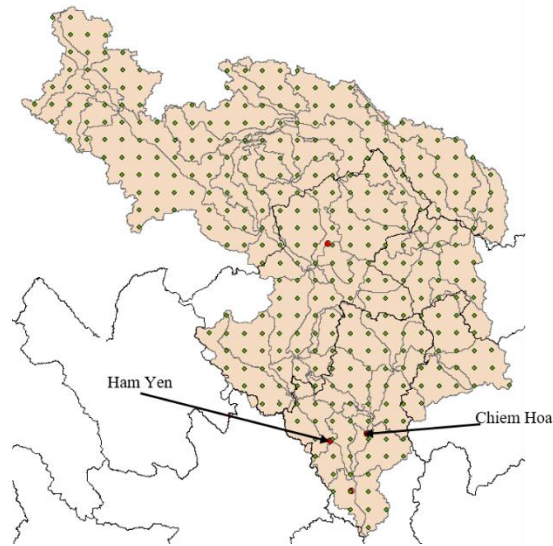


Figure 2.24 Location of Ham Yen and Chiem Hoa stations

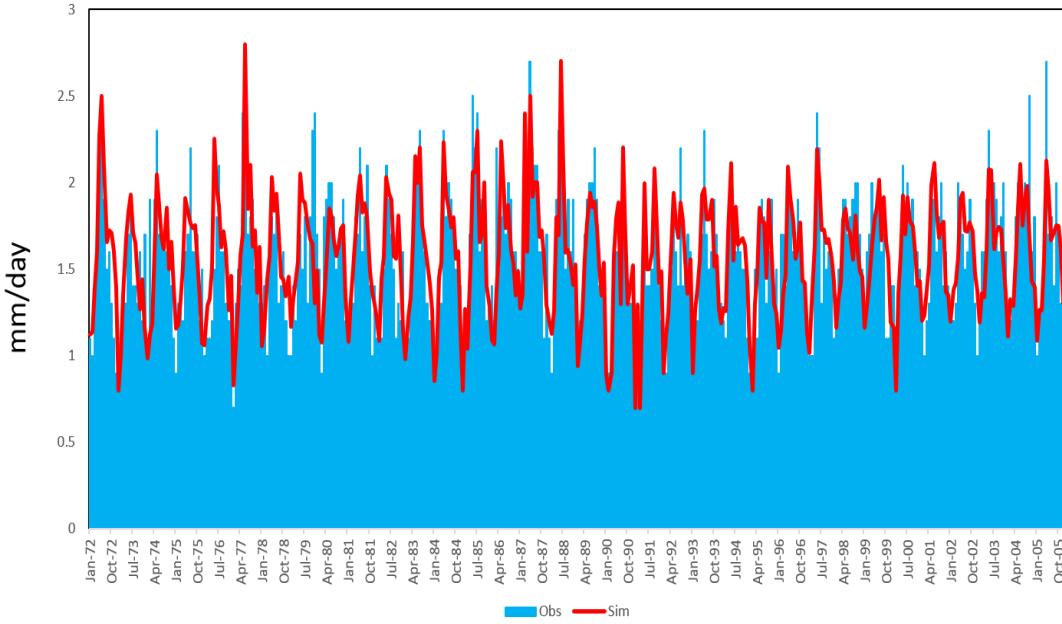


Figure 2.25 Historical mean monthly results at Ham Yen from 1972 to 2005, for calculated and observed evapotranspiration

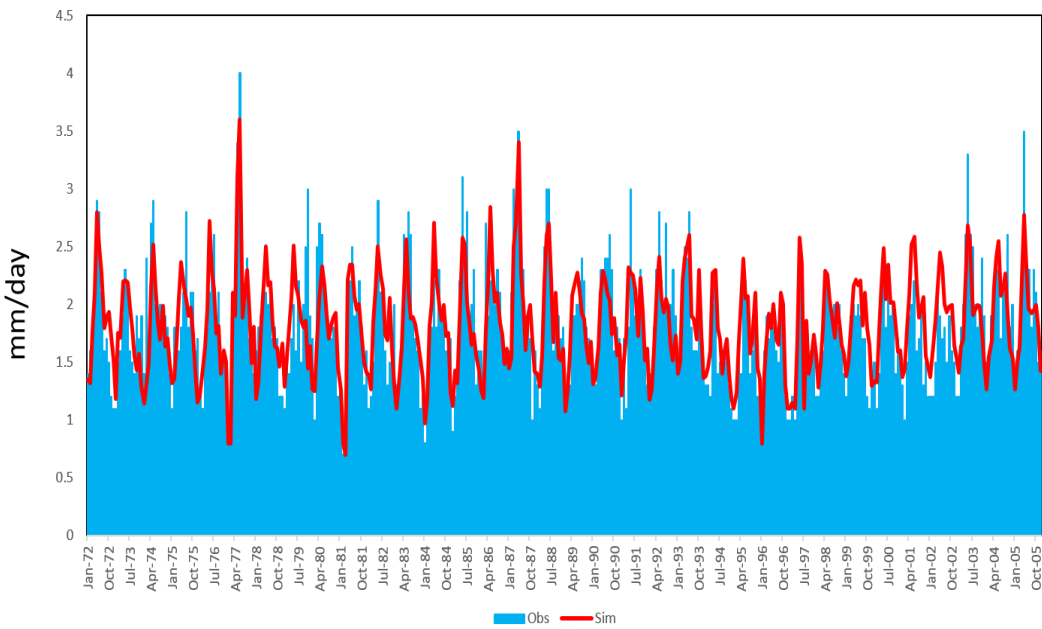


Figure 2.26 Historical mean monthly results at Chiem Hoa from 1972 to 2005, for calculated and observed evapotranspiration

Annual basin average evapotranspiration data during the period from 1900–2015, as well as their trend line are shown in Figure 2.27. It can be observed that annual evapotranspiration shows an increasing trend over the LRW.

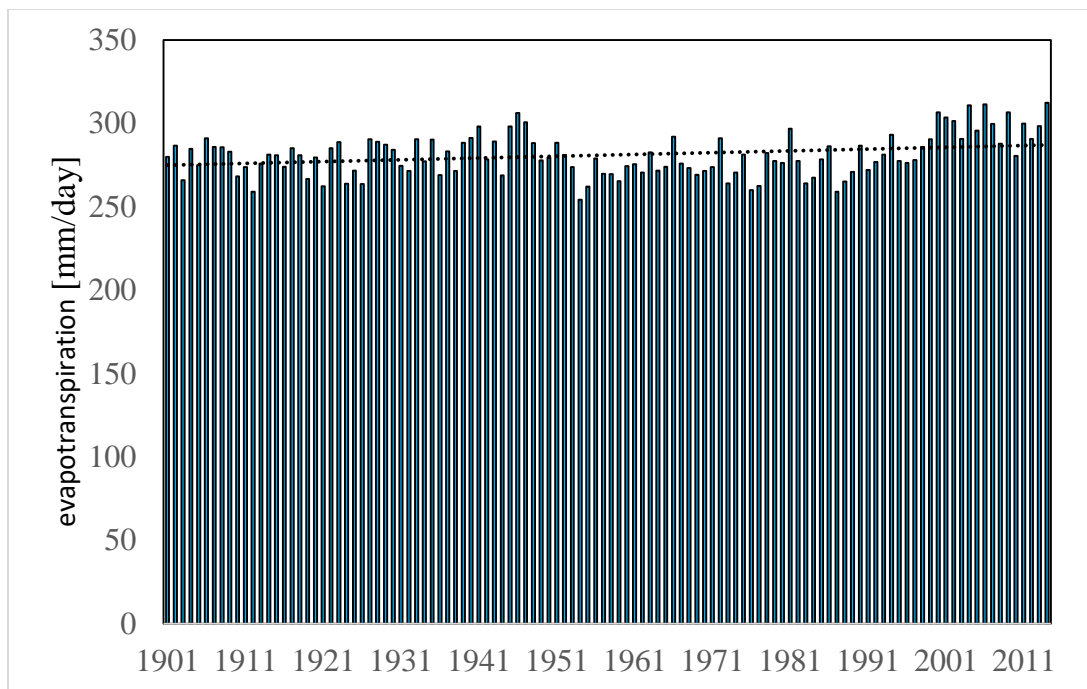


Figure 2.27 Annual basin-average evapotranspiration over LRW during 1900–2015

The analysis of historical flow conditions is illustrated in the next chapter of bias correction.

## 2.5 Conclusions

This study describes the historical changes in atmospheric-hydrologic conditions over the LRW during 1900–2015. Data from the numerical regional hydro-climate WRF and WEHY models, based on inputs provided from the global reanalysis data – ERA20C, were validated and showed good agreement with observation data. The downscaled precipitation data from the WRF

simulations were compared against available observations in Vietnam's territories and from global Aphrodite precipitation data. The simulations matched the precipitation observations well with respect to magnitude and spatial distribution at both point location and the watershed scale. From these results, it is concluded that the application of WRF over the transboundary region LRW is successful. Similarly, the WEHY model was implemented and evaluated at the outlet point with time series analysis. Both the calibration and validation have high correlation as the WEHY model satisfactorily simulates the timing and general magnitude of streamflow. These comparisons confirmed that the WEHY hydrologic model and reservoir sub-programs are reliable techniques to simulate hydrologic conditions over the LRW.

From the time series analysis of modeled results, it is found that there is no significant trend in the annual accumulated precipitation depth at the basin average, while upward trends in annual temperature and evapotranspiration were detected at watershed scale. From a scientific perspective, the increase in temperature and evapotranspiration over the LRW (about 5%) is evidence of recent climatic warming, and this change did not affect the precipitation condition significantly over the watershed.

Based on the analyses in this study, it is possible to identify changes in precipitation, temperature, and evapotranspiration over the study region during the period from 1900–2015. Such information may be useful for climate strategic adaptation with the purpose of reducing the effects of risks on human society in an economically and environmentally sustainable manner. The results of this chapter can be used for the projection of future water supply from the watershed using atmospheric inputs from global climate models' future climate projections.

## References

Skamarock, W.C., Klemp, J.B., Dudhia, J., Gill, D.O., Barker, D.M., Wang, W. and Powers, J.G., 008. A description of the Advanced Research WRF version 3. NCAR Technical note-475+ STR.

Trinh, T., Ishida, K., Fischer, I., Jang, S., Darama, Y., Nosacka, J., Brown, K. and Kavvas, M.L., 2016. New methodology to develop future flood frequency under changing climate by means of physically based numerical atmospheric-hydrologic modeling. *Journal of Hydrologic Engineering*, 21(4), p.04016001.

Jang, S., Kavvas, M.L., Ishida, K., Trinh, T., Ohara, N., Kure, S., Chen, Z.Q., Anderson, M.L., Matanga, G. and Carr, K.J., 2017. A performance evaluation of dynamical downscaling of precipitation over northern California. *Sustainability*, 9(8), p.1457.

Ohara, N., Chen, Z.Q., Kavvas, M.L., Fukami, K. and Inomata, H., 2011. Reconstruction of historical atmospheric data by a hydroclimate model for the Mekong River basin. *Journal of Hydrologic Engineering*, 16(12), pp.1030-1039.

Compo, G.P., Whitaker, J.S. and Sardeshmukh, P.D., 2006. Feasibility of a 100-year reanalysis using only surface pressure data. *Bulletin of the American Meteorological Society*, 87(2), pp.175-190.

Brower, M.C., Barton, M.S., Lledó, L. and Dubois, J., 2013. A study of wind speed variability using global reanalysis data. *AWS Truepower*.

Fuka, D.R., Walter, M.T., MacAlister, C., Degaetano, A.T., Steenhuis, T.S. and Easton, Z.M., 2014. Using the Climate Forecast System Reanalysis as weather input data for watershed models. *Hydrological Processes*, 28(22), pp.5613-5623.

Krishnamurti, T.N., Jha, B., Rasch, P.J. and Ramanathan, V., 1997. A high resolution global reanalysis highlighting the winter monsoon. Part I, reanalysis fields. *Meteorology and Atmospheric Physics*, 64(3-4), pp.123-150.

Anderson, M.L., Chen, Z.Q., Kavvas, M.L. and Yoon, J.Y., 2007. Reconstructed historical atmospheric data by dynamical downscaling. *Journal of Hydrologic Engineering*, 12(2), pp.156-162.

Milly, P.C., Betancourt, J., Falkenmark, M., Hirsch, R.M., Kundzewicz, Z.W., Lettenmaier, D.P. and Stouffer, R.J., 2008. Stationarity is dead: Whither water management?. *Science*, 319(5863), pp.573-574.

Trinh, T., Ishida, K., Fischer, I., Jang, S., Darama, Y., Nosacka, J., Brown, K. and Kavvas, M.L., 2016b. New methodology to develop future flood frequency under changing climate by means of physically based numerical atmospheric-hydrologic modeling. *Journal of Hydrologic Engineering*, 21(4), p.04016001.

Jang, S., Kure, S., Ohara, N., Kavvas, M.L., Chen, Z.Q., Carr, K.J. and Anderson, M.L., 2017b. Application of WEHY-HCM for Modeling Interactive Atmospheric-Hydrologic Processes at Watershed Scale to a Sparsely Gauged Watershed. *Sustainability*, 9(9), p.1554.

Jucker, M.; Lane, T.P.; Vincent, C.L.; Webster, S.; Wales, S.A.; Louf, V. (2020). Locally forced convection in sub-kilometre scale simulations with the Unified Model and WRF. *Quarterly Journal of the Royal Meteorological Society*. 146 (732): 3450–3465

Poli, P., Hersbach, H., Tan, D., Dee, D., Thepaut, J.N., Simmons, A., Peubey, C., Laloyaux, P., Komori, T., Berrisford, P. and Dragani, R., 2013. *The data assimilation system and initial performance evaluation of the ECMWF pilot reanalysis of the 20th-century assimilating surface observations only (ERA-20C)*. European Centre for Medium Range Weather Forecasts.

Poli, P., Hersbach, H., Dee, D., Berrisford, P., Simmons, A. and Laloyaux, P., 2015. *ERA-20C deterministic*. European Centre for Medium Range Weather Forecasts.

Poli, P., Hersbach, H., Dee, D.P., Berrisford, P., Simmons, A.J., Vitart, F., Laloyaux, P., Tan, D.G., Peubey, C., Thépaut, J.N. and Trémolet, Y., 2016. ERA-20C: An atmospheric reanalysis of the twentieth century. *Journal of Climate*, 29(11), pp.4083-4097

Predictia (2020, October 19). WRF: One model powering a myriad of weather solutions. <https://predictia.es/en/news/wrf-weather-model-applications>

Yatagai, A., Kamiguchi, K., Arakawa, O., Hamada, A., Yasutomi, N. and Kitoh, A., 2012. APHRODITE: Constructing a long-term daily gridded precipitation dataset for Asia based on a dense network of rain gauges. *Bulletin of the American Meteorological Society*, 93(9), pp.1401-1415.

Nguyen-Xuan, T., Ngo-Duc, T., Kamimera, H., Trinh-Tuan, L., Matsumoto, J., Inoue, T. and Phan-Van, T., 2016. The Vietnam gridded precipitation (VNGP) dataset: construction and validation. *SOLA*, 12, pp.291-296.

Kavvas, M., et al., 2006. Watershed environmental hydrology model: environmental module and its application to a California watershed. *J. Hydrol. Eng.* 3 (261), 261–272.

Kavvas, M.L., Kure, S., Chen, Z.Q., Ohara, N., Jang, S., 2013. WEHY-HCM for modeling interactive atmospheric-hydrologic processes at watershed scale. I: model description. *J. Hydrol. Eng.* 18 (10), 1262–1271

Kavvas, M.L., Chen, Z.Q., Dogrul, C., Yoon, J.Y., Ohara, N., Liang, L., Aksoy, H., Anderson, M.L., Yoshitani, J., Fukami, K., Matsuura, T., 2004. Watershed environmental hydrology (WEHY) model based on upscaled conservation equations: hydrologic module. *J. Hydrol. Eng.* 9 (6), 450–464

Chen, Z., et al., 2004a. Geomorphologic and soil hydraulic parameters for Watershed Environmental Hydrology (WEHY) model. *J. Hydrol.Eng.* 6 (465), 465–479.

Chen, Z., Kavvas, M., Fukami, K., Yoshitani, J., Matsuura, T., 2004b. Watershed environmental hydrology (WEHY) model: model application. *J. Hydrol. Eng.* 9:6 (480), 480–490.

Chen, Z.R., Kavvas, M.L., Ohara, N., Anderson, M.L. and Yoon, J., 2011. Coupled regional hydroclimate model and its application to the Tigris-Euphrates basin. *Journal of Hydrologic Engineering*, 16(12), pp.1059-1070.

Hersbach, H., Peubey, C., Simmons, A., Poli, P., Dee, D. and Berrisford, P., 2013. ERA-20CM: a twentieth century atmospheric model ensemble, ERA Report Series 16, European Centre for Medium-Range Weather Forecasts.

Hersbach, H., Peubey, C., Simmons, A., Berrisford, P., Poli, P. and Dee, D., 2015. ERA-20CM: a twentieth-century atmospheric model ensemble. *Quarterly Journal of the Royal Meteorological Society*, 141(691), pp.2350-2375.

Bougeault, P. and Lacarrere, P., 1989. Parameterization of Orography-Induced Turbulence in a Mesobeta--Scale Model. *Monthly Weather Review*, 117(8), pp.1872-1890.

Benjamin, S.G., Dévényi, D., Weygandt, S.S., Brundage, K.J., Brown, J.M., Grell, G.A., Kim, D., Schwartz, B.E., Smirnova, T.G., Smith, T.L. and Manikin, G.S., 2004. An hourly assimilation–forecast cycle: The RUC. *Monthly Weather Review*, 132(2), pp.495-518.

Han, J. and Pan, H.L., 2011. Revision of convection and vertical diffusion schemes in the NCEP global forecast system. *Weather and Forecasting*, 26(4), pp.520-533.

Tao, W.K., Simpson, J. and McCumber, M., 1989. An ice-water saturation adjustment. *Monthly Weather Review*, 117(1), pp.231-235.

Chou, M.D. and Suarez, M.J., 1999. A Solar Radiation Parameterization for Atmospheric Studies. Volume 15

Tachikawa, T., Hato, M., Kaku, M. and Iwasaki, A., 2011, July. Characteristics of ASTER GDEM version 2. In *2011 IEEE international geoscience and remote sensing symposium* (pp. 3657-3660). IEEE.

Hengl, T., de Jesus, J.M., MacMillan, R.A., Batjes, N.H., Heuvelink, G.B., Ribeiro, E., Samuel-Rosa, A., Kempen, B., Leenaars, J.G., Walsh, M.G. and Gonzalez, M.R., 2014. SoilGrids1km—global soil information based on automated mapping. *PloS one*, 9(8), p.e105992.

Trinh, T., Kavvas, M.L., Ishida, K., Ercan, A., Chen, Z.Q., Anderson, M.L., Ho, C. and Nguyen, T., 2018. Integrating global land-cover and soil datasets to update saturated hydraulic conductivity parameterization in hydrologic modeling. *Science of the Total Environment*, 631, pp.279-288.

## **CHAPTER 3. PRECIPITATION AND STREAM FLOW BIAS CORRECTION**

### **3.1 Introduction**

Because future projection simulations and even historical control runs do not include data assimilation process (unlike reanalysis data), model products may be biased. These biases necessitate a technology to correct simulated data and provide reliable future projection over the target watershed. There are various sources of uncertainty recognized in hydro-climate studies, such as GCM structure and parameter uncertainty, greenhouse gas emissions scenarios uncertainty, GCMs' initial conditions uncertainty, downscaling technique, and hydrologic model uncertainty. One recommendation to decrease uncertainty is the application of both atmospheric and hydrologic bias correction. In this study, two global climate models are applied, including the fifth generation of the Model for Interdisciplinary Research on Climate - MIROC5, and the fourth version of the Community Climate System Model - CCSM4 under two scenarios, the Representative Concentration Pathway - RCP 4.5 and 8.5. These scenarios were recommended by the Vietnam Ministry of Natural Resources and Environment. The bias precipitation and streamflow were corrected first by dynamically-downscaling and hydrologically modeling the historical control run climate simulations of MIROC5 and CCSM4 GCMs, and then bias corrections were applied to future periods.

### **3.2 Methodology**

In order to dynamically downscale both GCMs' (CCSM4 and MIROC5) historical control runs and climate projections of the 21<sup>st</sup> century, the regional climate model (WRF) whose application was described in detail in CHAPTER 2, was applied to downscale each to 9-km grid resolution. Downscaling was applied for the historical control runs of the GCMs from 1980-2005 and the future climate data (2006-2100). Although GCMs might be one of the best tools for the

estimation of future climate change, the use of GCMs' simulations introduces considerable uncertainty (Dosio and Paruolo, 2011; Hawkins and Sutton, 2009; Trinh et al., 2017). Uncertainty may come from the GCMs' structure and the selection of parameters and scenarios. Furthermore, there have been studies introducing downscaling methods' uncertainty and hydrologic model uncertainties. Uncertainty may be minimized by validating GCMs' outputs, downscaling, and hydrologic results and quantifying differences between historical simulated and observed data (Trinh et al., 2016). In this study, there are two different bias-correction applications: (1) precipitation bias-correction in which a bias-correction method is applied to quantify differences between WRF simulation and observation data; and (2) streamflow bias-correction in which a bias-correction is applied to quantify differences between the WEHY-hydrologic module flow simulations and observed flow data.

### 3.2.1. Precipitation Bias Correction

Before using the future projections of the CCSM4 and MIROC5 for further applications, such as atmospheric and hydrologic processes, it is necessary to incorporate historical biases into the future downscaled results. To do so, downscaled precipitation simulations can be compared to corresponding historical model simulations in terms of monthly mean statistics over the whole modeling domain in order to quantify the trend over the model domain.

Bias correction of historical precipitation climatology should be made before applying them to future simulations.

$$P_{bc}^{ijk} = P_s^{ijk} \frac{P_{op}^{ij}}{P_{sp}^{ij}} \quad (3.1)$$

$P_{bc}^{ijk}$ : Projection precipitation after incorporating the bias correction

j is the month (k = 1, 2, ..., 12)

$i$  number of grids over the model domain ( $i = 1, \dots, 8190$ )

$k$  is the year

$P_s^{ijk}$ : Projection precipitation before incorporating the bias correction.

$P_{sp}^{ij}$ : Control-run precipitation (during 1980-2005 water years).

$P_{op}^{ij}$ : Observation precipitation. (VNGP—10-km resolution, monthly intervals, Vietnam coverage—during 1980-2005 water years).

Control-run simulated hydrological data were used to create bias correction by means of comparisons with observed precipitation data. These bias-corrected precipitation data were then used to reconstruct and project hydrological processes and water balance analysis.

### 3.2.2. Streamflow Bias Correction

This section introduces a new approach to correct control-run flow data. Similar to the previous section, flow bias correction compares the monthly mean WEHY simulated hydrologic data against the corresponding historical observed monthly mean data. The following is the application of the equation.

$$Q_{bc}^{ijk} = \left[ \frac{(Q_{sf}^{ijk} - \mu_{sf}^{ij})}{\delta_{sf}^{ij}} \right] \delta_{of}^{ij} + \mu_{of}^{ij} \quad (3.2)$$

$Q_{bc}^{ijk}$ : Bias-corrected flow data after incorporating the bias correction with  $i = 1, 2, \dots, 12$

( $i$  corresponding to 12 months in a year); year  $k$  falling within the 15-year period  $j = I, II, III$ , where I is the period from 1961-1975; II is period from 1976-1990; and III is period from 1991-2005)

$Q_{sf}^{ijk}$ : Flow data before incorporating the bias correction. ( $sf$  stands for simulated flow)

$\mu_{sf}^{ij}$ : Mean of simulated flow data before incorporating the bias correction at month i and during 15-year period j.

$\delta_{sf}^{ij}$ : Standard deviation of simulated flow data before incorporating the bias correction.

$\mu_{of}^{ij}$ : Mean of observed flow data at month i and during 15-year period j.

$\delta_{of}^{ij}$ : Standard deviation of observed flow data

$Q_{bc}^{ijk}$  are obtained from simulated flow data by means of the WEHY model with inputs provided from WRF model's outputs.  $Q_{bc}^{ijk}$  is monthly flow data at future year k at the outlet point at Lo watershed (Tuyen Quang Station).  $\mu_{sf}^{ij}$  and  $\delta_{sf}^{ij}$  are calculated based on  $Q_{bc}^{ij}$  time series data. Meanwhile  $\mu_{of}^{ij}$  and  $\delta_{of}^{ij}$  are calculated based on observed flow data at Tuyen Quang station.

The historical  $\mu_{of}^{ij}$  and  $\delta_{of}^{ij}$  are calculated during 1961-2005 using 45 years of observation data. The observations are divided into 3 different periods with intervals of 15 years including: I from 1961-1975; II from 1976 to 1990; and III from 1991 to 2005. Within each 15-year period, there are 12 values for  $\mu_{of}^{ij}$  and 12 values for  $\delta_{of}^{ij}$  corresponding to the 12 months. To begin bias-correction, the standardized-simulated flow data are calculated, and then  $\mu_{of}^{ij}$  and  $\delta_{of}^{ij}$  are calculated. Once  $\mu_{sf}^{ij}$  and  $\delta_{sf}^{ij}$  are obtained, the trend of  $\mu_{of}^{ij}$  and  $\delta_{of}^{ij}$  from the first window to the third window period is estimated. Then, future  $\mu_{of}^{ij}$  and  $\delta_{of}^{ij}$  are estimated based on the historical trend from observation data. Finally, the  $Q_{bc}^{ijk}$  is calculated based on standardized-simulated flow data and  $\mu_{of}^{ij}$  and  $\delta_{of}^{ij}$  as shown in equation 3.2.

### **3.3 Results**

#### **3.3.1. Precipitation Bias Correction Results**

GCM-based CCSM4 and MIROC5 historical climate simulations for the late twentieth and early twenty first centuries (CCSM4: 1980-2005, MIROC5: 1980-2005) were applied over the Lo River watershed by means of dynamical downscaling using the WRF model with spatial resolution of 9 km at hourly increments. Bias correction was conducted based on the monthly climatology of precipitation from the VNGP data and then incorporated into the CCSM4-GCM-based and MIROC5-GCM-based future precipitation projections. First, the downscaled historical precipitation from MIROC5 and CCSM4 were averaged over the LRW and converted to monthly data as shown in Figure 3.1-a. WRF-simulated monthly precipitation from CCSM4 and MIROC5 were compared to corresponding observation data (VNGP) (Figure 3.1-a). Applying the proposed bias correction method for precipitation over the LRW, the bias-corrected basin-averaged precipitation were also compared to VNGP as shown in Figure 3.1-b. As shown, the bias-corrected WRF simulation results are a better match to the VNGP data than the uncorrected results. A similar comparison is provided for annual precipitation. Figure 3.2 a and b respectively show comparisons between uncorrected and bias-corrected WRF-simulated and VNGP observed data from water year 1980 to water year 2005 for the LRW.

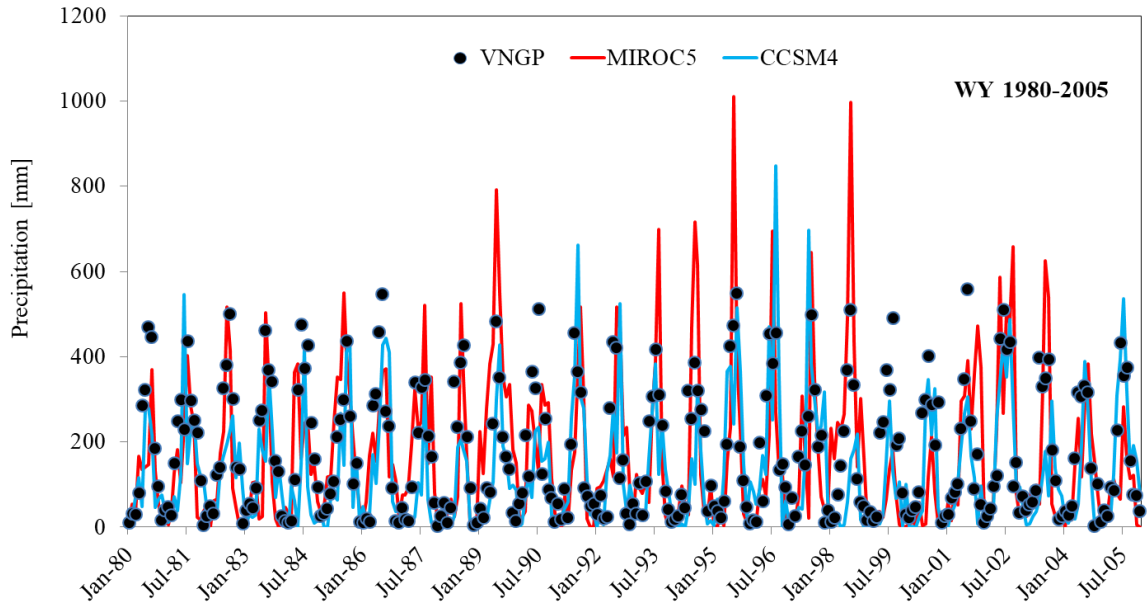


Figure 3.1a Comparisons of WRF-simulated monthly precipitation versus VNGP monthly precipitation from water year 1980 to water year 2005 for the LRW (before precipitation bias-correction)

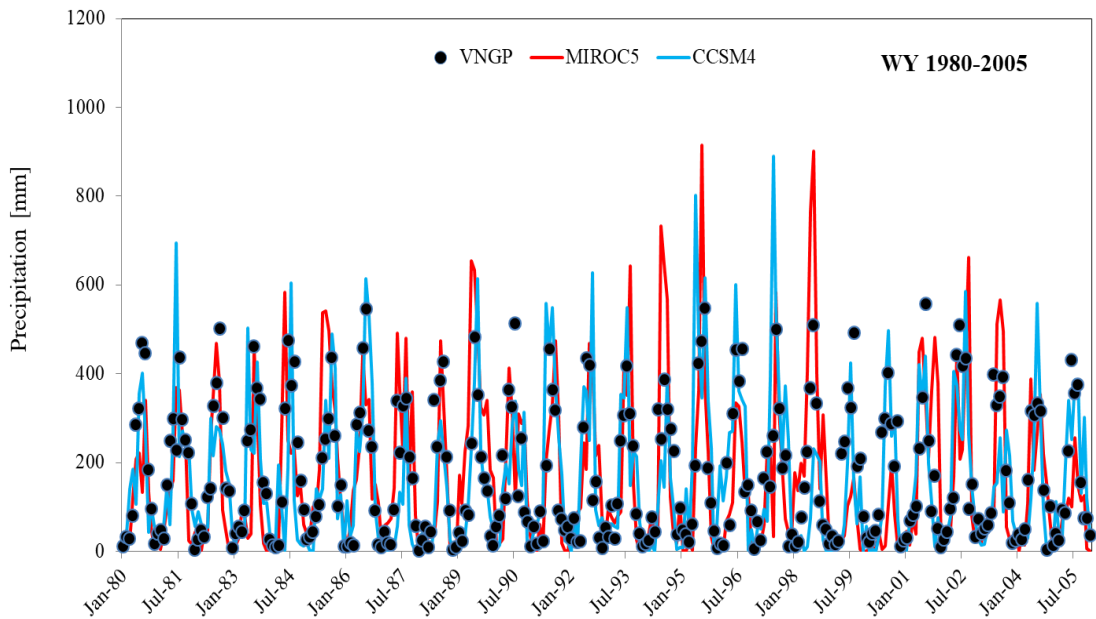


Figure 3.1b Comparisons of WRF-simulated monthly precipitation versus VNGP monthly precipitation from water year 1980 to water year 2005 for the LRW (after precipitation bias-correction).

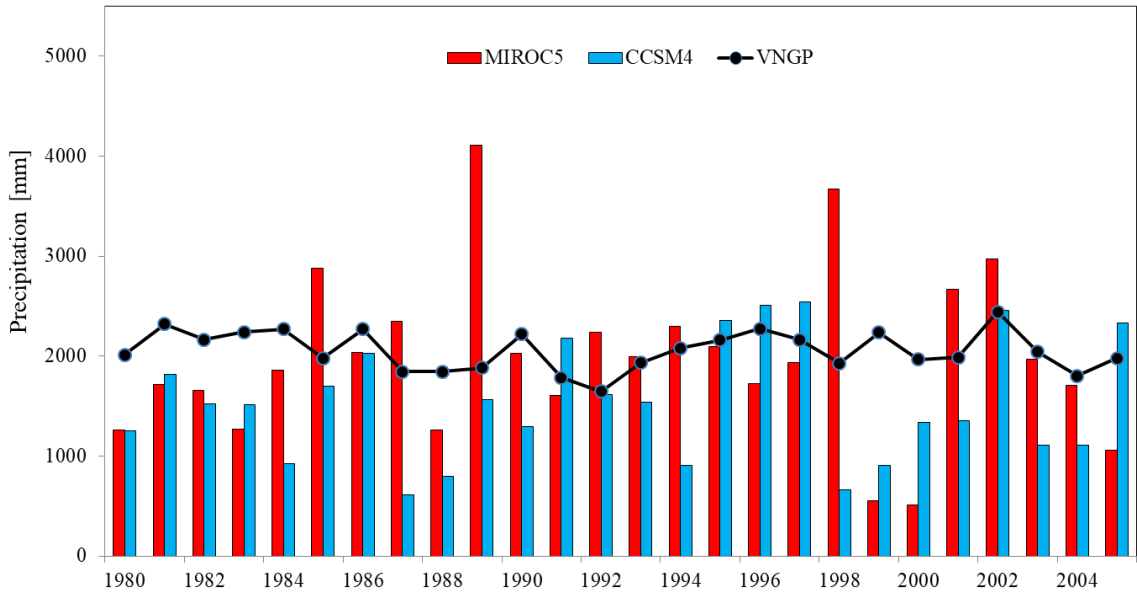


Figure 3.2a Comparisons of WRF-simulated annual precipitation versus VNGP annual precipitation from water year 1980 to water year 2005 for the LRW (before precipitation bias-correction)

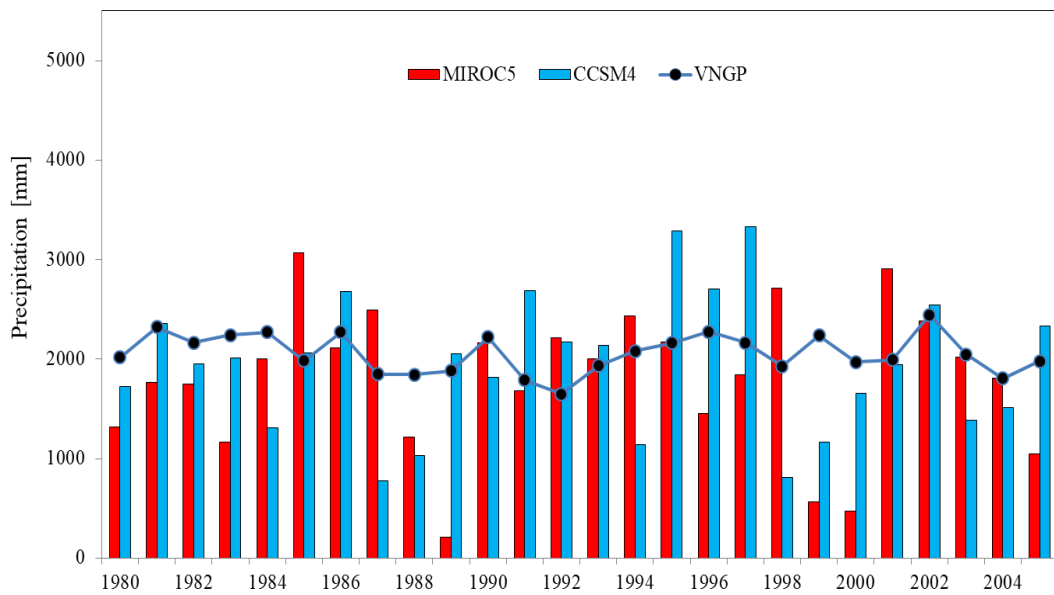


Figure 3.2b Comparisons of WRF-simulated annual precipitation versus VNGP annual precipitation from water year 1980 to water year 2005 for the LRW (after precipitation bias-correction).

The data resulting from simulations based on GCM-CCSM4 or MIROC5 are different from using reconstructed reanalysis data, such as ERA-20C. The simulations of GCM-based CCSM4/MIROC5 focus on the climatology of the specified period rather than the prediction of actual precipitation during the period. Thus, these simulations are not comparable with the time-series of observed precipitation (VNGP). One method for comparing GCMs-based WRF simulations and a time-series of observed precipitation is to look at long-term precipitation trends using the 5-year moving average of annual precipitation. These trends are compared for water years 1980 to 2005 in Figures 3.3-a, and b.

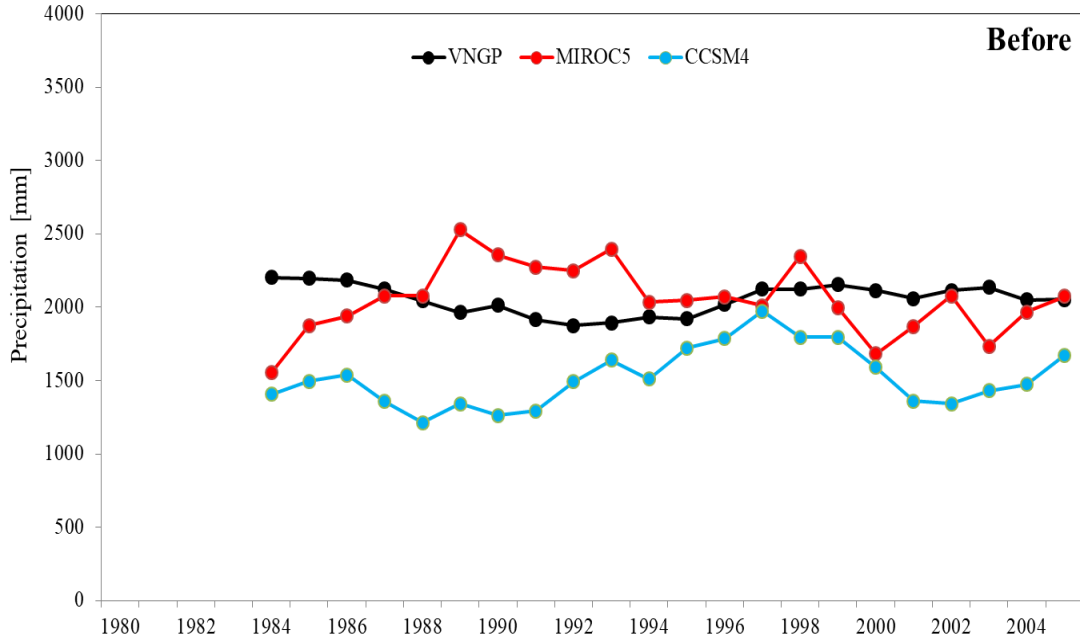


Figure 3.3a Comparisons of 5-year moving LRW average annual precipitation between VNGP and WRF-simulated precipitation during water year 1980 to water year 2005 (before precipitation bias-correction)

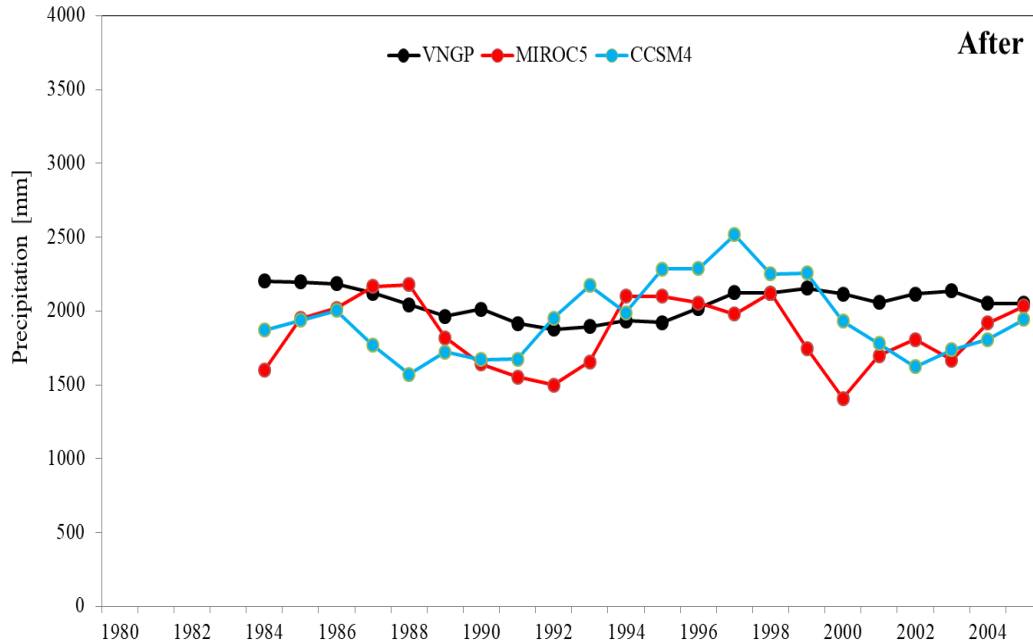


Figure 3.3b Comparisons of 5-year moving Lo watershed average annual precipitation between VNGP and WRF-simulated precipitation from water year 1980 to water year 2005(after precipitation bias-correction)

After applying a mean-monthly basin averaged bias correction, the WRF simulated precipitation trend improved and was similar to the corresponding precipitation trends. Furthermore, the statistics for GCMs-based WRF simulations, evaluated against observation values during 1980 to 2005 for the LRW, were also improved after applying the bias-correction method (Table 3.1). Statistical tests indicate the reliability and capability of WRF simulations for downscaling of atmospheric variables from a GCM output.

Table 3.1 Mean, standard deviation, and correlation coefficient of LRW average monthly precipitation observations and WRF-simulations with CCSM4 and MIROC5 inputs

Statistics	VNGP (1980- 2005)	CCSM4 before-bias (1980-2005)	CCSM4 after-bias (1980-2005)	MIROC5 before-bias (1980-2005)	MIROC5 after-bias (1980-2005)
Mean	171.94	128.26	162.43	165.42	169.32
STDEV	149.65	140.87	157.12	179.39	169.05
Correlation coefficient	/	0.651	0.71	0.629	0.677

After successfully reconstructing the historical climate data based on the two GCM outputs (CCSM4 and MIROC5) from 1980 to 2005, the bias-corrected precipitation data can be used as input for the WEHY model simulations. The bias-corrected precipitation in combination with other variables such as short and long wave radiation, wind speed, relative humidity, and air temperature, are input into the WEHY model in order to quantify the flow condition over the LRW.

### 3.3.2. Streamflow Bias Correction Results

Bias-corrected precipitation data from the WRF simulation of both GCMs were input into the WEHY model to simulate flow over the LRW from 1980-2005. The parameters applied in WEHY are unchanged from the validated parameters of Chapter 2. The WEHY-simulated flow data were then compared to corresponding observation data at Tuyen Quang. In Figure 3.4, monthly observed flow at Tuyen Quang is plotted along with four sets of simulated flow data at Tuyen Quang for the simulation period. The four sets of simulated flow data represent WEHY simulation results using WRF downscaled CCSM4 (C\_be) and MIROC5 data (M\_be), and precipitation bias-corrected WRF downscaled CCSM4 (C\_af) and MIROC5 data (M\_af). Mean-

monthly observation data and monthly means of the four sets of simulated flow data (C\_be, M\_be, C\_af and M\_af) at Tuyen Quang station are shown in Figure 3.5. Streamflow bias-correction has yet to be applied to the data shown in Figures 3.4 and 3.5.

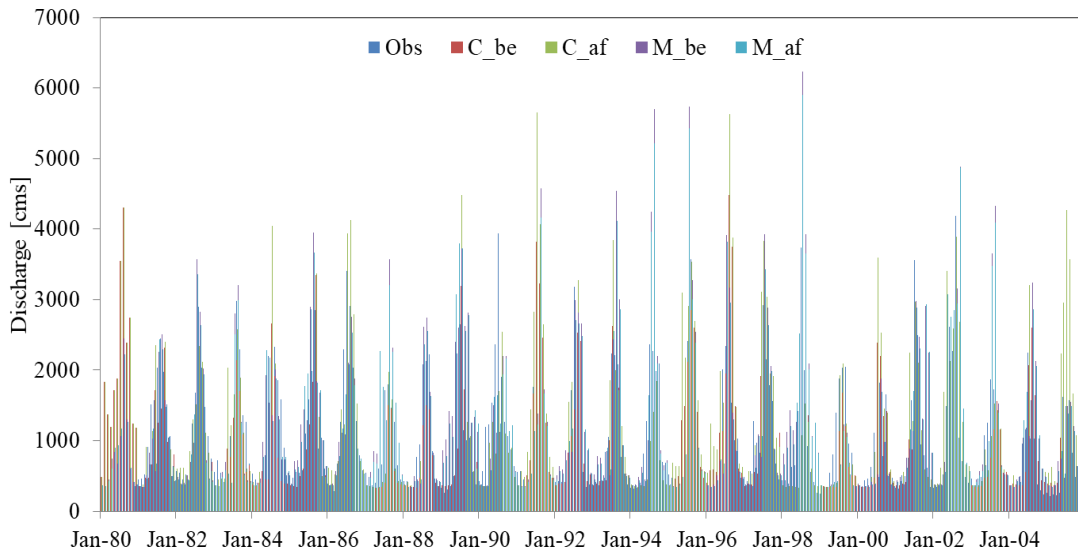


Figure 3.4 Monthly observation data and simulated flow data using four different climate inputs (before and after bias-correction downscaled atmospheric data from CCSM4 and MIROC5) at Tuyen Quang station

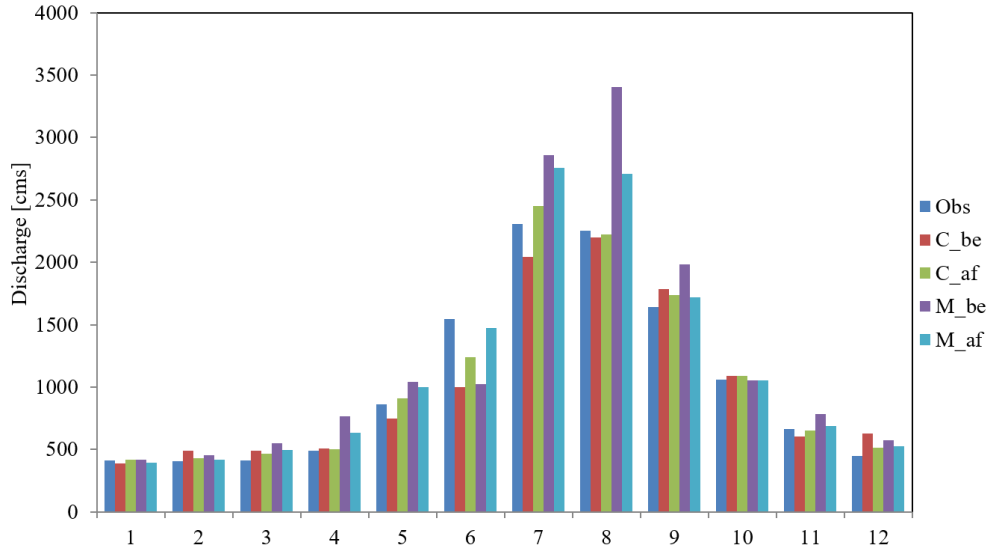


Figure 3.5 Mean monthly observation data and simulated flow data using four different climate inputs (before and after bias-correction downscaled atmospheric data from CCSM4 and MIROC5) at Tuyen Quang station

Similar to GCM-based CCSM4 and MIROC5 precipitation, flow data simulation results from GCM outputs may not be suitable for comparison to the time-series of observed flow due to the focus of GCM simulations on the climatology of the specified period rather than the prediction of actual flow during the period. It is more important to focus on long-term flow trends based on annual flow data and the 5-year moving average of annual flow between GCMs-based WRF simulations and observed values during water year 1980 to water year 2005. As shown in Figure 3.6, which contains the observed and simulated annual flow data, the simulated flow still includes bias and should be corrected after bias-correcting precipitation.

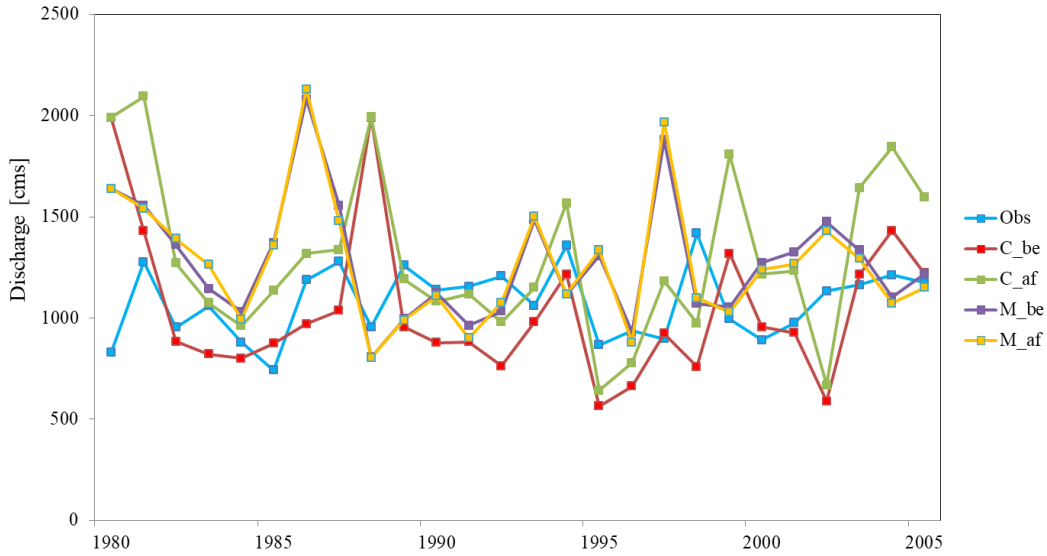


Figure 3.6 Observed and WEHY-simulated annual flow data during water year 1980 to water year 2005 (before and after precipitation bias-correction of downscaled atmospheric data from CCSM4 and MIROC5) at Tuyen Quang station

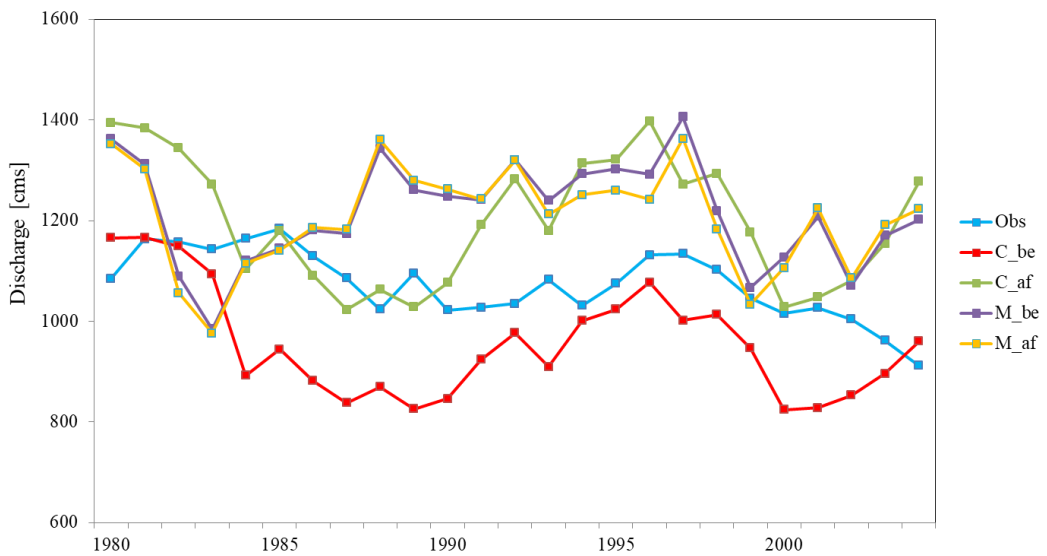


Figure 3.7 Observed and WEHY-simulated 5-year moving average annual flow data during water year 1980 to water year 2005 (before and after precipitation bias-correction of downscaled atmospheric data from CCSM4 and MIROC5) at Tuyen Quang station

To initiate the proposed streamflow bias-correction method, flow data must be standardized. There are five different sets of flow data including: observation data at Tuyen Quang station, WEHY simulated flow data resulting from downscaled GCMs, CCSM4 and MIROC5, and WEHY simulated flow data resulting from downscaled GCMs, CCSM4 and MIROC5 which have been precipitation bias-corrected. The standardization equation is the following:

$$Q_{j\text{sd}}^i = \left[ \frac{(Q_j^i - \mu^i)}{\delta^i} \right] \quad (3.3)$$

$Q_{j\text{sd}}^i$ : standardized flow data at month i and year j

$Q_j^i$ : Flow data at month i and year j

$\mu^i$  : Mean value of simulated flow data at month i

$\delta^i$  : Standard deviation value of simulated flow data at month i

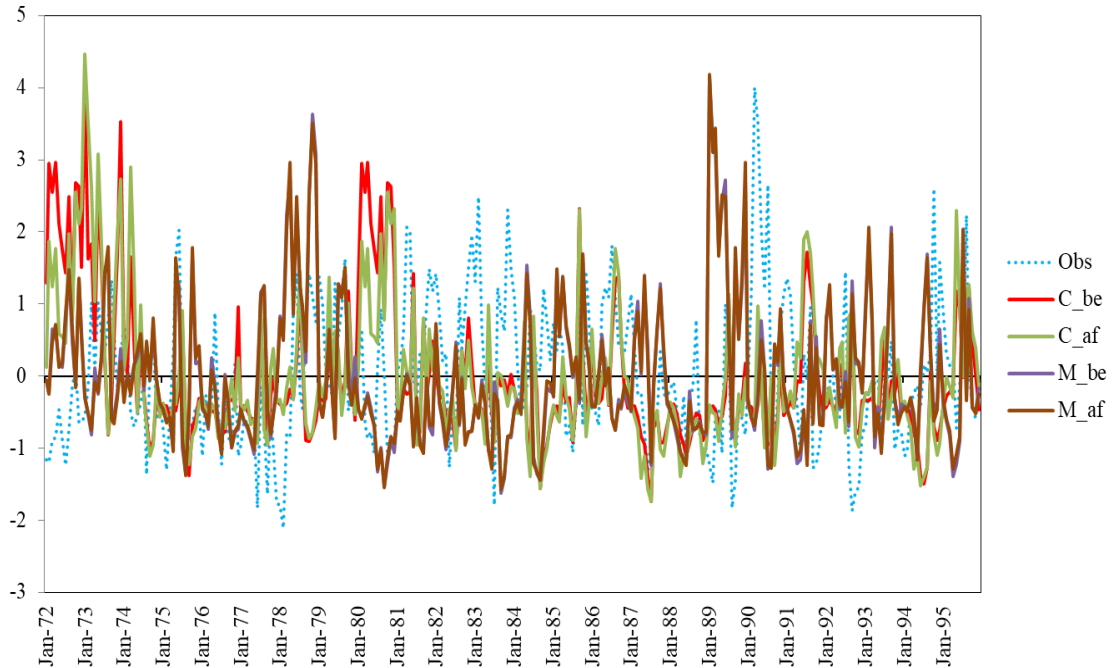


Figure 3.8 Time series data of Standardized flow data under observation and simulation conditions

Standardized flow data are shown in Figure 3.8. Following standardization, the mean and standard deviation of observation data were calculated based on three different time periods including, 1961-1975, 1976-1990, and 1991-2005. The mean and standard deviation values are shown in Figures 3.9 and 3.10 respectively, and tabulated in Tables 3.2 and 3.3 respectively. After quantifying the mean and standard deviation, estimates are made for the next period, based on the current trend as shown in the figures and tables. The trend is roughly estimated based on linear regression and values from the subsequent time period. The trends for each month increased in the wet season and decreased in dry season. Once the mean and standard deviation values for one time period are obtained, it is possible to apply the estimated mean and standard deviation to standardize the flow data in the next time period through application of Equation

3.2. Figure 3.11 contains monthly observed and bias-corrected simulation flow data at Tuyen Quang station during an 8-year period (2006-2015) for validation purposes.

Table 3.2 Mean monthly flow data at Tuyen Quang in each of the three periods

Period	1	2	3	4	5	6	7	8	9	10	11	12
1961-1975	357.9	310.8	293.0	375.2	789.3	1570.5	2226.7	2416.3	1626.8	1080.1	765.9	469.0
1976-1990	448.2	441.1	427.9	487.6	828.7	1536.6	2231.3	2367.9	1571.7	979.0	601.4	502.2
1991-2005	352.6	325.5	405.4	515.0	803.3	1585.9	2338.3	2449.7	1745.6	998.5	743.0	390.2

Table 3.3 Standard deviation of monthly flow data at Tuyen Quang in each of the three periods

Period	1	2	3	4	5	6	7	8	9	10	11	12
1961-1975	98.3	577.4	1212.9	1938.2	2013.2	538.2	1120.1	1608.0	1117.8	726.4	459.2	204.6
1976-1990	189.4	642.5	1319.6	1914.6	1943.1	634.4	1118.4	1651.1	1147.1	718.8	440.9	231.3
1991-2005	198.6	647.5	1331.3	2022.7	1939.5	604.5	1138.2	1745.1	1208.4	704.0	411.5	245.9

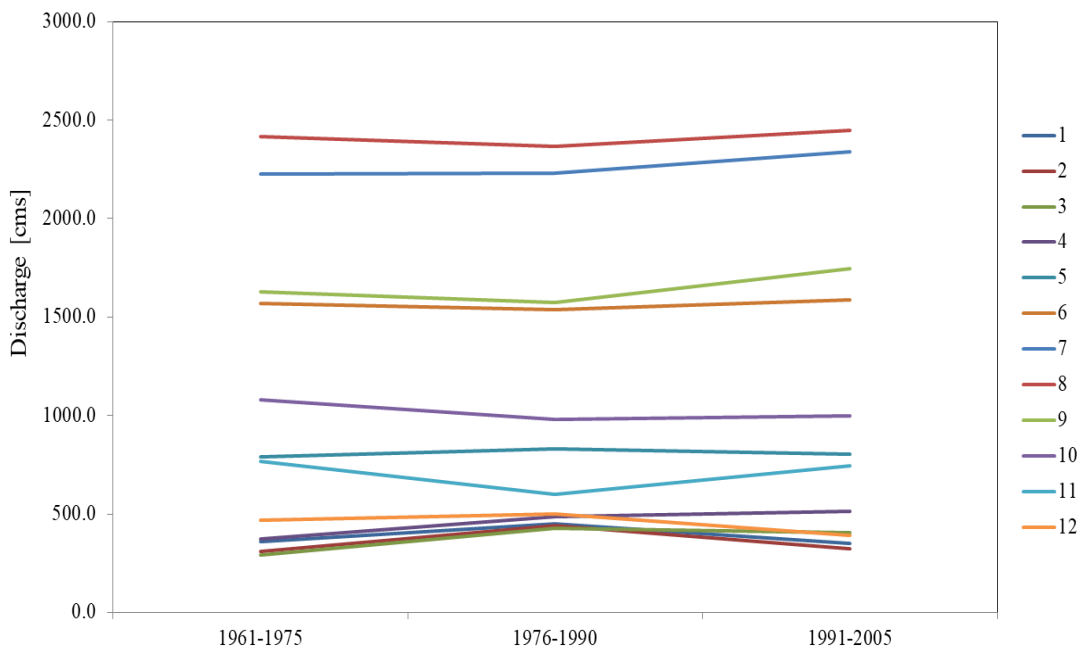


Figure 3.9 Monthly climatology of mean flow data at Tuyen Quang in three periods

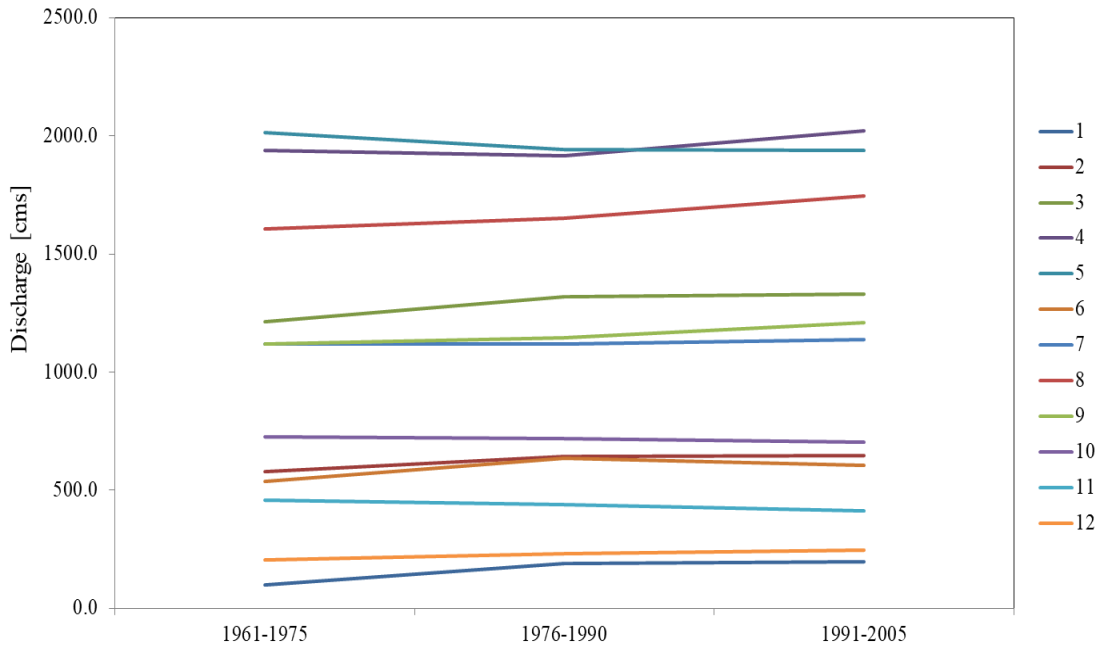


Figure 3.10 Monthly climatology of standard deviation flow data at Tuyen Quang in three periods

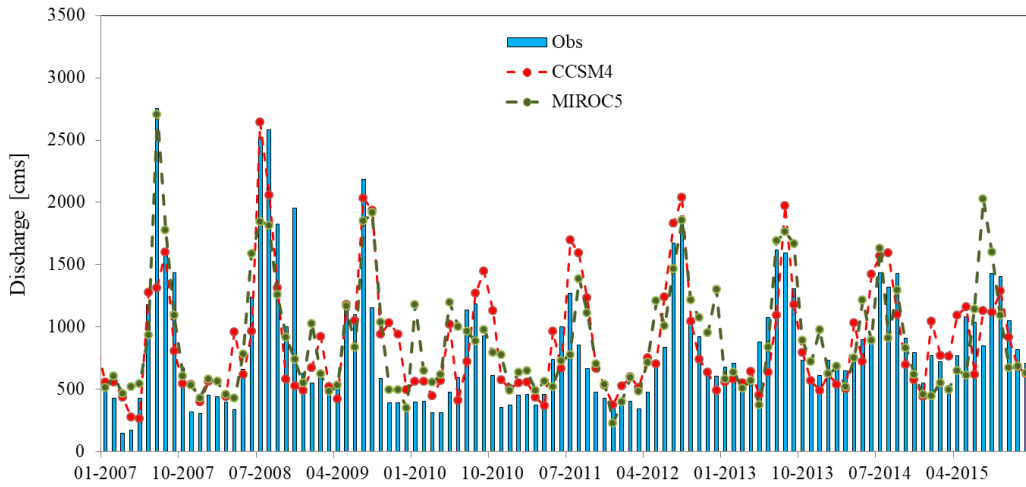


Figure 3.11 Observed and bias-corrected simulation flow data at Tuyen Quang (2007-2015)

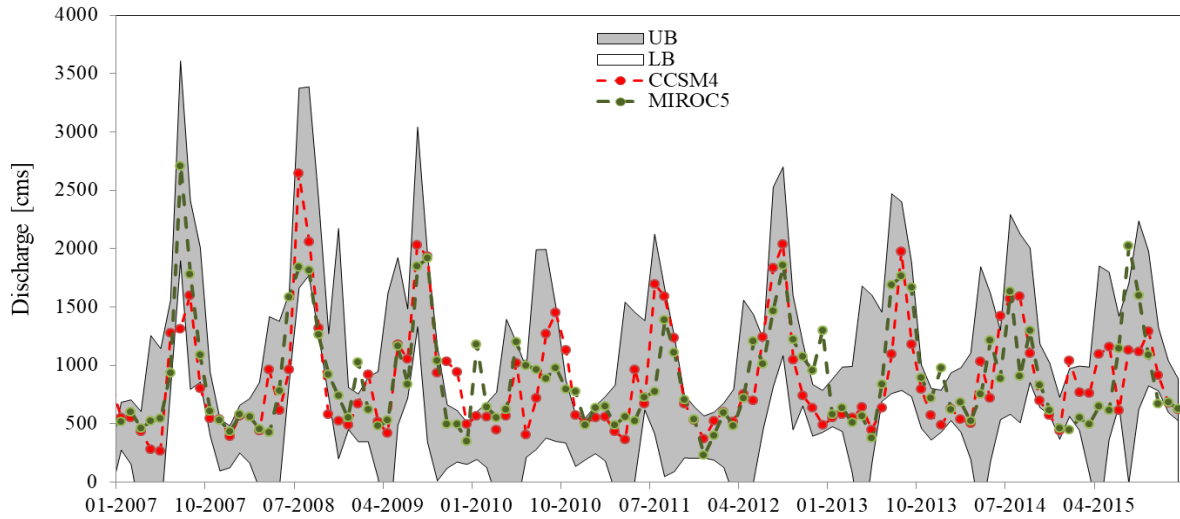


Figure 3.12 Bias-corrected simulation flow data at Tuyen Quang (2007-2015) and lower and upper band of monthly observed (corresponding to 5 and 95 % confidence band)

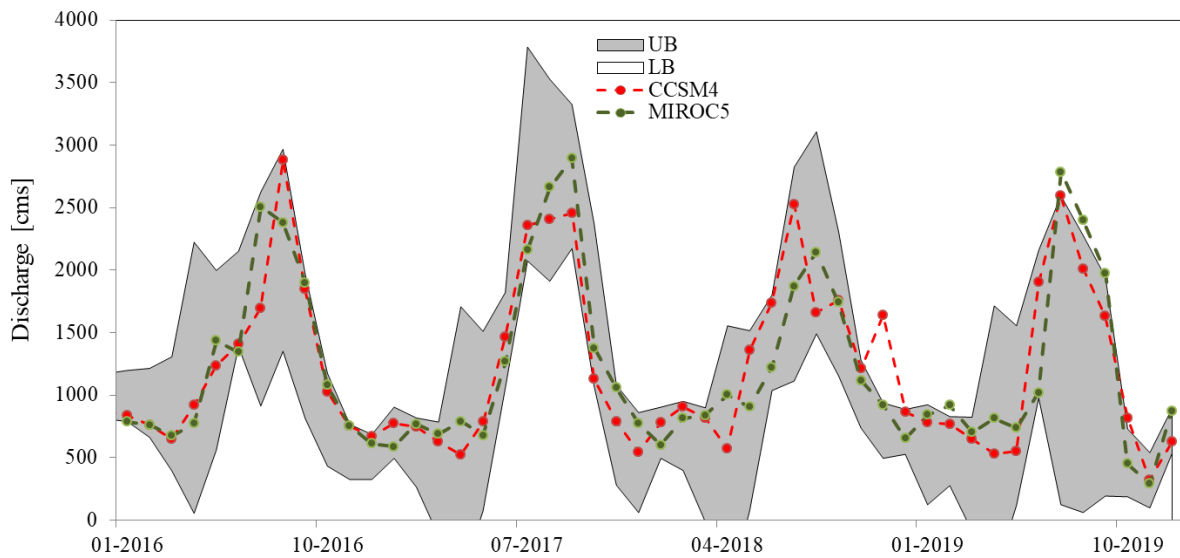


Figure 3.13 Bias-corrected simulation flow data at Tuyen Quang (2016-2019) and lower and upper band of monthly observed (corresponding to 5 and 95 % confidence band)

As seen in Figure 3.12, simulated monthly streamflow from bias-corrected CCMS4 and MIROC5 were plotted along with and lower and upper band of monthly observed data in gray (corresponding to 5 and 95 % confidence). Based on visual inspection, most of the observation values were inside the upper and lower bands. For CCSM4, 94 of the 108 points, or 87%, were within the confidence bands. For MIROC5, 97 of the 108 points, or approximately 90%, were within the confidence bands. Similarly, Figure 3.13 also shows bias-corrected simulated flow data at Tuyen Quang (2016-2019) and lower and upper band of monthly observed (corresponding to 5 and 95 % confidence band), with similar results.

### **3.4 Conclusions**

Precipitation and streamflow bias correction were successfully applied over the LRW. Comparison of observation and bias-corrected simulation precipitation and stream flow data showed that the corrected data agreed with the observations for both yearly and monthly data. After applying bias correction, the WRF simulated precipitation trend improved and was more similar to the corresponding precipitation trends. Furthermore, statistical coefficients for GCMs-based WRF simulations, evaluated against observation values during 1980 to 2005 for the LRW, were also improved after applying the bias-correction method (Table 3.1). Similarly, the streamflow bias correction data has a high correlation with observation data. The large majority of monthly observation points were inside the upper and lower bands. For CCSM4, 94 of the 108 points, or 87%, were within the confidence bands. For MIROC5, 97 of the 108 points, or approximately 90%, were within the confidence bands. These proposed methodologies are therefore reliable methods of estimating future water supply and will be useful in calculating the water balance and projecting drought conditions over the LRW.

## References

Dosio, A., Paruolo, P., 2011. Bias correction of the ENSEMBLES high-resolution climate change projections for use by impact models: evaluation on the present climate. *J. Geophys. Res. Atmos.* 116 (D16).

Hawkins, E., Sutton, R., 2009. The potential to narrow uncertainty in regional climate predictions. *Bull. Am. Meteorol. Soc.* 90 (8), 1095.

Trinh, T., Ishida, K., Kavvas, M.L., Ercan, A. and Carr, K., 2017. Assessment of 21st century drought conditions at Shasta Dam based on dynamically projected water supply conditions by a regional climate model coupled with a physically-based hydrology model. *Science of the Total Environment*, 586, pp.197-205.

Trinh, T., Ishida, K., Fischer, I., Jang, S., Darama, Y., Nosacka, J., Brown, K. and Kavvas, M.L., 2016. New methodology to develop future flood frequency under changing climate by means of physically based numerical atmospheric-hydrologic modeling. *Journal of Hydrologic Engineering*, 21(4), p.04016001.

Brown, J.D. and Seo, D.J., 2013. Evaluation of a nonparametric post-processor for bias correction and uncertainty estimation of hydrologic predictions. *Hydrological Processes*, 27(1), pp.83-105.

Piani, C., Weedon, G.P., Best, M., Gomes, S.M., Viterbo, P., Hagemann, S. and Haerter, J.O., 2010. Statistical bias correction of global simulated daily precipitation and temperature for the application of hydrological models. *Journal of hydrology*, 395(3-4), pp.199-215.

## **CHAPTER 4. DYNAMICAL DOWNSCALING OF GLOBAL CLIMATE MODELS TO PROJECT WATER SUPPLY OVER THE LO RIVER WATERSHED**

### **Abstract**

Global Climate Model outputs can provide the whole Earth's climate for decades, even centuries, but in order to gain economy in numerical computations their spatial resolutions are quite coarse. The resolutions of GCM data are usually larger than  $1^\circ$  (~ 110 km around the tropics), making them too coarse to resolve the fundamental influence of steep topography. This is true for the source regions of the LRW, and for the convective precipitation due to orographic effects in these regions. In order to achieve realistic precipitation projections, it is necessary to downscale the coarse-grid-resolution GCM climate projections to finer space and time resolutions over the basin. In this chapter, the future climate projections, based on two emission scenarios simulated by two GCMs, the fifth generation of Model for Interdisciplinary Research on Climate - MIROC5, and the fourth version of the Community Climate System Model - CCSM4 are utilized to help in the projection of water supply of the LRW. These two GCMs were selected with two scenarios: Representative Concentration Pathways - RCP 4.5 and 8.5, as recommended by the Vietnam Ministry of Natural Resources and Environment. These global datasets were downscaled to 9-km spatial resolution at hourly intervals by means of the WRF model (Chapter 2). The downscaled precipitation data were then adjusted by bias correction using ground observation data, and used to simulate flow conditions over the LRW by the hydrologic model WEHY before applying streamflow bias-correction to provide reliable flow data and water supply for the LRW (Chapter 3).

Analysis of the WEHY-WRF applications shows that the ensemble mean of the annual mean air temperature is expected to increase by  $2.04^\circ\text{C}$  from 2011 to 2100. No significant trend

was found in the annual mean solar radiation toward the end of the 21st century. Based on the Mann-Kendall test (at 95% confidence level), no trend in annual precipitation over the LRW can be determined. However, a slightly increasing trend is detected for flow data at Vu Quang station. Additionally, analysis shows that flow has no trend in the early 21st century (2011-2035), but does have 3 significant wave-like increasing and decreasing trends in the later 21<sup>st</sup> century (2035-2053; 2054-2074; and 2075-2093). Results from this chapter are used to compare water demand (Chapter 5) to provide early drought forecasting events through drought analysis.

#### **4.1 Introduction**

Fundamentally, the Lo River watershed (LRW) as a transboundary region is an area of complex water resources management. The Upper LRW lies in China and the Lower LRW lies in Vietnam. Differences among these countries in terms of physical features, governmental policies, and priorities in short- and long-term water resources management may lead to conflicts in the management and sharing of water. While countries compete to protect their own interests, upstream countries hold an advantage, while downstream countries must usually remain passive in using these water resources. Any upstream development; mainly dams, reservoirs, deforestation, large scale irrigation schemes, urbanization, upstream flood protection, and other forms of land use change, will have a direct impact on the river flow, both in wet and dry seasons.

To develop a better understanding of the hydrologic regimes of the LRW, especially considering the impacts of climate change, understanding the timing and duration of hydro-meteorological hazards is essential to reduce socio-economic effects. There is an urgent need to develop advanced models, which apply to the LRW while accounting for the balance between data availability and model complexity. The output of such models will be used to develop water

balances for the future, in which a rising water demand, declining water supply, and more frequent and intense drought events are expected. These models' outputs can also be used as seasonal forecasting systems providing early warning information across the river basin.

Currently, GCMs are considered the best tool for estimating future climate change (Dosio and Paruolo, 2011; Hawkins and Sutton, 2009; Maurer, 2007; Maurer and Duffy, 2005; Teutschbein and Seibert, 2012). GCM outputs can provide the whole Earth's climate for decades, even centuries. However, their spatial resolutions are necessarily quite coarse in order to be able to gain economy in numerical computations (Trinh et al., 2017). Resolutions of GCM data are usually larger than  $1^\circ$  (~ 110 km around the tropics) making them too coarse to resolve the fundamental influence of steep topography of the source regions of the LRW, on the convective precipitation due to orographic effects in these regions. Since none of the GCMs can resolve the steep topography of the source regions of the LRW, they cannot model the precipitation over the vital source regions of the basin reliably. Therefore, in order to obtain realistic results on the assessment of the climate change impact on the LRW with respect to water balances and hydrologic extremes (floods and droughts), it is necessary to obtain realistic precipitation projections over the LRW source regions. Realistic precipitation projections require coarse-grid-resolution (larger than  $1^\circ$ ) GCM climate projections to be downscaled to finer space and time resolutions. There are two main approaches to downscaling GCM climate projections over a selected geographical region: a) statistical downscaling approach, and b) dynamical downscaling approach. As shown in Chapter 2, dynamical downscaling is a feasible method because it represents spatial trends well in the projected precipitation fields over Vietnam, including the LRW, while statistical downscaling showed limitations in projecting future precipitation.

In this chapter, the future climate projections, based on two emission scenarios simulated by two global climate models (GCMs), the fifth generation of Model for Interdisciplinary Research on Climate - MIROC5, and the fourth version of the Community Climate System Model - CCSM4 are utilized to help in the projection of water supply of the LRW. These two GCMs were selected with two scenarios: Representative Concentration Pathways - RCP 4.5 and 8.5, as recommended by the Vietnam Ministry of Natural Resources and Environment. These global datasets were downscaled to 9-km spatial resolution at hourly intervals by means of the WRF model (Chapter 2). The downscaled precipitation data were then adjusted by bias correction using ground observation data. The downscaled-corrected atmospheric data were then used to simulate flow conditions over LRW with the hydrologic model- WEHY before applying streamflow bias-correction to provide reliable flow data and water supply for the LRW (Chapter 3). The WEHY-WRF models used were set up and described in the Chapter 2.

## **4.2 Methodology**

The projection of water supply described here was carried out over LRW as part of a larger study to assess water balance and drought conditions based on projected water supply and water demand during the 21<sup>st</sup> century. This chapter introduces a methodology to provide a reliable projection of future atmospheric-hydrologic conditions over the LRW. The method for projection of water supply starts by obtaining GCM data, which are the construction of mathematical formulations of the climate processes system. The system can be classified as the atmosphere, oceans, and land components which are constituted by processes such as radiation, energy transfer by winds, cloud formation, evaporation and precipitation of water and heat transportation by ocean currents (Earth Exploration Toolbook, 2014). GCMs utilize numerical methods which calculate, in a 3-dimensional grid system developed by physically based equation

and parameterizations, approximate solutions. The essential physical variables are temperature, pressure, east-west wind and north-south wind and specific humidity. The Intergovernmental Panel on Climate Change, in their fifth assessment report on climate change (IPCC AR5), recommended a new set of scenarios, denoted as “Representative Concentration Pathways (RCPs). RCPs are defined by their approximate total radiative forcing in year 2100 relative to 1750: 2.6 W/m<sup>2</sup> for RCP2.6, 4.5 W/m<sup>2</sup> for RCP4.5, 6.0W/m<sup>2</sup> for RCP6.0, and 8.5W/m<sup>2</sup> for RCP8.5. For RCP6.0 and RCP8.5 radiative forcing does not peak by 2100. For RCP2.6 it peaks and declines during the 21st century, and for RCP4.5 it stabilizes by 2100. RCPs are based on a combination of integrated assessment models, simple climate models, atmospheric chemistry, and global carbon cycle models. Including the prescribed concentrations of other greenhouse gases, the combined CO<sub>2</sub>-equivalent concentrations are: 475 ppm (RCP2.6), 630 ppm (RCP4.5), 800 ppm (RCP6.0), and 1313 ppm (RCP8.5) (From the ICPP AR5 Working Group I Report). RCP 4.5 and 8.5 emission scenarios are highly recommended by the Vietnamese government (MONRE 2016).

As mentioned in the previous section, the grid resolutions of GCMs are usually larger than 1° (110km) which is too large for regional studies. Therefore, dynamical downscaling is required to refine the quality of data. The WRF model was used to refine the selected GCM’s data, requiring 3-dimensional atmospheric data as initial and boundary conditions. For the historical climate simulations such data are available from global control run datasets. For the simulation of future climate projections, such 3-dimensional data are obtained from the latest CMIP5 (of IPCC Assessment Report 5) GCM climate projections of the 21st century. Dynamical downscaling is computationally intensive. However, new computing technologies make it possible to complete the simulation of the selected climate projections of the 21st century from 2

GCMs of CMIP5 under different emission scenarios at 9-km grid resolution over the entire LRW.

After dynamical downscaling, the GCM's output from coarse to fine resolutions, these downscaled data can be used to project streamflow by means of the WEHY model. Soil and land cover characteristics are assumed the same as historical conditions, while the historical atmospheric data are replaced by future data. The WEHY model, including hillslope and river channel routing processes, in combination with the WEHY reservoir sub-program were used to simulate water supply over the LRW. After applying WEHY-WRF with inputs provided from the GCM's data, the future atmospheric-hydrologic data over the LRW was generated and these data can be used to analyze projected trends in atmospheric and hydrologic processes.

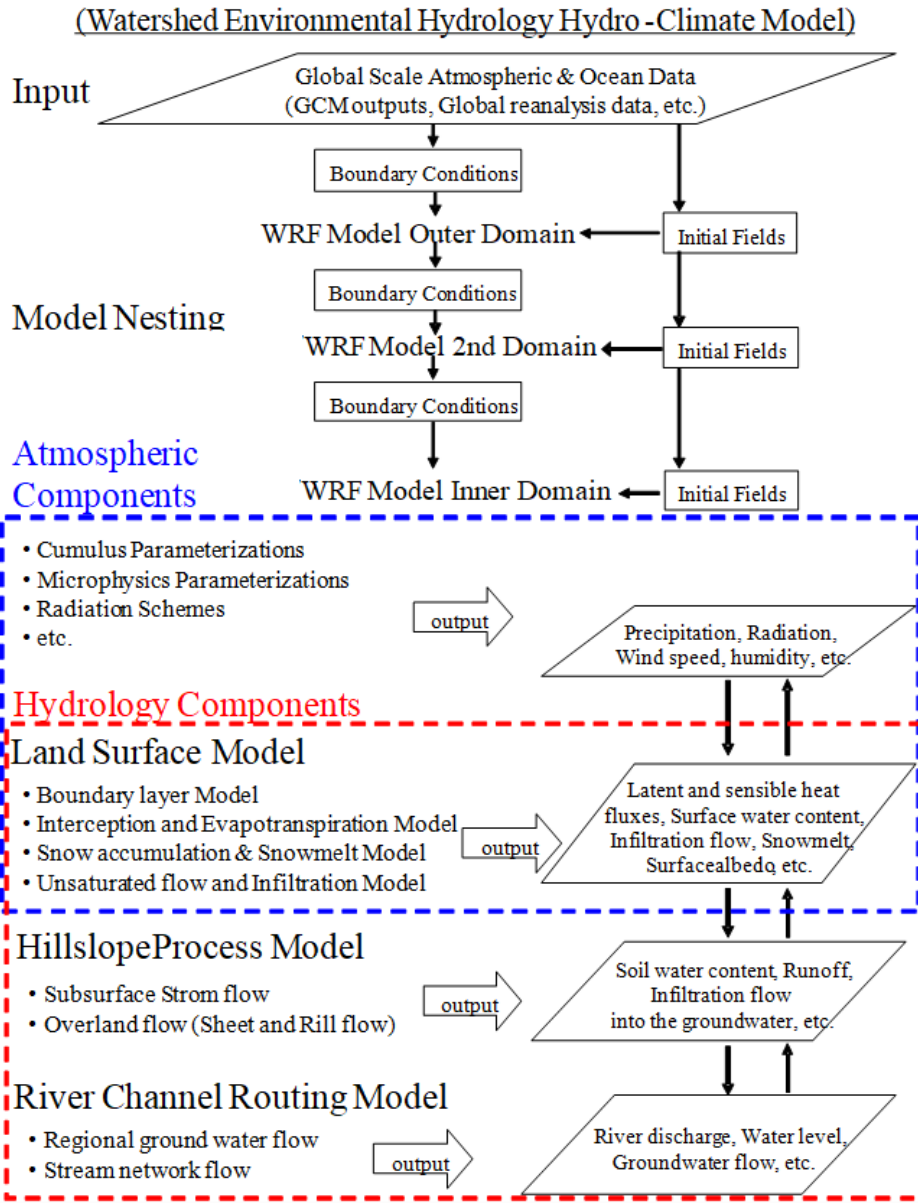


Figure 4.1 Structure and components of WEHY-WRF (Watershed Environmental Hydrology Hydro-Climate Model) (Kavvas et al. 2013)

### 4.3 Results

The validated WRF-WEHY-Reservoir models in Chapter 2 were applied over the LRW, with input from GCMs' outputs including MIROC5 and CCSM4. It is difficult to characterize

the future climate based on individual GCMs due to the temporal and spatial uncertainty in future climate conditions. It is recommended that a combination of GCM outputs be used as input to regional models for the projection of the future climate. In this study, the future projection of atmospheric-hydrologic conditions under a changing climate is based on the ensemble of projections by the regional atmospheric model WRF, based on 2-projection realizations from MIROC5 GCM (under RCP 8.5), and CCSM4 GCM (under RCP 4.5 scenarios).

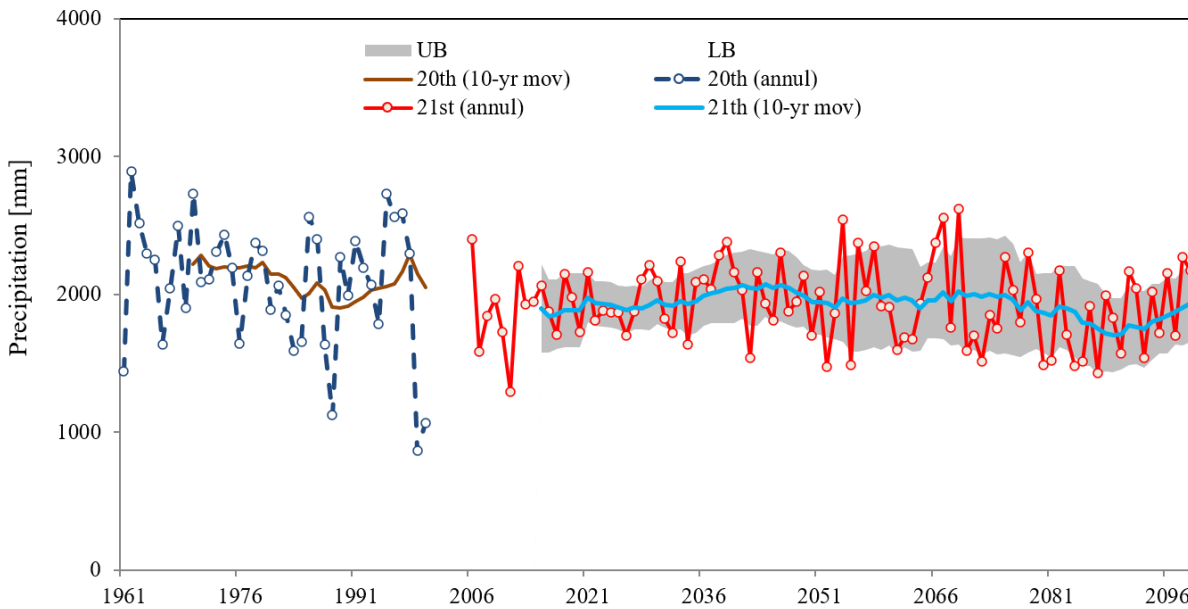


Figure 4.2 Historical and future GCM (MIROC5 and CCSM4)-based WRF projection of ensemble average annual precipitation for the LRW

Figure 4.2 contains historical annual LRW precipitation values and GCM-based future WRF-projected ensemble average annual LRW-average precipitation with 95% confidence interval. As shown in this figure, a trend in annual precipitation over the LRW cannot be determined, based on the Mann-Kendall test (at 95% confidence level).

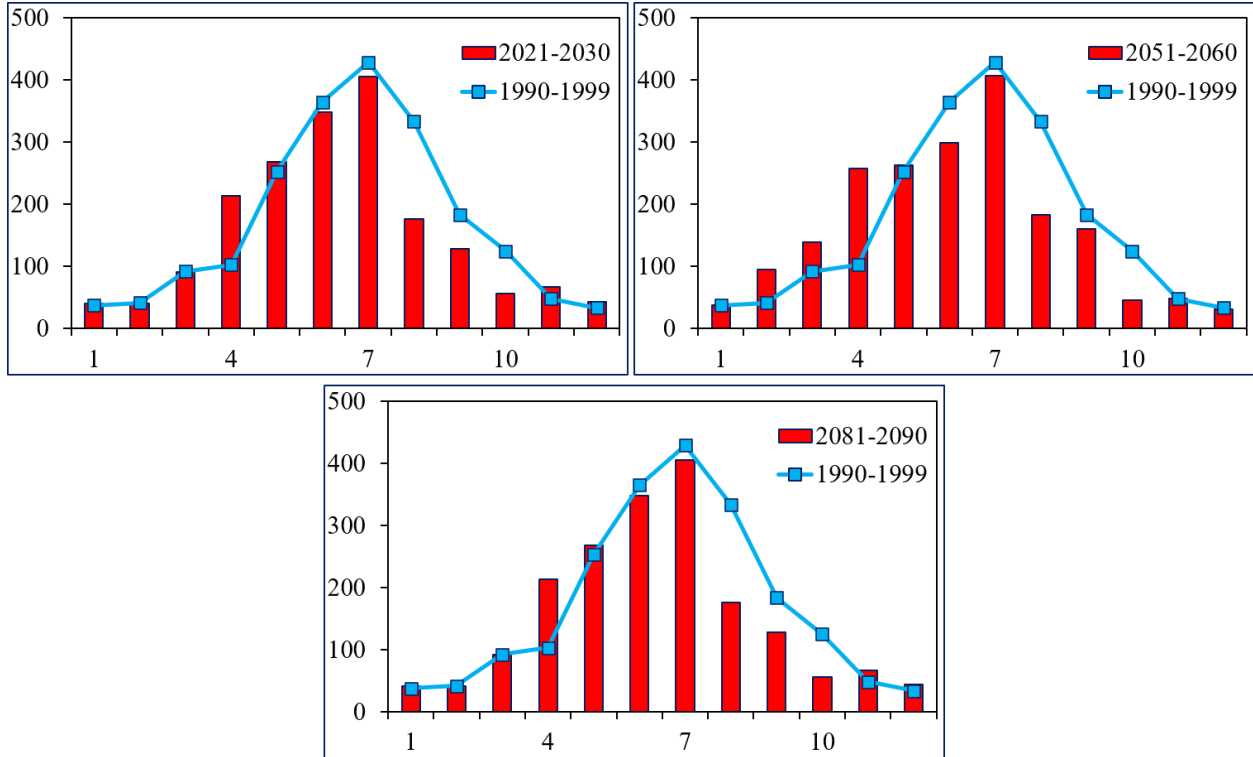


Figure 4.3 Future mean monthly precipitation in the early 21st century, mid-21st century and end of the 21st century and historical mean monthly precipitation during WY 1990 - WY1999 over the LRW

In order to analyze changes in the precipitation regime during 1950–2010, the monthly climatology basin average of annual precipitation was divided into three time windows of 10 years length, 2021–2030, 2051–2060, and 2081-2090, as shown in Figure 4.3. The figure shows that the dry season lasts for 7 months, and that the 2-month period from September to October has a decreasing trend compared to the control run (1990-1999). The wet season lasts for 5 months from April to September with no significant difference, except for August, in which there is a significantly decreasing trend compared to the historical precipitation.

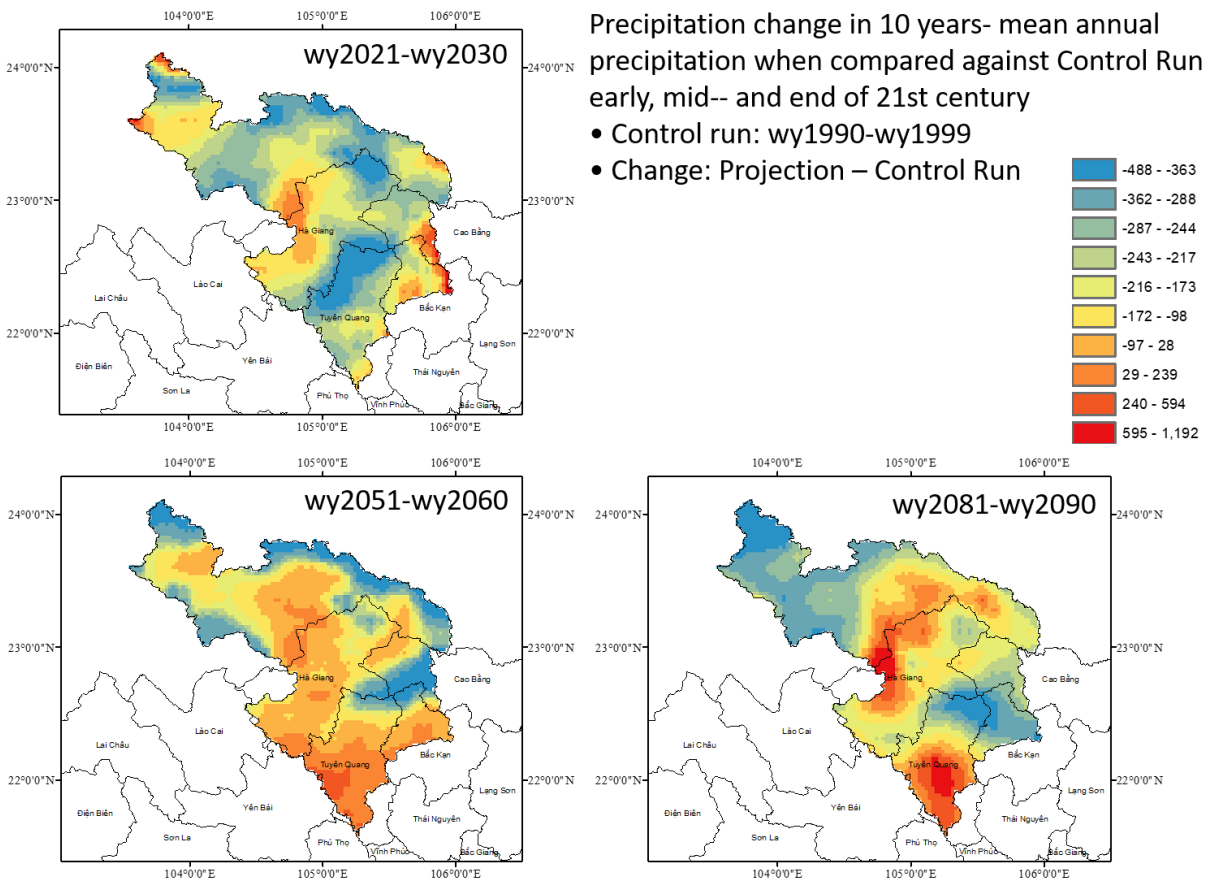


Figure 4.4 Comparison of the spatial change of precipitation against control run (10 years mean annual precipitation)

To identify the precipitation distribution for the whole study region, monthly climatology precipitation spatial distribution maps were applied (Figure 4.4). It may be inferred from visual observation that the projected mean monthly precipitation is significantly increased at the mid-21<sup>st</sup> century (WY 2051- WY 2060) and at the end of the 21<sup>st</sup> century (WY 2090 – WY 2099) when compared against the corresponding historical mean monthly precipitation (WY 1990 - WY 1999) over some sectors of the LRW. The projected mean monthly precipitation is

significantly increased over the south and the middle east areas of the LRW. The precipitation depth has a decreasing trend in the northern and western areas as seen in Figure 4.4

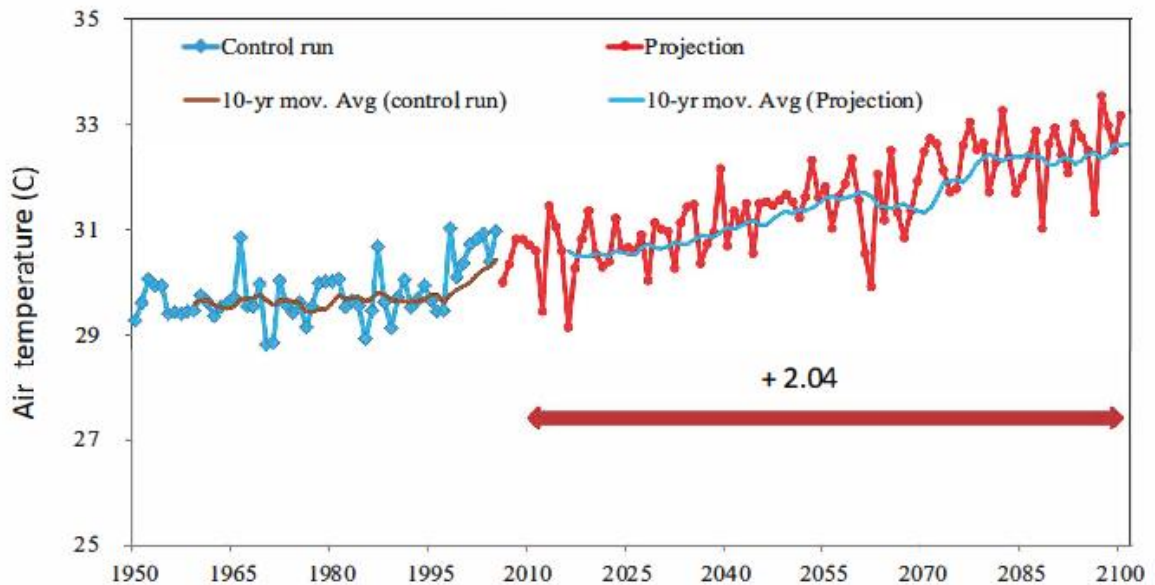


Figure 4.5 Historical and future GCM (MIROC5 and CCSM4)-based WRF projection of ensemble average annual air temperature for the LRW

Air temperature and solar radiation under the future 21<sup>st</sup> century climate was also projected, based on the downscaling of MIROC5 and CCSM4 GCM projections. Unlike precipitation, the annual mean air temperature, which is shown in Figure 4.5, has a clear warming trend toward the end of the 21<sup>st</sup> century when compared against the historical period. The change in annual mean air temperature is about 2.04 °C at the end of the 21<sup>st</sup> century over the LRW. Meanwhile, no significant trend was found in the annual mean solar radiation toward the end of the 21<sup>st</sup> century, as shown in Figure 4.6.

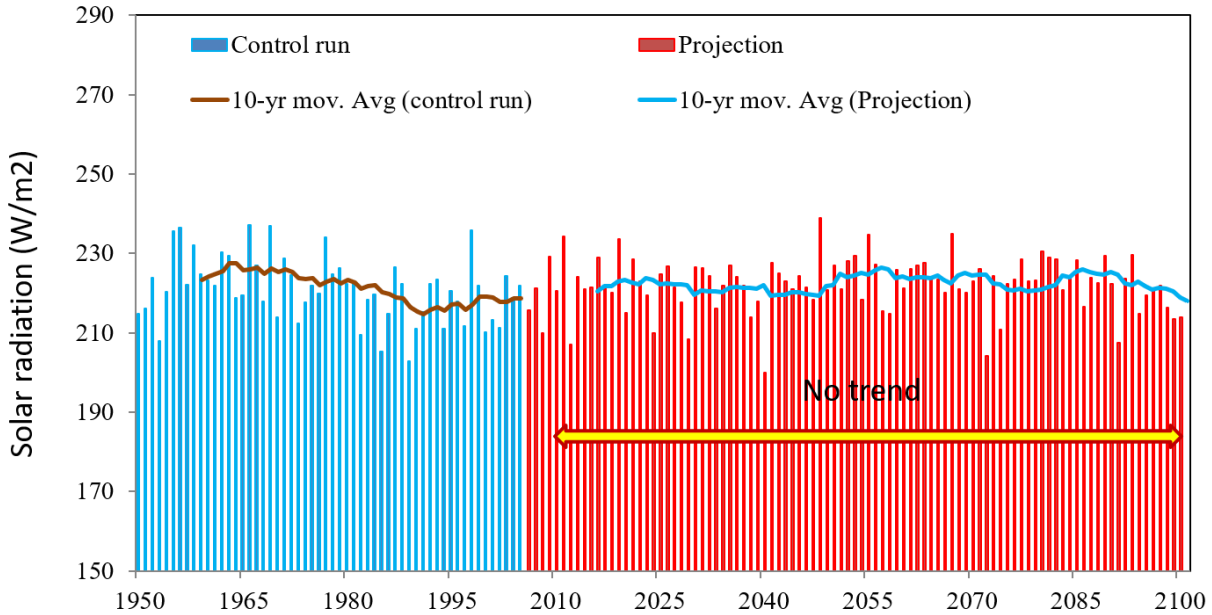


Figure 4.6 Comparison of historical and future GCM (MIROC5 and CCSM4)-based WRF projection of ensemble average annual solar radiation for Lo River watershed

Downscaled atmospheric data were input to the WEHY hydrologic model and the WEHY reservoir sub-program for simulations of future hydrologic conditions over the LRW. Figure 4.7 contains historical and future GCM (MIROC5 and CCSM4)-based WEHY projection of ensemble average annual flow. While the simulation was conducted for the entire LRW, the water supply or outflow from the LRW was retrieved from flow data at Vu Quang Station. A slightly increasing trend of flow data at Vu Quang station was detected. As depicted in Figure 4.7, there is no trend for flow in the early 21<sup>st</sup> century (2011-2035). However, there are 3 significant wave-like increasing and decreasing trends in the later part of the 21<sup>st</sup> century (2035-2053; 2054-2074; and 2075-2093).

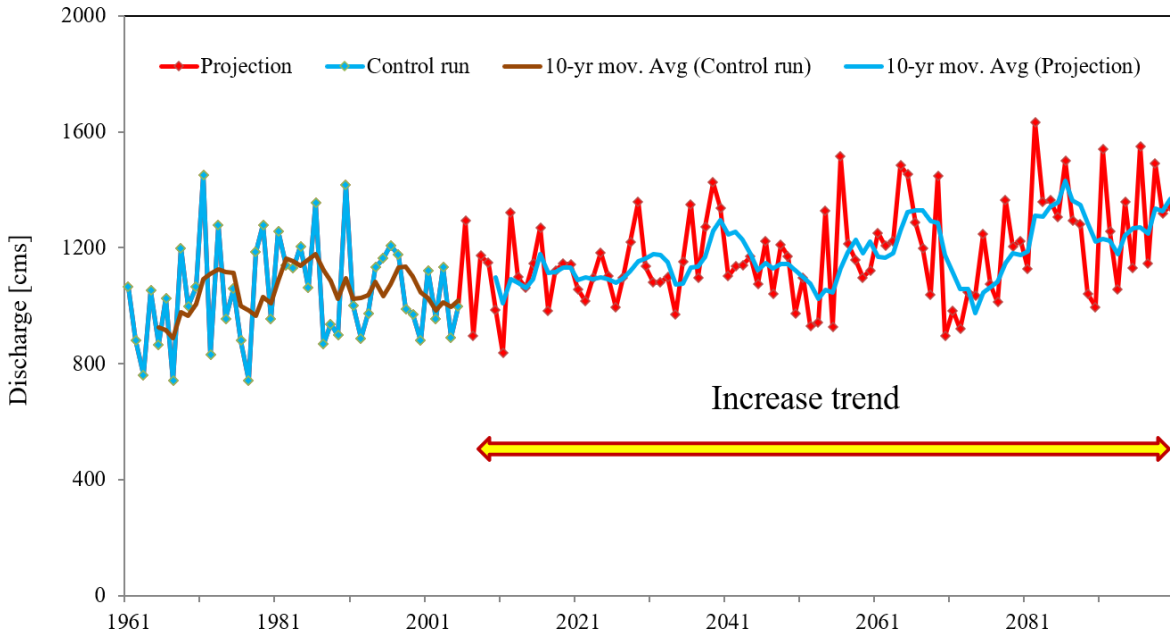


Figure 4.7 Comparison of historical and future GCM (MIROC5 and CCSM4)-based WEHY projection of ensemble average annual flow for Lo River watershed

Future mean monthly flow in the early 21<sup>st</sup> century, mid-21<sup>st</sup> century and at the end of the 21<sup>st</sup> century, along with historical mean monthly flow during WY 1990 – WY 1999 over the LRW, are presented in Figure 4.8. Similar to the precipitation analyses above, flow conditions are increasing in the wet season months of May, June, and Jul, and decreasing in the dry season in September, October and November.

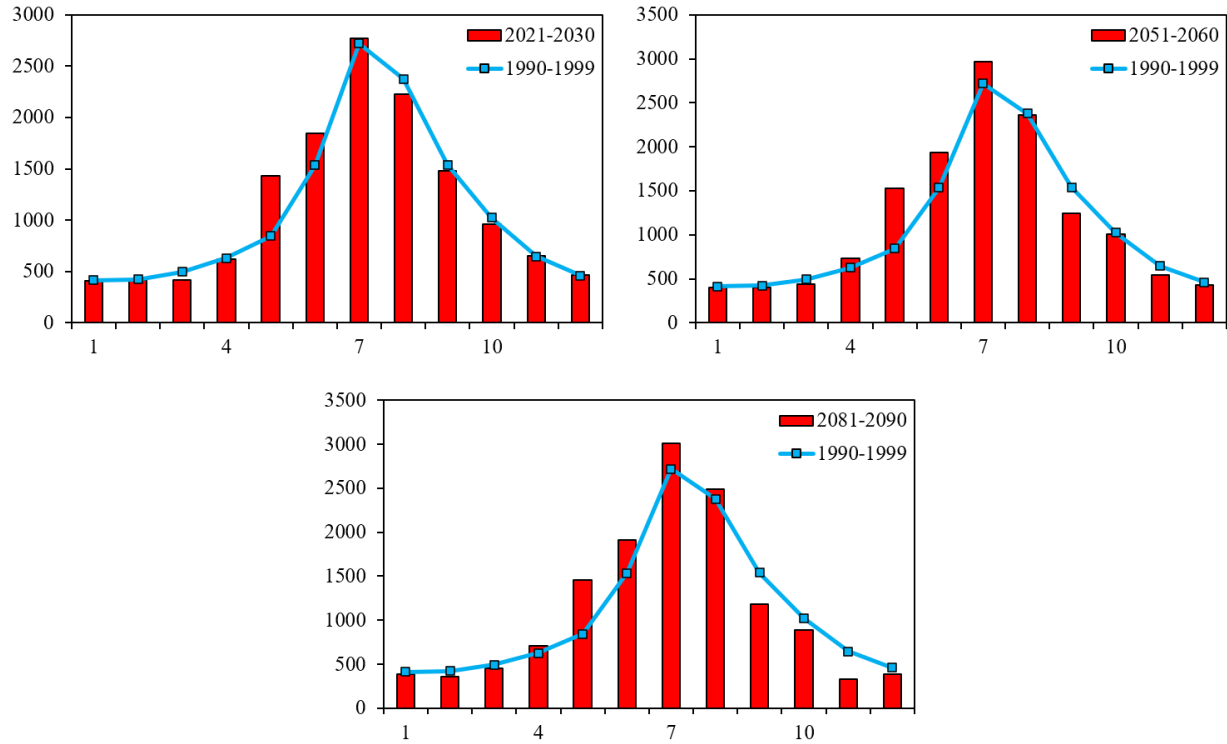


Figure 4.8 Comparison of the future mean monthly flow at early 21st century, at mid-21st century and at the end of the 21st century against the historical mean monthly flow during wy1990-wy1999 over the LRW

#### 4.4 Conclusion

The validated WEHY-WRF models provided control run values and projections of water supply over the LRW during the 21st century. The control run data were used for bias-correction application as described in Chapter 3. The bias-corrected atmospheric and hydrologic data were used to analyze the future trends of precipitation, temperature, solar radiation, evapotranspiration, and flow data.

From the analyses of the WEHY-WRF applications, the following conclusions related to the future climate conditions may be stated:

1. The ensemble means of the annual mean air temperature are expected to increase 2.04 °C from 2011 to 2100.

2. No significant trend was found in the annual mean solar radiation toward the end of the 21st century.

3. Based on the projected mean monthly precipitation, the dry season lasts for 7 months (October to April). However, both September and October show a decreasing trend compared to the control run (1990-1999). The wet season lasts for 5 months from April to September, with no significant difference except for August which shows a significant decreasing trend compared to the historical precipitation. The projected mean monthly precipitation is significantly increased at the mid-21st century (WY 2051 – WY 2060) and at the end of the 21st century (WY 2090 – WY 2099) when compared against the corresponding historical mean monthly precipitation (WY 1990 – WY 1999) over the LRW. Meanwhile the projected mean monthly precipitation is significantly increased over the south and the Middle East areas of the LRW, while the precipitation depth decreased in the northern and western areas.

5. A slightly increasing trend in flow data at Vu Quang station was detected. The flow has no trend in early part of 21st century (2011-2035) before showing 3 significant wave-like increasing and decreasing trends in the later part of the 21st century (2035-2053; 2054-2074; and 2075-2093).

6. Flow data increased in the wet season months of May, June, and Jul, and decreased in the dry season in September, October and November.

## References

Ministry of Natural Resources and Environment (MONRE), Climate Change and Sea Level rise scenarios for Vietnam, summary for policymakers. (2016)

Taylor, K.E., Stouffer, R.J. and Meehl, G.A., 2012. An overview of CMIP5 and the experiment design. *Bulletin of the American meteorological Society*, 93(4), pp.485-498.

Mastrandrea, M.D., Mach, K.J., Plattner, G.K., Edenhofer, O., Stocker, T.F., Field, C.B., Ebi, K.L. and Matschoss, P.R., 2011. The IPCC AR5 guidance note on consistent treatment of uncertainties: a common approach across the working groups. *Climatic Change*, 108(4), pp.675-691.

Dosio, A. and Paruolo, P., 2011. Bias correction of the ENSEMBLES high-resolution climate change projections for use by impact models: Evaluation on the present climate. *Journal of Geophysical Research: Atmospheres*, 116(D16).

Hawkins, E. and Sutton, R., 2009. The potential to narrow uncertainty in regional climate predictions. *Bulletin of the American Meteorological Society*, 90(8), pp.1095-1108.

Maurer, E.P., 2007. Uncertainty in hydrologic impacts of climate change in the Sierra Nevada, California, under two emissions scenarios. *Climatic Change*, 82(3), pp.309-325.

Maurer, E.P. and Duffy, P.B., 2005. Uncertainty in projections of streamflow changes due to climate change in California. *Geophysical Research Letters*, 32(3).

Teutschbein, C. and Seibert, J., 2012. Bias correction of regional climate model simulations for hydrological climate-change impact studies: Review and evaluation of different methods. *Journal of hydrology*, 456, pp.12-29.

Trinh, T., Ishida, K., Kavvas, M.L., Ercan, A. and Carr, K., 2017. Assessment of 21st century drought conditions at Shasta Dam based on dynamically projected water supply

conditions by a regional climate model coupled with a physically-based hydrology model. *Science of the Total Environment*, 586, pp.197-205.

Earth Exploration Toolbook, 2014. Part 2—Understand Climate Models.

## **CHAPTER 5. WATER DEMAND**

### **5.1 Introduction**

Water balance evaluations and drought analyses require calculation of both water supply and water demand. Chapters 2, 3 and 4 presented the methodology and analysis of historical and future water supply over the Lo River watershed. This chapter focuses on water demand data collected from different sources.

Water demand in different economic sectors is calculated based on norms and standards of water use established by the Vietnamese government, and some related studies. The calculation of water demand will focus on the following sources: (i) Irrigation; (ii) Livestock; (iii) Aquaculture; (iv) Domestic purposes; (v) Industry; (vi) Tourism and services; and (vii) Environmental sanitation. Among those demands, irrigation, or agriculture, is the most significant as it accounts for 81% of total water demand (2030 WRG (2017)).

Historical and future water demands were collected and estimated by the Department of Water Resources Management (DWRM). Based on DWRM calculations, a number of sources of data have been used in the preparation of water demand forecasts, founded on water use data from the World Bank. This dataset has been adapted for use in the forecasts using additional information sourced from numerous reports. There is a challenge in utilizing the data due scattered sourcing and contradictory information. The World Bank has data on water use from different sources for Vietnam from 1982 to present at a five-year interval. This dataset includes identical numbers for the years 2007, 2012 and 2017 – indicating that the 2007 data, at 14-years old, may be the most recent supplied. The Department of Water Resources Management (DWRM) has generated estimates of agricultural production, population, and areas of industrial development for 2019, 2025, 2030 and 2050. These forecasts appear to be incomplete for later

years, but the 2019 forecast appears to be a reliable starting point for agricultural and industrial water use. Additionally, the total population numbers for 2019 in the DWRM domestic (urban and rural) water estimates are higher than the official population figures for Vietnam.

## 5.2 Key Assumptions

### 5.2.1. Agricultural Production

While there is some potential for the expansion of agricultural production, data from the Food and Agriculture Organization of the United Nations (FAO) suggests that cereal production is tapering (**Error! Reference source not found.**). This may be indicative of the increased competition for land and resources.

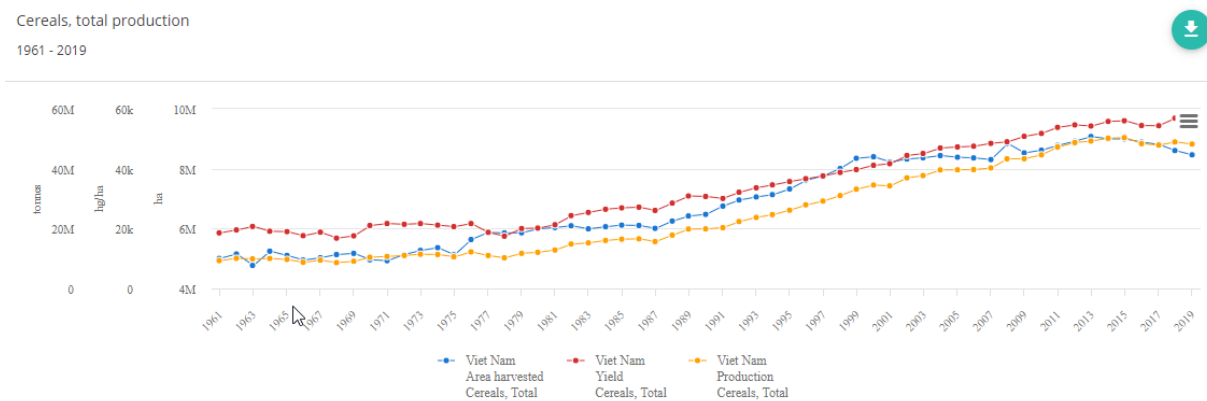


Figure 5.1 Total cereal production – Vietnam (Reproduced from the Food and Agriculture Organisation of the United Nations, 2021)

An important consideration in the preparation of forecasts is understanding how much water is used in agriculture to support export markets. The Vietnam General Statistics Office maintains a database on the volumes of crops produced and exported. These have been used to estimate the proportion of different crop types allocated to export markets. While there are some anomalous results in the table, possibly as a result of different tonnage at different points in the production process, these results provide an indication of the proportions going to export

markets. The 2020 data have not been used in this study due to the assumed impacts of the COVID-19 pandemic on normal trade patterns.

To estimate the volumes of water required to sustain export crops in each year, areas and water use data from the DWRM have been utilized. This estimate (for crop types where export volumes can be estimated) is shown in Table 5.1.

Of all of the crops utilizing water, rice and coffee are likely to be the most significant export uses with approximately 17% going to export each year.

Table 5.1 Irrigation water use generating exports (Vietnam General Statistics Office, 2021)

Crop type	Volume (m <sup>3</sup> x 10 <sup>6</sup> )	% of total water use	Assumed export % (2015-2019)	Proportion of water used for export
Rice	40,466	69.3%	13.6%	9.4%
Corn-potatoes	4,637	7.9%	0%	0.0%
Vegetables	2,300	3.9%	0%	0.0%
Cassava	388	0.7%	0%	0.0%
Sugar cane	1,510	2.6%	0%	0.0%
Coffee	5,237	9.0%	90% <sup>1</sup>	8.1%
Cover tree	210	0.4%	0%	0.0%
Fruit trees	3,648	6.2%	0%	0.0%
Total	58,397	100.0%		17.5%

During forecasting it is assumed that the current export volumes will be maintained, with any increase in irrigation demand resulting from domestic consumption. This assumption has a significant impact on the demand forecasts and is also the assumption with highest degree of

---

<sup>1</sup> This proportion has been assumed to allow for some domestic consumption

uncertainty. To demonstrate the impact of efficiency improvements on future demand in agriculture, the efficiency improvements in Table 5.2 have been adopted for all scenarios.

Table 5.2 Assumed improvement in agricultural water use efficiency

Year	2020	2030	2040	2050
Increase in efficiency	0%	5%	10%	15%

### 5.2.2. Tourism

Inbound tourism numbers have shown strong growth in recent years with a growth rate of 20% per annum (p.a.) over the period from 2015 to 2021 (General Statistics Office of Vietnam, 2021). With an average stay of approximately 8 nights, growth in the tourist sector is not anticipated to have a significant impact on water demands. This growth has been assumed to increase in all scenarios in the medium term, with market saturation later in the forecasting period and the growth in tourism equaling the rate of growth in population. Water use per visitor is projected to increase over time (Table 5.3).

Table 5.3 Tourist water demand forecasting assumptions (Vietnam General Statistics Office, 2021)

Indicator	Units	2020	2030	2040	2050
Tourist growth rate	% p.a.	19%	9.8%	0.3%	0.2%
Tourist demand	L/person/night	135.0	192.5	250.0	250.0

### 5.2.3. Industry

Rising gross domestic product per capita will fuel the domestic demand for manufactured goods. While some of these goods will be manufactured outside Vietnam, many will be manufactured overseas. This water resources planning study utilizes three economic forecasts

(Table 5.4). Economic growth is assumed to impact industrial demand in accordance with the elasticity of demand shown in Table 5.5. This elasticity of demand is anticipated to decline over time due to decreased focus on water-intensive manufacturing as a driver of growth.

Table 5.4 Economic growth scenarios (Vietnam General Statistics Office, 2021)

Period	Low growth (% p.a.)	Average growth (% p.a.)	High growth (% p.a.)
2021 - 2025	6.20%	6.80%	7.50%
2026 - 2030	5.80%	6.40%	7.20%
2021 - 2030	6.00%	6.60%	7.40%
2031 - 2045	4.70%	5.70%	6.30%

Table 5.5 Assumed GDP elasticity of industrial demand – all scenarios

Year	2020	2030	2040	2050
Elasticity	0.50	0.40	0.30	0.25

#### 5.2.4. Population forecasts

Population forecasts of total population have been taken from the World Population Review (World Population Review, 2021). Forecasts have been assumed to be identical in all scenarios (Table 5.6). Rural populations have been shown to be declining in recent years (World Bank, 2021), which are important for estimating the future transition from rural to urban demands.

Table 5.6 Population forecasts (World Population Review, 2021)

Location	2020	2030	200	2050
Rural	60,992,000	55,160,000	49,886,000	45,116,000
Urban	36,346,000	49,003,000	57,909,000	64,489,000
Total	97,338,000	104,163,000	107,795,000	109,605,000

### 5.2.5. Domestic water use

Domestic water use will have three primary drivers:

- Coverage of the urban service area (currently 86%) (World Bank, 2019);
- The proportion of the total population in urban areas;
- The level of customer service per person (currently 100 L/person/day) (World Bank, 2019).

The forecasts for these parameters under each scenario are shown in Table 5.7 and Table 5.8. It is assumed that economic growth will accelerate the provisions and the level of urban water servicing.

Table 5.7 Assumed urban service area coverage (World Bank, 2019)

Scenario	2020	2030	200	2050
Low economic growth	86.0%	90.7%	95.3%	100.0%
Average economic growth	86.0%	93.0%	100.0%	100.0%
High economic growth	86.0%	100.0%	100.0%	100.0%

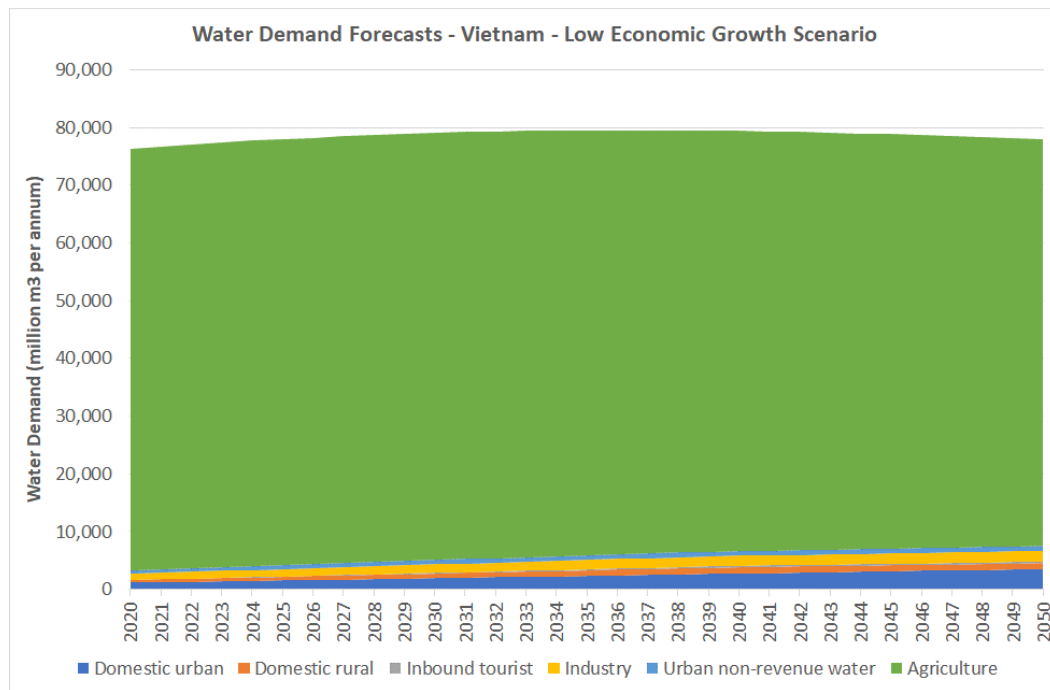
Table 5.8 Assumed urban per capita demands (L/person/day)

Scenario	2020	2030	200	2050
Low economic growth	100.0	116.7	133.3	150.0
Average economic growth	100.0	125.0	150.0	150.0
High economic growth	100.0	150.0	150.0	150.0

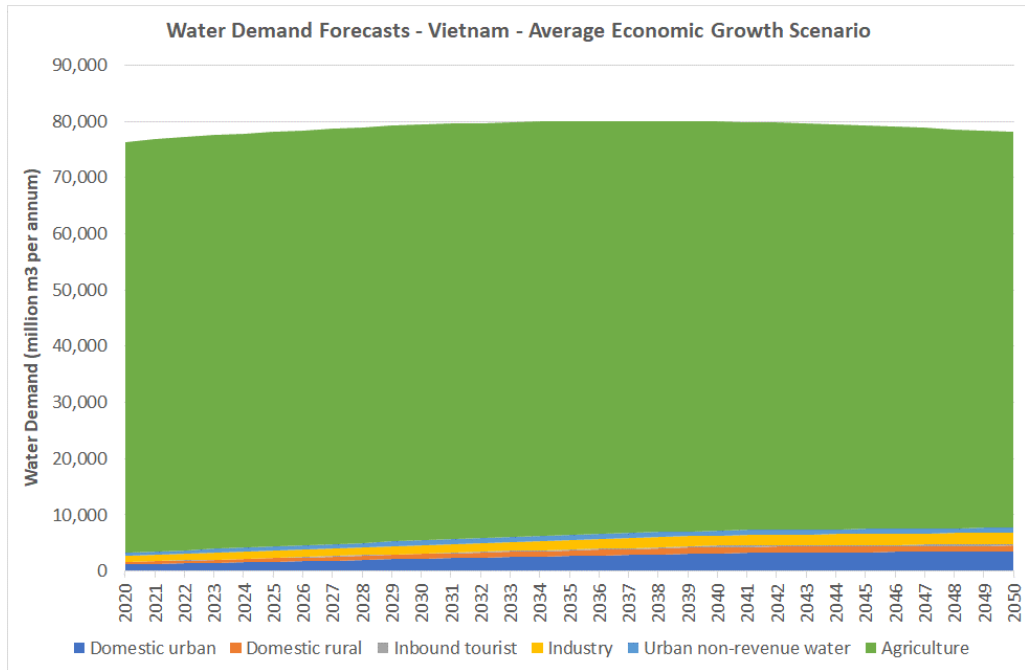
### 5.3 Demand forecasting scenarios

In the preparation of demand forecasts, there are no correct or incorrect solutions. Each is dependent on the number of assumptions regarding the drivers stated above. All scenarios have a common forecast of irrigation water use – with the main differentiator being differences in urban and industrial water use.

#### Scenario 1 – Low economic growth



### Scenario 2 – Average economic growth



### Scenario 3 – High economic growth

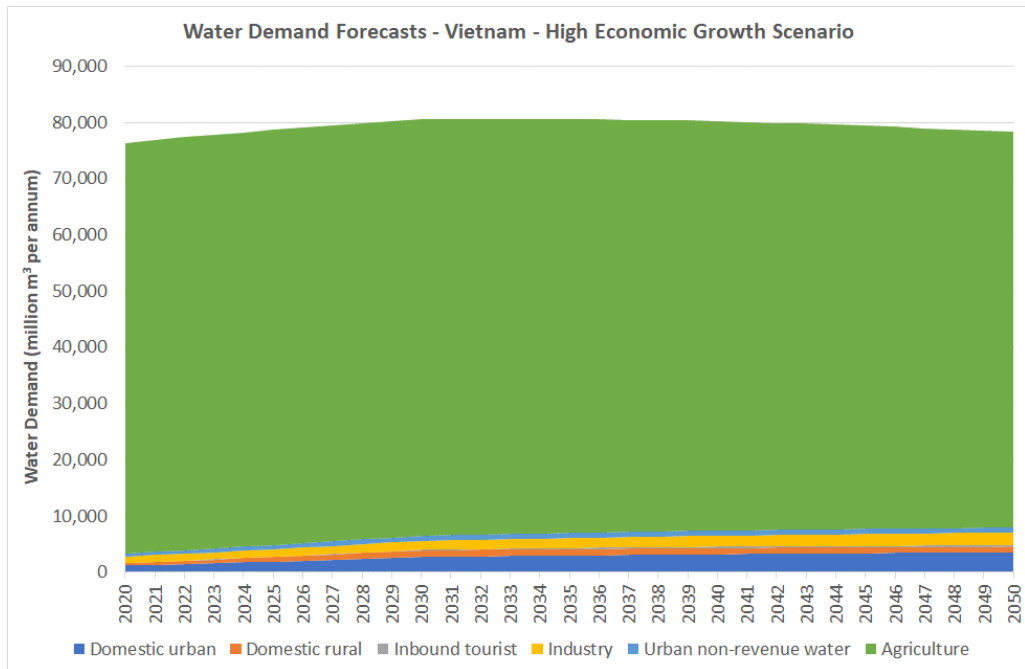


Figure 5.2 Water Demand Forecasts

### 5.3.1. Comparison of scenarios

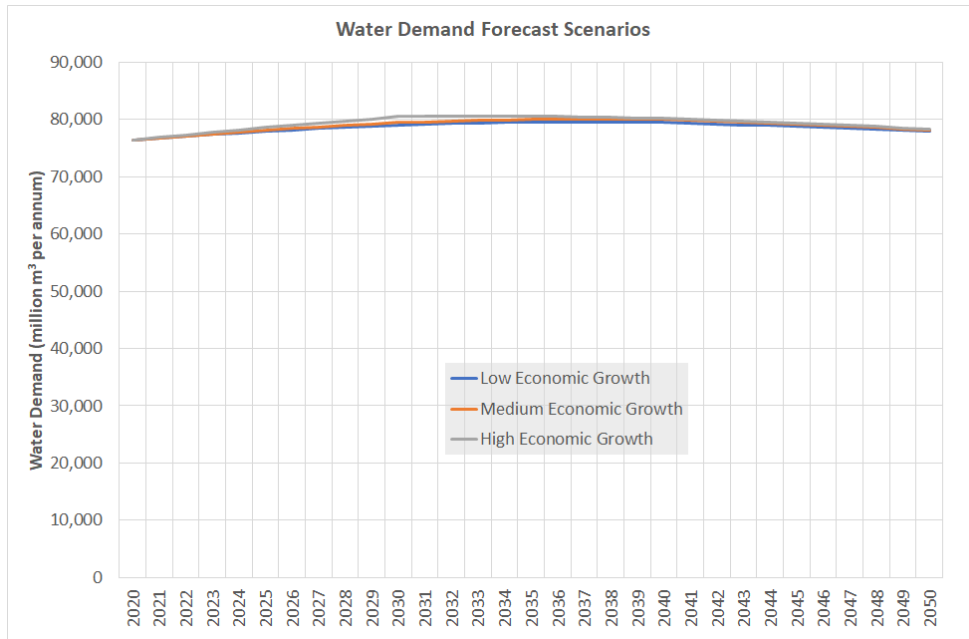


Figure 5.3 Comparison of forecasts - total water demand

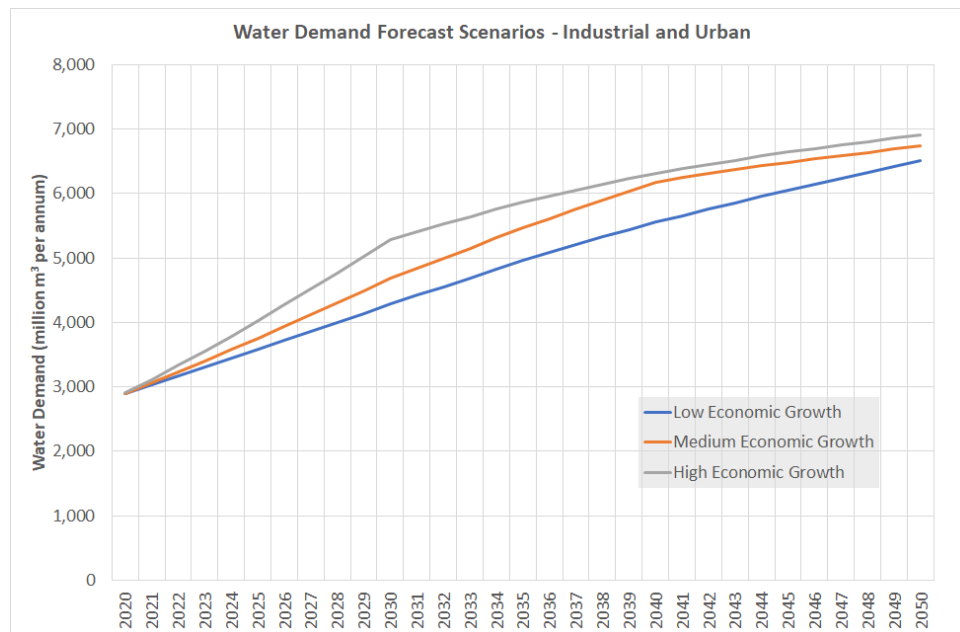


Figure 5.4 Comparison of forecasts - urban and industrial demand

In this chapter, the water demand for the LRW is estimated based on the above method. The following is water demand over the LRW in 2019, 2025, 2030, 2050 with Medium Economic Growth.

Table 5.9 Estimated water demand for LRW in 2019 (unit:  $10^9$  m<sup>3</sup>)

Jan	Feb	Mar	Apr	May	Jun	Jul	Aug	Sep	Oct	Nov	Dec	Year
0,10	0,13	0,14	0,14	0,10	0,09	0,14	0,14	0,14	0,12	0,06	0,06	1,36

Table 5.10 Estimated water demand for LRW in 2025 (unit:  $10^9$  m<sup>3</sup>)

Jan	Feb	Mar	Apr	May	Jun	Jul	Aug	Sep	Oct	Nov	Dec	Year
0,12	0,14	0,16	0,15	0,11	0,10	0,15	0,15	0,15	0,13	0,07	0,07	1,52

Table 5.11 Estimated water demand for LRW in 2030 (unit:  $10^9$  m<sup>3</sup>)

Jan	Feb	Mar	Apr	May	Jun	Jul	Aug	Sep	Oct	Nov	Dec	year
0,12	0,14	0,16	0,15	0,11	0,10	0,15	0,15	0,15	0,13	0,07	0,07	1,52

Table 5.12 Estimated water demand for LRW in 2050 (unit:  $10^9$  m<sup>3</sup>)

Jan	Feb	Mar	Apr	May	Jun	Jul	Aug	Sep	Oct	Nov	Dec	year
0,120	0,1	0,171	0,1666	0,126	0,117	0,1587	0,1587	0,1536	0,1470	0,0827	0,0843	1,642

## 5.4 Conclusions

The demand forecasting scenarios prepared provide the following conclusions:

1. There are a number of sources of data on existing water demand, and some provide different estimates of current demand, so there is some uncertainty about how much water is currently used.
2. Agricultural water use dominates the total water use and assumptions about future water efficiency in that sector will determine the ultimate forecast.
3. Other drivers in future increase in demand in the urban and industrial sectors are:
  - a) Economic growth, which will impact industrial water use and urban water servicing standards;
  - b) Increasing urbanization of the population;
  - c) Improved standards of service and wider coverage in urban areas;
  - d) The level of non-revenue water in urban systems.
4. Projected increases in inbound tourists in the medium term are unlikely to have significant impacts.

## References

Zhang, B. and He, C., 2016. A modified water demand estimation method for drought identification over arid and semiarid regions. *Agricultural and Forest Meteorology*, 230, pp.58-66.

Food and Agriculture Organisation of the United Nations. (2021). *Selected Indicators - Vietnam*. Retrieved from Food and Agriculture Organisation of the United Nations: <http://www.fao.org/faostat/en/#country/237>

General Statistics Office of Vietnam. (2021). *Exports of goods by kinds of economic sectors and by commodity group*. Retrieved from General Statistics Office: <https://www.gso.gov.vn/en/px-web/?pxid=E0810&theme=Trade%2C%20Price%20and%20Tourist>

World Bank. (2019). Vietnam: Towards a Safe, Clean and Resilient Water System.

World Bank. (2021). *Rural population - Vietnam*. Retrieved from The World Bank Data: <https://data.worldbank.org/indicator/SP.RUR.TOTL?start=2008&locations=VN>

World Population Review. (2021). *Vietnam Population (2021)*. Retrieved from World Population Review: <https://worldpopulationreview.com/countries/vietnam-population>

## **CHAPTER 6. WATER BALANCE AND FUTURE DROUGHT ANALYSIS**

### **Abstract**

Drought has been considered one of the most complex natural phenomena related to a shortage. The occurrence and intensity of meteorological disasters such as drought and flood are projected to increase in the future. In this study, drought properties such as drought duration, drought severity, relationship between duration and severity, were analyzed by means of comparing historical and future water supply of the Lo River Watershed (Chapter 4) versus water demand (Chapter 5) to obtain changes in water balance and drought conditions in the future. Future projections show more drought events in the early 21<sup>st</sup> century compared to the end of the century. Additionally, future water demand has an increasing trend, and future water supply in the LRW tends to be insufficient to meet that demand. Thus, it is crucial to take actions now and prepare for possible water scarcity in the future to eliminate the future loss related to droughts in the region.

### **6.1 Introduction**

Global warming, a consequence of the industrial revolution, is a serious threat to human life, agriculture, energy, ecosystem, wildlife, and other aspects of the earth system (An et al., 2020; Mikhaylov et al., 2020). Consequently, the occurrence and intensity of meteorological disasters such as drought and flood are likely to increase in future (Trinh et al., 2017; Hari et al., 2020). In Vietnam, drought has recently become one of the nation's most important problems. According to collected statistics from MONRE and the World Bank, droughts have occurred in 40 of the last 50 years to different extents and locations across Vietnam. Drought has caused many negative impacts on the local agriculture and livelihoods. In order to deal with drought

issues in the past, the Vietnamese government put effort into developing drought management measures. However, drought remains a complex problem.

In the LRW, the wet season ends in September or October. Droughts, resulting from a shortage of rainfall and low water level in reservoirs, mainly occur during the winter-spring crop season. For example, a drought from the end of 1998 until April of 1999 affected about 86,140 ha of rice paddy, with severe drought in 17,077 ha, and 10,930 ha of vegetables and other crops. A drought in 2004 left water levels of the Red River from January to February at the lowest in 40 years, and flood retention capacity of reservoirs was below their designed level. Local communities had to mobilize all possible resources to cope with this drought.

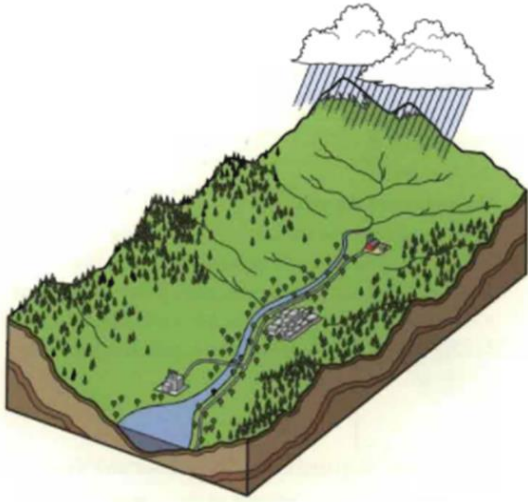
In this study, drought properties such as drought duration, drought severity, and the relationship between duration and severity, were analyzed by means of comparing historical and future water supply (Chapter 4) versus water demand (Chapter 5) to obtain changes of water balance and drought conditions in the future. The results of this study could be highly beneficial for developing strategic adaptation to reduce the potential risks related to water scarcity in the region.

## **6.2 Methodology**

### **6.2.1 Estimation of water supply**

Water balance at a watershed is calculated based on projected water supply and water demand over the target watershed.  $\text{Water balance} = \text{Water supply} - \text{water demand}$ .

In this study, water supply is calculated based on the government decree number 21/2013/ND-CP as illustrated in Figure 6.1.



- $W_{su} = W_{sw} - W_{tw} - W_{out}$

Figure 6.1 Water supply calculation (MONRE, 2019)

$$W_{su} = W_{sw} - W_{tw} - W_{out} \quad (6.1)$$

$W_{su}$ : the total amount of water that can be used (water supply)

$W_{tw}$ : the total amount of surface water that is transferred/conveyed out of watershed

$W_{sw}$ : the total amount of water within the watershed

$W_{ec}$ : the total amount of water loss from evapotranspiration or conveyed out of a watershed

$W_{out}$ : the total amount of water that flows out from the watershed at the outlet point.

For the Lo River watershed,  $W_{ec}$  was calculated in Chapters 2 and 4;  $W_{out}$  is the required minimum environmental flow; and  $W_{sw}$  is the total natural flow at the outlet point (according to decree number 21/2013/ND-CP) which was simulated from the hydro-climate model with input provided from GCM-based CCSM4 and MIROC5 climate projections. Equation 6.1 can be rewritten as follows:

$$W_{su} = W_{FNo} + W_s - W_{env} \quad (6.2)$$

Where all data are at a monthly interval

$W_{su}$  is the volume of water supply;

$W_{FNO}$  is the volume of full natural flow at outlet point (in this case, Vu Quang station);

$W_s$  is the volume stored in reservoirs Thac Ba and Tuyen Quang;

$W_{env}$  is the volume of environmental flow (at the outlet point, Vu Quang station);

According to decree number 71/2017/BTNMT of the Vietnam Ministry of Natural Resources and Environment,  $W_{env}$  can be estimated at 95% exceedance probability of flow at Vu Quang station.  $W_{ev}$  was calculated in Chapters 2 and 4, and  $W_s$  can be estimated based on utilizable storage capacity (Figure 6.2). The 95% exceedance probability of flow, based on observations at Vu Quang, is shown in Figure 6.3, and corresponds to 159 m<sup>3</sup>/s.  $W_{FNO}$  is the volume of full natural flow at the outlet point that is full natural flow at Vu Quang station. The  $W_{FNO}$  was estimated by means of WEHY-WRF model with inputs provided from GCM-based CCSM4 and MIROC5 climate projections. Through application of Equation 2, the result of water supply is plotted in Figure 6.4.

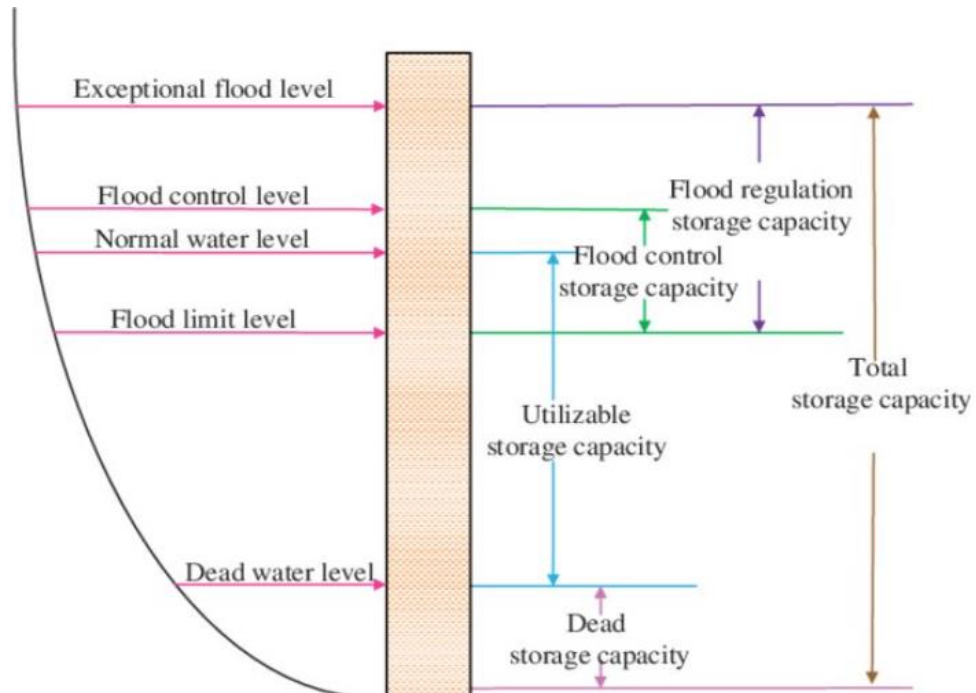


Figure 6.2 Characteristics of a reservoir: relationship between water level and storage capacity (Trinh et al., 2017)

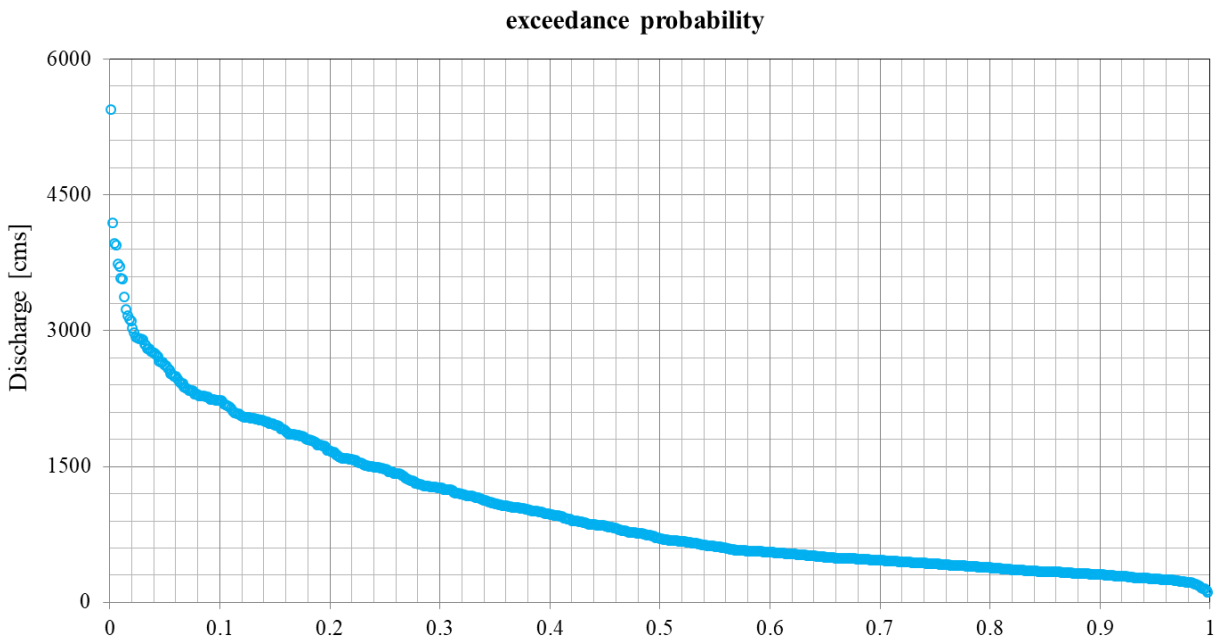


Figure 6.3 Exceedance probability of flow data at Vu Quang station

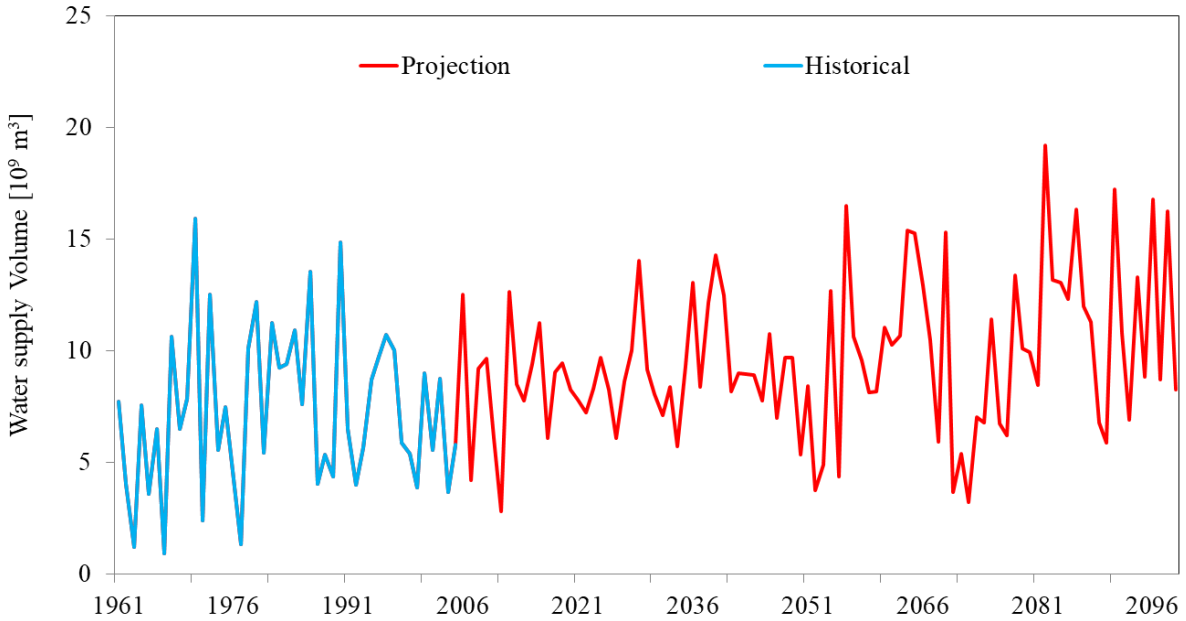


Figure 6.4 Estimation of water supply for the LRW

### 6.2.2 Water balance analysis

Based on calculated water supply and water demand, it is possible to obtain water balance over the target watershed. This comparison suggests instances of deficit as well as surplus in both the historical and future periods. Water surplus is defined as water supply being in excess of water demand, while water deficit is quantified as water supply being insufficient to meet water demand. A deficit period is defined as the duration of time when water supply is below the water demand (Trinh et al., 2017; Shiao and Shen, 2001; Yevjevich 1967) (Figure 6.5). In the meantime, the non-drought (surplus) duration and non-drought severity (cumulative surplus) are the period of time and cumulative volume above the truncation level for a non-drought event (Shiao and Shen, 2001).

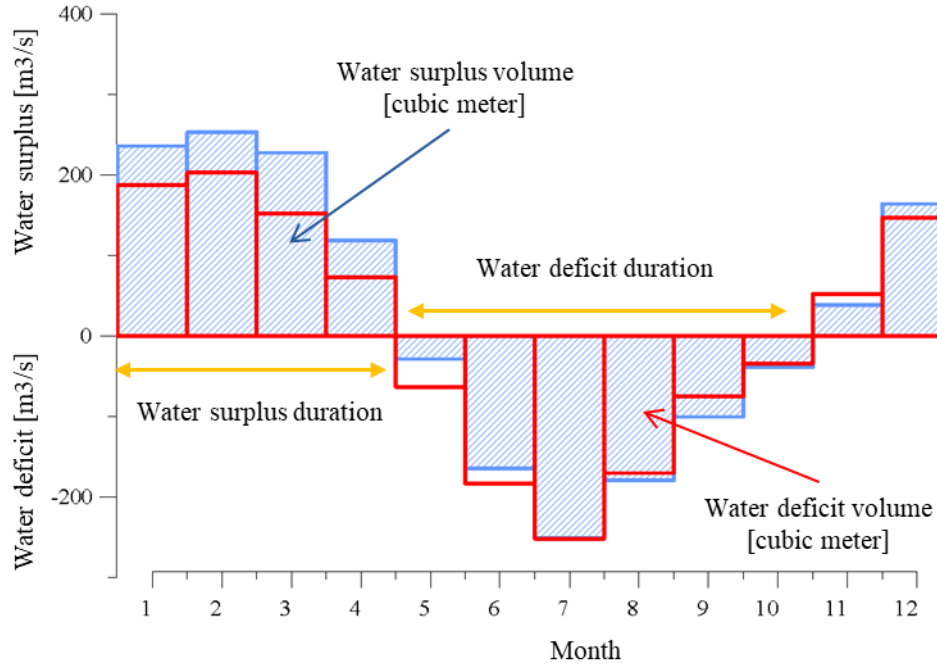


Figure 6.5 The concept and definition of water surplus and deficit duration and volume (Trinh et al., 2017)

In this analysis, residual values are a month's water deficit or surplus. For this study, the water deficit duration,  $D_d$ , is the number of months for which the residual values are below zero, and the deficit volume,  $V_d$ , is the cumulative sum of the monthly deficit for that particular deficit event. The deficit/drought intensity ( $I_d$ ) is the ratio between the deficit volume ( $V_d$ ) and duration ( $D_d$ ). Similarly, water surplus duration,  $D_s$  is the number of months for which the monthly residual values are above zero, and the surplus volume,  $V_s$ , is the cumulative sum of the monthly surplus for that particular surplus event. The surplus intensity ( $I_s$ ) is the ratio between the surplus volume ( $V_s$ ) and duration ( $D_s$ ).

$$I_d = \frac{V_d}{D_d} \quad I_s = \frac{V_s}{D_s} \quad (6.3)$$

This analysis can be performed with either yearly or monthly water balance data. After obtaining a water deficit/surplus duration and volume, it is possible to calculate exceedance

probability. Exceedance probability is a fundamental method to analyze a series of data. In this analysis, both the probability of deficit/surplus duration and volume were computed.

### **6.3 Result and Discussion**

Based on the calculated water supply and collected water demand, a comparison between the future average water supply and water demand is possible for the LRW. Figure 6.6 contains three different water demand levels corresponding to current water demand, 2025 water demand, and 2050 water demand, overlaid on historical and projected water supply. Water supply is increasing, as is water demand, but at a slower rate. In the historical period of Figure 6.6, several historical droughts are obvious in years where annual mean water supply did not meet annual water demand. They occur in 1963, 1967, 1972, 1977, and 1999–2000. In the future period, there are several drought years with small water deficit, however, the drought duration can last up to 5 continuous years. Longer drought duration may lead to more critical drought conditions. Based on the water balances calculated, the volume of annual deficit may be less in the future compared with historical values, but the deficit duration will be longer.

In order to further assess the water balance, monthly climatology was examined for future water surplus and deficit as shown in Figure 6.7. Based on Figure 6.7, it may be inferred that the droughts may be less extreme from February to April, while they tend to be more extreme in November when compared to historical periods. There is a time shift of drought season in that it tends to start earlier and more extreme in November and ends earlier in May, a water balance shift from deficit to surplus in the future period.

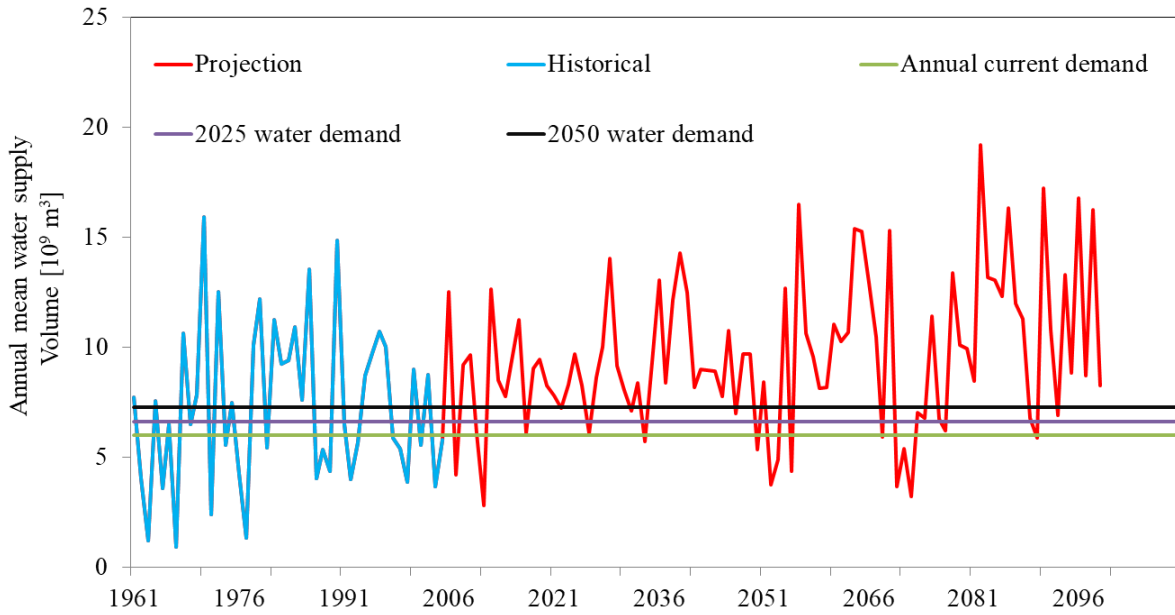


Figure 6.6 Comparison between future average water supply and water demand

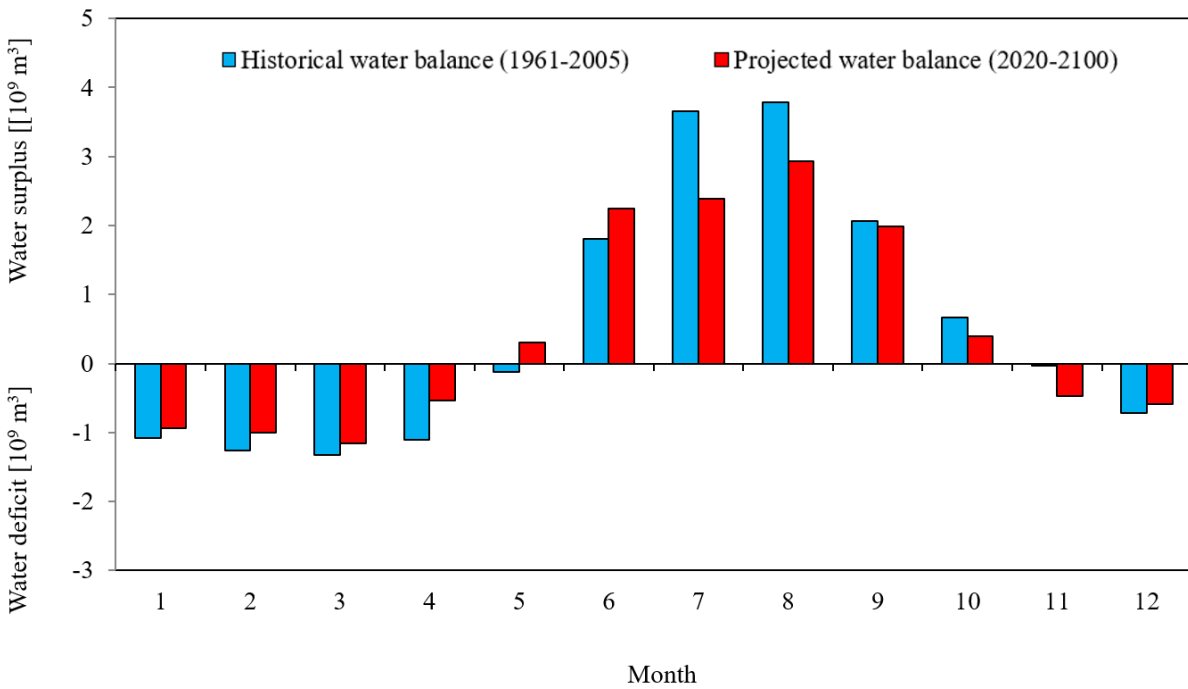


Figure 6.7 Comparison of the monthly climatology of historical and the future water surplus and deficit based on current water demand

Further analysis on the water balance of the LRW was conducted based on projected water demand volumes. Figure 6.8 shows the monthly climatology of historical and future water balance based on the projected 2025 and 2050 water demands. Water deficit based on 2050 demand is even more severe than the historical period. This phenomenon can be seen clearly in Figure 6.9 since the total future water deficit during the dry season is larger than the historical condition. Additionally, as shown in Figure 6.10, the future water surplus during the wet season could be less than the historical condition, which agrees with previous analysis.

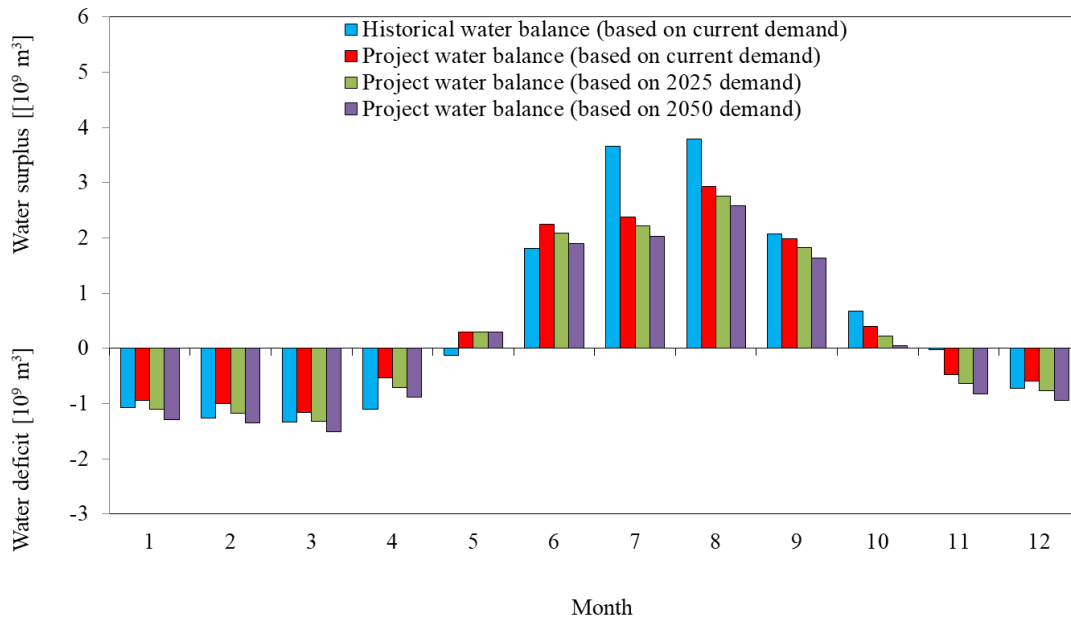


Figure 6.8 Comparison of the monthly climatology of historical and future water surplus and deficit for the LRW based on different water demand scenarios

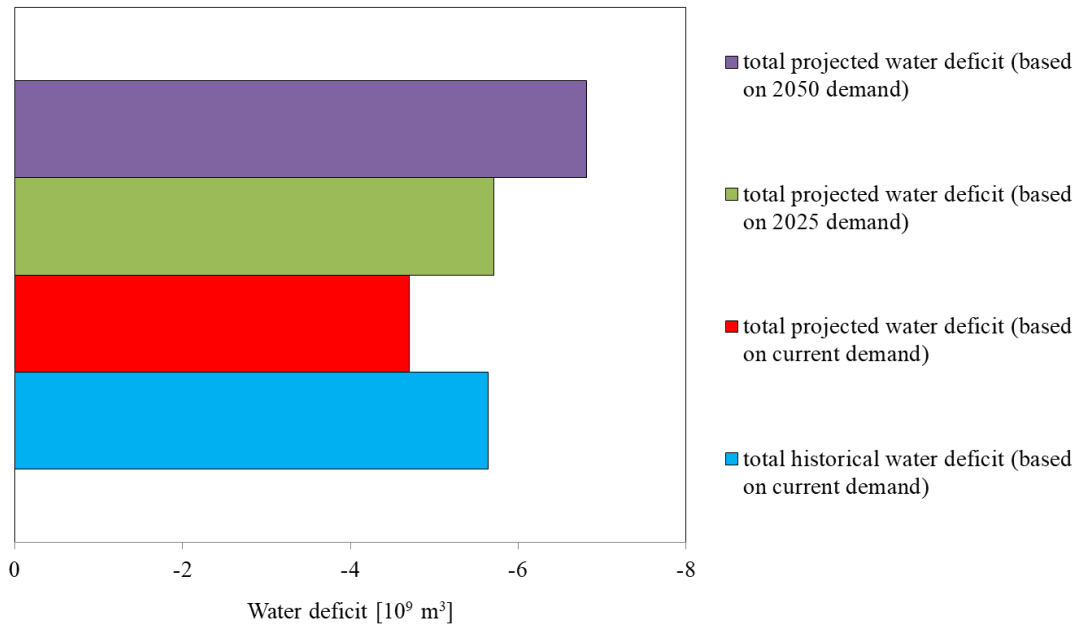


Figure 6.9 Comparison of the total historical and the future water deficit during the dry season.

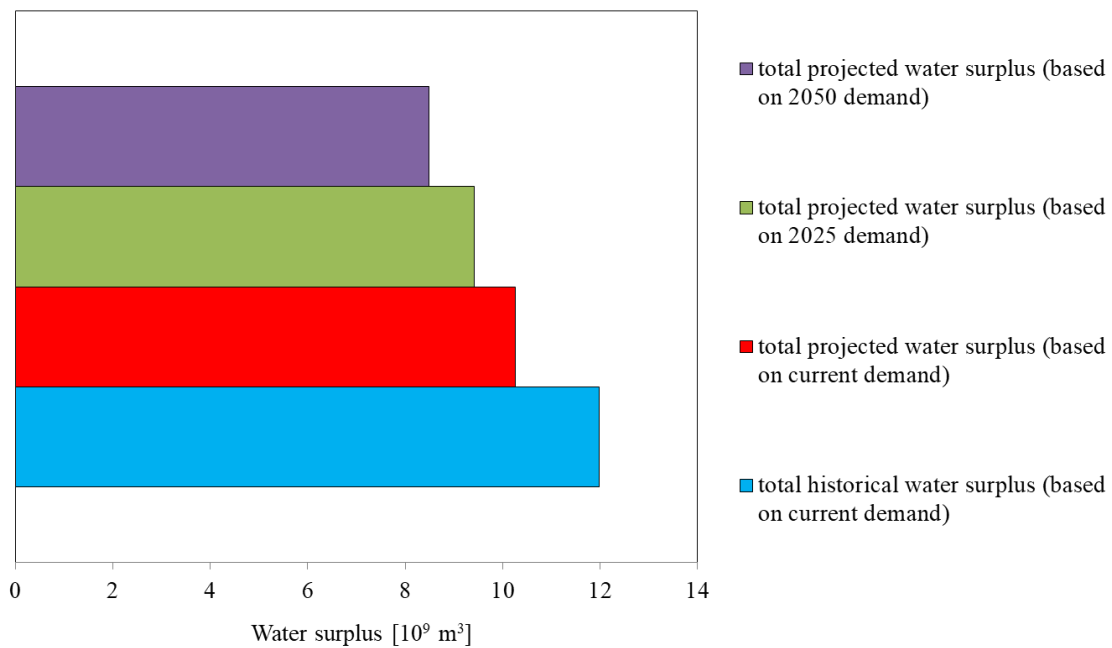


Figure 6.10 Comparison of the total historical and the future water surplus during the wet season

Projected drought severity and duration were analyzed according to Equation 6.3. A scatter plot of the severity of the projected water deficit events versus their duration, utilizing current water demand, is presented in Figure 6.11. Based on the plot, deficit durations can reach up to 20 months (almost 2 years) in MIROC5 projections. The longest drought duration of CCSM4 projection is 19 months, with a deficit volume of approximately  $14 \times 10^9 \text{ m}^3$ . The longest historical drought event was 18 months, but that event did not represent the maximum historical water deficit. The maximum historical deficit volume was about  $17 \times 10^9 \text{ m}^3$ . Applying current water demand to the projected supply volumes does not represent a realistic comparison. Therefore, projected drought severity and duration were analyzed using both future supply and projected 2025 and 2050 water demand conditions. The scatter plots in Figures 6.12 and 6.13 were created based on the future supply and 2025, and 2050 water demand conditions respectively. The plotted values for the historical drought duration and severity in Figures 6.12 and 6.13 are still based on current water demand conditions. Under the 2025 water demand condition, the longest drought duration of 22 months came from both MIROC5 and CCSM4 projections. The largest drought severity under MIROC5 projection is roughly  $22 \times 10^9 \text{ m}^3$ , while the largest drought severity under CCSM4 projection is about  $19 \times 10^9 \text{ m}^3$ .

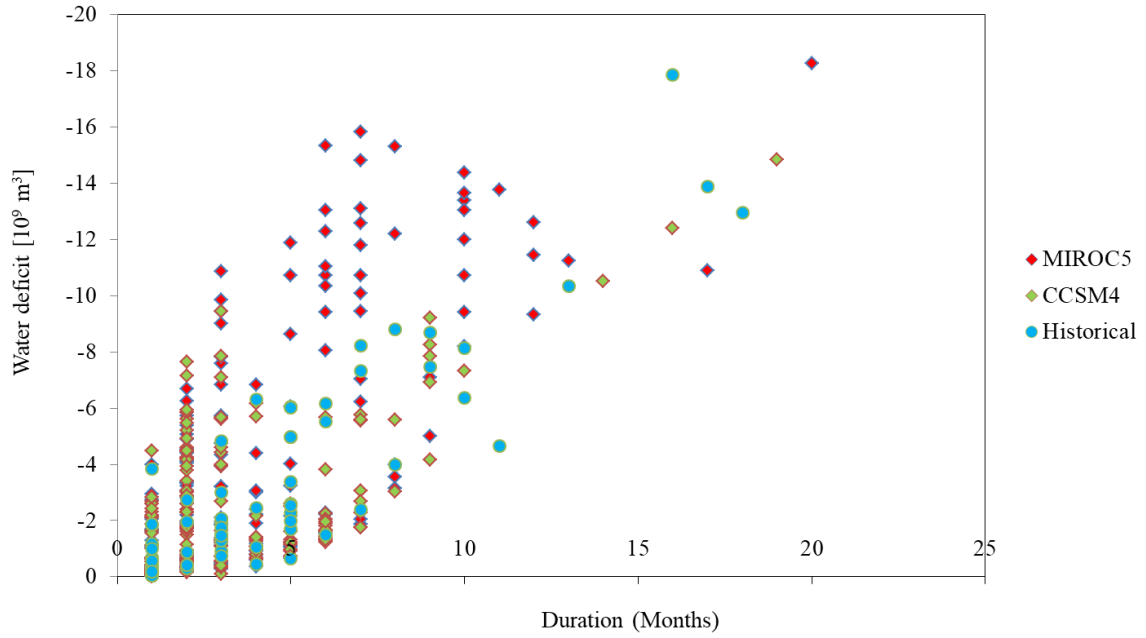


Figure 6.11 Relationship between drought duration and severity based on the current demand

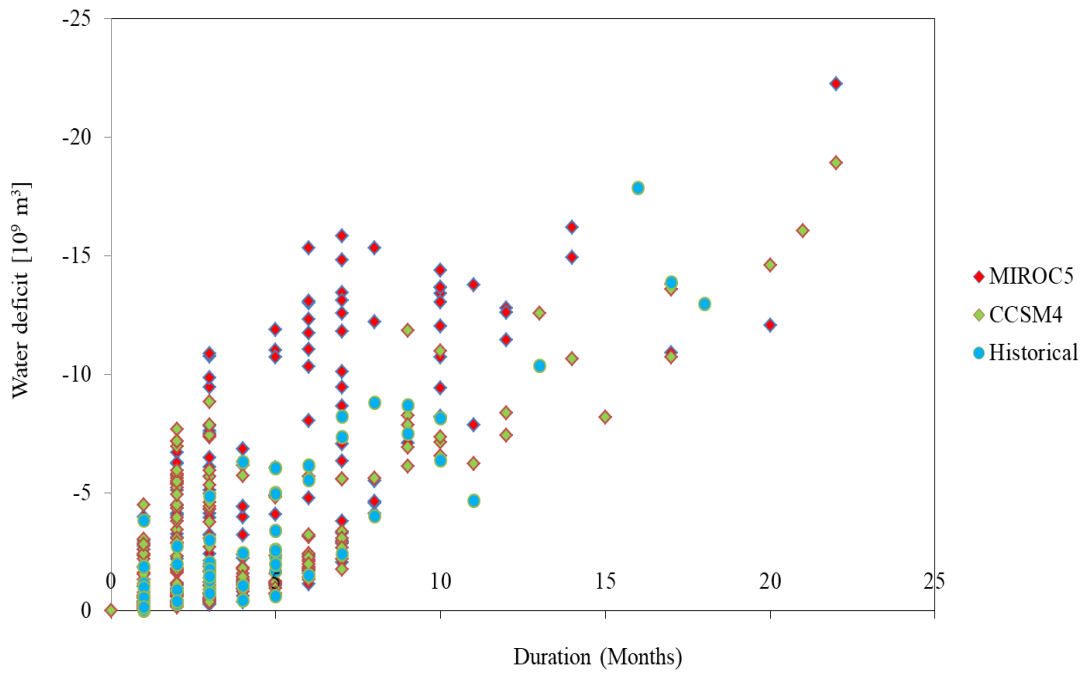


Figure 6.12 Relationship between drought duration and severity based on 2025 water demand

Under the 2050 water demand condition shown in Figure 6.13, the longest drought event is 23 months long and has a water deficit volume of  $24 \times 10^9 \text{ m}^3$  according to the MIROC5 scenario. This is the longest drought event calculated for any combination of scenarios, and is 7 months longer than the longest historical drought event. The most extreme drought volume projected is  $24 \times 10^9 \text{ m}^3$ , which is 35% higher than historical conditions. The MIROC5 projection under scenario RCP 8.5 is the basis for the worst-case climate change scenario, and is based on what proved to be overestimation of projected outputs.

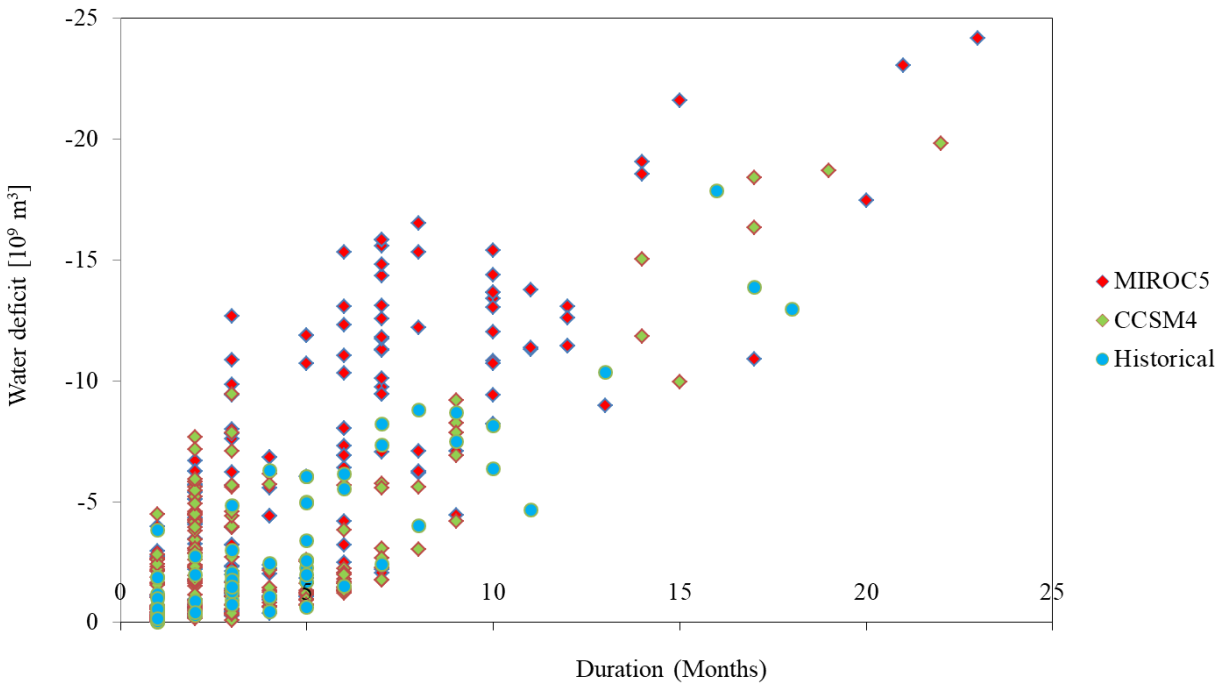


Figure 6.13 Relationship of drought duration and severity based on 2050 demand

The exceedance probability of drought intensity for historical and future conditions is presented in Figure 6.14. The results suggest that the future drought regime may have a more severe pattern than its historical counterpart.

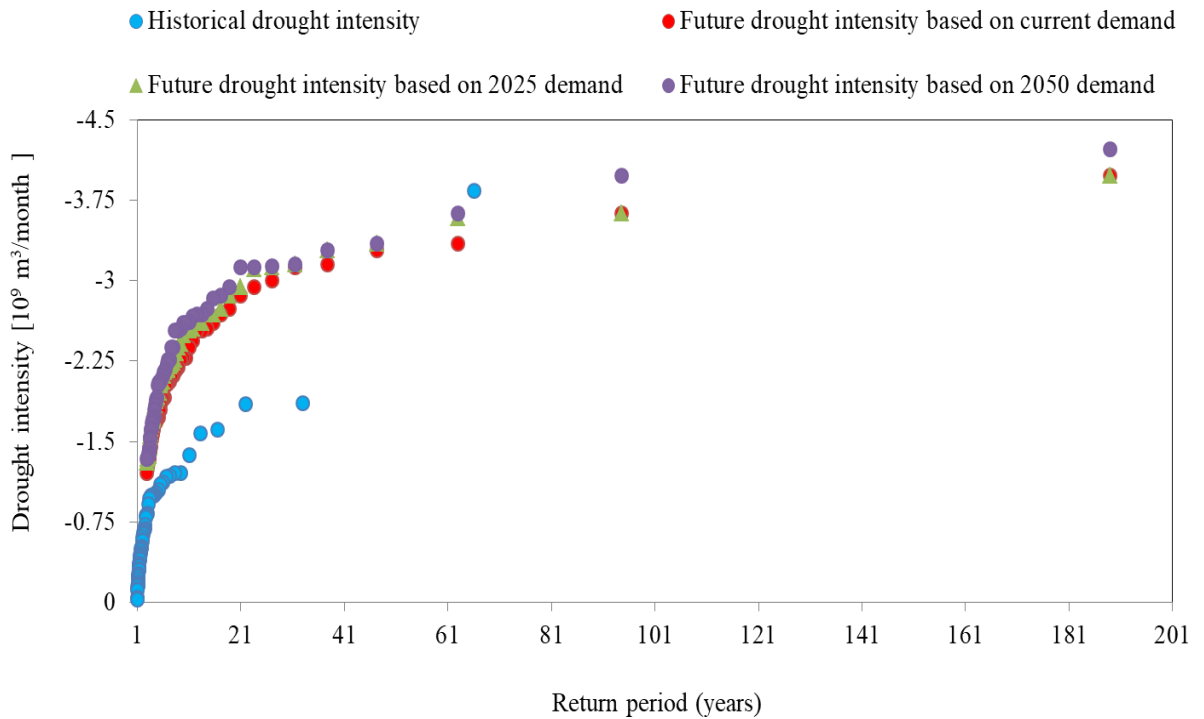


Figure 6.14 Evolution of the drought intensity as function of return period during historical and future conditions

## 6.4 Conclusion

In this study, drought properties such as drought duration, drought severity, and the relationship between duration and severity were analyzed by means of comparing historical and future water supply (Chapter 4) versus water demand (Chapter 5) to analyze changes of water balance and drought conditions in the future. The drought analyses indicate that:

1. Future projections showed more drought events in the early 21st century compared to the end of the century.
2. The majority of events, approximately 90%, had durations less than or equal to 11 months, and approximately 5% had durations between 12 and 24 months.

3. MIROC5 climate projection with scenario RCP 8.5 exhibits a more intense drought event than CCSM4 climate projection with scenario RCP4.5. The longest historical drought duration was 18 months, while the future duration of drought events can be up to 24 months.

4. The drought intensity may increase by 4.9% with projected 2025 demand and 10% with projected 2050 water demand.

5. Due to the increasing trend in both current water demand and future water demand, future water supply from the LRW is projected to be insufficient to meet demand. Thus, it is necessary to improve the water governance of the country, alter the operation rules of Tuyen Quang and Thac Ba reservoirs, and improve the efficiency of the water delivery system.

## References

Shiau, J.-T. and Shen, H.W., 2001. Recurrence analysis of hydrologic droughts of differing severity. *Journal of Water Resources Planning and Management*, 127(1): 30-40.

Yevjevich, V. et al., 1967. An objective approach to definitions and investigations of continental hydrologic droughts. Colorado State University Fort Collins.

Hari, V., Rakovec, O., Markonis, Y., Hanel, M., & Kumar, R. (2020). Increased future occurrences of the exceptional 2018–2019 Central European drought under global warming. *Scientific reports*, 10(1), 1-10.

An, R., Shen, J., Li, Y., & Bandaru, S. (2020). Projecting the Influence of Global Warming on Physical Activity Patterns: a Systematic Review. *Current Obesity Reports*, 1-12.

Mikhaylov, A., Moiseev, N., Aleshin, K., & Burkhardt, T. (2020). Global climate change and greenhouse effect. *Entrepreneurship and Sustainability Issues*, 7(4), 2897.

Trinh, T., Ishida, K., Kavvas, M.L., Ercan, A. and Carr, K., 2017. Assessment of 21st century drought conditions at Shasta Dam based on dynamically projected water supply conditions by a regional climate model coupled with a physically-based hydrology model. *Science of the Total Environment*, 586, pp.197-205.

Mao, Y., Ye, A., Liu, X., Ma, F., Deng, X. and Zhou, Z., 2016. High-resolution simulation of the spatial pattern of water use in continental China. *Hydrological Sciences Journal*, 61(14), pp.2626-2638.

Shukla, S. and Wood, A.W., 2008. Use of a standardized runoff index for characterizing hydrologic drought. *Geophysical Research Letters*, 35(2).

Cuong, H.V. and Toan, T.Q., 2019. Assessment of hydro-climatological drought conditions for Hong-Thai Binh river watershed in Vietnam using high-resolution model simulation. *Vietnam Journal of Science, Technology and Engineering*, 61(2), pp.90-96.

Cường, H.V., Nhãn, N.T.N., Bách, T.V. and Toàn, T.Q., Nghiên cứu diễn biến hạn hán trên lưu vực sông Hồng – Thái Bình bằng bộ dữ liệu khí tượng, thủy văn khôi phục từ mô hình kết hợp WEHY-WRF.

## CHAPTER 7. DISCUSSION AND CONCLUSIONS

### 7.1 Summary

This study introduced a new approach to assess water balance and drought conditions over a transboundary region, the Lo River watershed in Vietnam. The Lo River is a tributary of the Red River system. The Red River system is the second largest river system in Vietnam after the Mekong River. With a catchment area of 39,000 km<sup>2</sup>, the Lo River watershed is considered one of the major international rivers in Vietnam. The upstream section is located in China and accounts for 52% of the area. The downstream section is located in Vietnam with 48% of the area. The basin has an important political and military strategic position, and is considered a key economic and agricultural region in Vietnam. Thus, studying the future water balance and drought conditions over the LRW is crucial to providing solutions, recommendations and better preparation for adapting and mitigating negative impacts from climate change conditions over the 21st century. This study started by implementing a hydro-climate model over the LRW. The regional climate model-WRF and a watershed model WEHY were selected for reconstruction and projection of historical and future water supply over the LRW during the 21st century. WEHY-WRF was successfully implemented and validated based on comparisons between simulation and corresponding observation data. The simulations matched well with the observation data with respect to magnitude (Nash-Sutcliffe 0.79, and correlation coefficient was 0.89) and spatial distribution. These comparisons confirmed that the selected models are reliable techniques to simulate atmospheric and hydrologic conditions over the LRW.

After successful implementation and validation of WEHY-WRF, it is possible to apply these models for projection of future water supply over the LRW. Because future projection simulations and even historical control runs do not include data assimilation process (unlike

reanalysis data), model products may be biased. These biases necessitate a technology which is able to correct simulated data and provide reliable future projection over the target watershed. There are various sources of uncertainty recognized in hydro-climate studies, such as GCM structure and parameter uncertainty, greenhouse gas emissions scenarios uncertainty, GCM initial conditions uncertainty, downscaling technique, and hydrologic model uncertainty. One method of decreasing uncertainty is the application of both atmospheric and hydrologic bias correction. In this study, two global climate models were applied, including the fifth generation of the Model for Interdisciplinary Research on Climate - MIROC5, and the fourth version of the Community Climate System Model - CCSM4. These two GCMs were applied with two scenarios, Representative Concentration Pathway - RCP 4.5 (CCSM4) and 8.5 (MIROC5). These scenarios were recommended by the Vietnam Ministry of Natural Resources and Environment. The biases in precipitation and streamflow were corrected first by dynamically-downscaling and hydrologically modeling the historical control run climate simulations of MIROC5 and CCSM4 GCMs, and then the bias corrections were applied to future periods.

After bias-correcting both atmospheric and hydrologic data, it is possible to project the future water supply. First, the downscaled-corrected atmospheric data were used to simulate flow conditions over the LRW with the hydrologic model WEHY. Then streamflow bias-correction was applied to provide reliable flow data and water supply for the LRW. Analysis of the WEHY-WRF applications revealed that the ensemble mean of the annual mean air temperature increased by 2.04 °C from 2011 to 2100. No significant trend was found in the annual mean solar radiation toward the end of the 21st century. A trend in annual precipitation over the LRW watershed cannot be determined, based on the Mann-Kendall test (at 95% confidence level), however, a slightly increasing trend of flow magnitude at Vu Quang station was detected. No trend was

detected for flow in the early 21st century (2011-2035). However, 3 significant wave-like increasing and decreasing trends occur in the later part of the 21st century (2035-2053; 2054-2074; and 2075-2093). These results were then used in combination with the estimated water demand (Chapter 5) to provide early detection of drought events through drought analysis.

Projected water supply was compared to water demand as collected and estimated by the Department of Water Resources Management (DWRM) in Vietnam. The calculation of water demand considers the following fields: (i) Irrigation; (ii) Livestock; (iii) Aquaculture; (iv) Domestic purposes; (v) Industry; (vi) Tourism and services; (vii) Environmental sanitation. These water demands were estimated for three future periods including 2025, 2030 and 2050. The estimated water demand displayed a distinct increasing trend over the LRW.

Drought properties such as drought duration, drought severity, and the relationship between duration and severity were analyzed through comparison of historical and future water supply (Chapter 4) and water demand (Chapter 5) to obtain changes of water balance and drought conditions in the future. The drought analyses indicated that:

- Future projections showed more drought events in the early 21st century compared to the end of century.
- The majority of events, approximately 90%, had durations less than or equal to 11 months, and approximately 5% had durations between 12 and 24 months.
- MIROC5 climate projection under scenario RCP 8.5 exhibits a more intense drought event than CCSM4 climate projection with scenario RCP4.5. The longest historical drought duration was 18 months, while the future duration of drought event can be up to 24 months.
- The drought intensity may increase by 4.9% with projected 2025 water demand and 10 % with projected 2050 water demand.
- Due to the increasing trend in both current water demand and future water demand, future water supply from the LRW is projected to be insufficient to meet demand. Thus, it is

necessary to improve water governance, increase the efficiency of water delivery systems and modify the operation rules of Tuyen Quang and Thac Ba reservoirs.

## **7.2 Future Perspectives**

Water balance and drought conditions were projected based on 2 scenarios: RCP 4.5 and RCP 8.5. Results show that future drought events are longer and more extreme than in the past, thus new strategic plans to reduce the risks to human society, in an economically and environmentally sustainable manner, are necessary. Expanded studies regarding the revision of the operation rules of Tuyen Quang and Thac Ba Reservoirs are needed to satisfy the water demand in the study area. Water demand was collected from 7 different sectors, but future studies may be expanded to include the projection of water demand up to year 2100 under different economic and population scenarios, particularly considering the current COVID-19 situation. Along with the projection of water demand, future studies should focus on changes in land use and its impact on streamflow response under future atmospheric conditions. Evaluating a variety of land cover and atmospheric conditions, along with various economic and population scenarios, will create a more comprehensive study capable of projecting future hydrologic conditions and estimating water risks such as future floods and droughts.

## **7.3 Conclusion**

This study introduced a comprehensive and reliable methodology to project water balance and drought conditions. The results provide informational support for managers and policy makers in the water sector, allowing for optimal benefit under multiple purpose operation, with a focus on the Lo River watershed. These study results are expected to contribute crucial information not only for the LRW but the national water resources plan in Vietnam. A similar methodology can be replicated in various regions in Vietnam and around the world.